University of Alberta

Model for Liquid Phase Flow on Sieve Trays

by

Bemal Mahendra Mehta

©

A thesis submitted to the Faculty of Graduate Studies and Research in partial fulfillment of the requirements for the degree of Master of Science

Department of Chemical and Materials Engineering

Edmonton, Alberta
Spring 1997

National Library of Canada
Acquisitions and Bibliographic Services
395 Wellington Street
Ottawa ON K1A 0N4
Canada

Bibliothèque nationale du Canada
Acquisitions et services bibliographiques
395, rue Wellington
Ottawa ON K1A 0N4
Canada

Your file Votre référence

Our file Notre référence

The author has granted a non-exclusive licence allowing the National Library of Canada to reproduce, loan, distribute or sell copies of his/her thesis by any means and in any form or format, making this thesis available to interested persons.

The author retains ownership of the copyright in his/her thesis. Neither the thesis nor substantial extracts from it may be printed or otherwise reproduced with the author's permission.

L'auteur a accordé une licence non exclusive permettant à la Bibliothèque nationale du Canada de reproduire, prêter, distribuer ou vendre des copies de sa thèse de quelque manière et sous quelque forme que ce soit pour mettre des exemplaires de cette thèse à la disposition des personnes intéressées.

L'auteur conserve la propriété du droit d'auteur qui protège sa thèse. Ni la thèse ni des extraits substantiels de celle-ci ne doivent être imprimés ou autrement reproduits sans son autorisation.

0-612-21191-6

Canada

University of Alberta

Library Release Form

Name of Author: Bemal Mahendra Mehta

Title of Thesis: Model for Liquid Phase Flow on Sieve Trays

Degree: Master of Science

Year this Degree Granted: 1997

Permission is hereby granted to the University of Alberta Library to reproduce single copies of this thesis and to lend or sell such copies for private, scholarly, or scientific research purposes only.

The author reserves all other publication and other rights in association with the copyright in the thesis, and except as herein before provided, neither the thesis nor any substantial portion thereof may be printed or otherwise reproduced in any material form whatever without the author's prior written permission.

Bemal Mehta

Bemal M. Mehta
26 Charlton Crescent
Sherwood Park, Alberta
T8H 1R1

April 14, 1997

University of Alberta

Faculty of Graduate Studies and Research

The undersigned certify that they have read, and recommend to the Faculty of Graduate Studies and Research for acceptance, a thesis entitled Model for Liquid Phase Flows on Sieve Trays submitted by Bemal Mahendra Mehta in partial fulfillment of the requirements for the degree of Master of Science.

K. Chuang

K. Nandakumar

R. Wood

R. Batycky

W. Finlay

April 4, 1997

To Meenakshi

Abstract

In this work, the liquid phase flow patterns on sieve trays are predicted using a fundamental model. The model uses the time and volume averaged momentum and continuity equations to predict steady state liquid velocities of froth regime flows. Vapor phase flows and the interphase interactions are specified as part of the model. Empirical correlations for distillation hydraulics that include froth height and vapor holdup are used to develop the constitutive relationships needed for closure of the model. The model was evaluated for F-factors (defined as $u_s\sqrt{\rho_G}$ ($kg^{0.5}/m^{0.5}$ s)) ranging from 0.462 to 1.464 and liquid loadings (volumetric flow per length weir) of 27 m^2/h to 68 m^2/h. Experimental data from the literature (primarily that of Solari and Bell, 1986) was used to evaluate the models. For most of the tested cases, the model is able to predict liquid velocities within 33 percent of measured values. At low vapor loading and high liquid loadings, the model breaks down and the degree of flow maldistribution is under-predicted.

Acknowledgment

The author would like to thank all of those whose help is greatly appreciated:

Dr. K. Nandakumar and Dr. K. Chuang for all of their guidance and encouragement.

The National Science and Engineering Research Council (NSERC) for their financial support.

Numerous friends, family, and colleagues who have helped and supported me in countless ways.

Table of Contents

Chapter 1. Introduction 1

Chapter 2. Literature Review - Fluid Mechanics 3
- 2.1 Introduction 3
- 2.2 Two-Fluid Model 3
- 2.3 Closure Relationships for Gas-Liquid Flows 5
  - 2.3.1 Viscous Stress 5
  - 2.3.2 Reynolds Stress 5
  - 2.3.3 Interphase Momentum Interaction 7
- 2.4 Numerical Methods and Solution Algorithms 7
  - 2.4.1 Geometric Transformations, Interpolation, and Discretization Schemes 8
  - 2.4.2 SIMPLE, SIMPLEC, and IPSA 8
- 2.5 Conclusions 9

Chapter 3. Literature Review - Distillation
- 3.1 Introduction 10
- 3.2 Flow Regimes 10
- 3.3 Void Fraction and Liquid Holdup 10
  - 3.3.1 Prediction of Liquid Holdup 12
  - 3.3.2 Volume Fraction Profiles 13
- 3.4 Eddy Diffusivity 13
- 3.5 Flow Patterns and Maldistribution 14
- 3.6 Liquid Phase Maldistribution Models 15
  - 3.6.1 Simplified Models 15
  - 3.6.2 Fundamental Models 15
- 3.7 Conclusions 16

Chapter 4. Single Phase Flow Model 17
- 4.1 Introduction 17
- 4.2 Liquid Phase Model 17
  - 4.2.1 Simplified Constitutive Relationships and Boundary Conditions 17
  - 4.2.2 Reduced Computational Difficulties 18
  - 4.2.3 Data Availablility 18
- 4.3 Key Model Assumptions 19
  - 4.3.1 Physical Properties 19
  - 4.3.2 Froth Regime Flows 19
  - 4.3.3 Flow Geometry 19
  - 4.3.4 Gas Phase Flow Pattern 19
  - 4.3.5 Transient Effects 19
  - 4.3.6 Mass Transfer 21

4.4 Single Phase Transport Equations 21
4.5 Constitutive Relationships 21
4.5.1 Interphase Momentum Interactions 22
4.5.2 Froth Height and Liquid Volume Fraction 22
4.5.3 Turbulent Viscosity 23
4.6 Flow Geometry and Boundary Conditions 23
4.6.1 Walls 23
4.6.2 Symmetry Plane 23
4.6.3 Liquid Exit 25
4.6.4 Sieve Plate 25
4.6.5 Liquid Inlet 25
4.7 Residence Time Distribution 26
4.8 Conclusions 26

Chapter 5. Results and Discussion 28
5.1 Introduction 28
5.2 Velocity Profiles 28
5.2.1 Data Sets 28
5.2.2 Results 31
5.2.3 Evaluation of Model Performance 55
5.2.4 Liquid Inlet Boundary Conditions 55
5.2.5 Prediction of Flow Patterns 57
5.2.6 Prediction for Recirculation and Large Flow Maldistribution 58
5.2.7 Prediction of Flow with High Weir Heights 60
5.3 Residence Time Distribution 60
5.3.1 Data Sets 60
5.3.2 Simulations 62
5.4 Conclusions 64

Chapter 6. Conclusions and Future Work 65
6.1 Introduction 65
6.2 Future Modelling Work 65
6.2.1 Mass Transfer Models 65
6.2.2 Two Fluid Model 66
6.3 Future Experimental Work 66
6.3.1 Further Model Evaluation 66
6.3.2 Downcomer Hydraulics 66
6.3.3 Vapor Phase Flow Patterns 67
6.3.4 Vapor-Liquid Interactions 67
6.4 Conclusions 67

Bibliography 68

Appendix I. Simulation Code 72

Appendix II. Grid Generation 99

Appendix III. Statistical Definitions 111

Appendix IV. Data Sets 113

List of Tables

5.1	Summary of Data Sets	32
5.2	Standard Error of Model Predictions	33
5.3	Transient Inlet Boundary Conditions	62

List of Figures

3.1	Flow Regime Map	11
4.1	Schematic Diagram of a Sieve Tray	20
4.2	Simulation Sieve Tray Geometry	24
5.1	Location of Velocity Measurements - Solari and Bell, 1986	29
5.2	Location of Velocity Measurements - Solari et al., 1982	30
5.3	Centerline U Velocity Versus Radial Position - Case B1	34
5.4	Downstream U Velocity Versus Radial Position - Case B1	35
5.5	Centerline U Velocity Versus Radial Position - Case B2	36
5.6	Downstream U Velocity Versus Radial Position - Case B2	37
5.7	Centerline U Velocity Versus Radial Position - Case B3	38
5.8	Downstream U Velocity Versus Radial Position - Case B3	39
5.9	Centerline U Velocity Versus Radial Position - Case B4	40
5.10	Downstream U Velocity Versus Radial Position - Case B4	41
5.11	Centerline U Velocity Versus Radial Position - Case A10	42
5.12	Centerline U Velocity Versus Radial Position - Case A12	43
5.13	Centerline U Velocity Versus Radial Position - Case A15	44
5.14	Centerline U Velocity Versus Radial Position - Case A17	45
5.15	Top View of the Liquid Phase Flow Pattern - Case B2	46
5.16	Side View of the Liquid Phase Flow Pattern - Case B2	47
5.17	Top View of the Liquid Phase Flow Pattern - Case B3	48
5.18	Top View of the Liquid Phase Flow Pattern - Case A12	49
5.19	U Velocity Versus Radial Position (z) - Case B2	50
5.20	U Velocity Versus Height (y) - Case B2	51
5.21	V Velocity Versus Radial Position (z) - Case B2	52
5.22	W Velocity Versus Radial Position (z) - Case B2	53
5.23	U Velocity Versus Radial Position (z) - Case B3	54
5.24	Experimentally Determined Residence Time Distribution - Case B5	61

5.25 Predicted Residence Time Distribution - Case B5 63

Nomenclature

A_B	Bubbling area, m^2
A_f	Fractional hole area, (A_h/A_B)
A_h	Hole area, m^2
B_d	Drop volume, m^3
C_D	Drag coefficient
$C_{1\varepsilon}$	Epsilon equation constant 1
$C_{2\varepsilon}$	Epsilon equation constant 2
$C_{3\varepsilon}$	Epsilon equation constant 3
C_μ	Eddy viscosity constant
d_h	Hole diameter, m
D	Column diameter, m
D_m	Diffusivity, m^2/s
De	Eddy diffusivity for liquid mixing, m^2/s
F_s	F-factor $(u_s\rho_G^{0.5})$, $kg^{0.5}m^{-0.5}s^{-1}$
F_{lv}	Flow parameter $((L/G)(\rho_G/\rho_L)^{0.5})$
Fr	Froud number (u_s^2/gh_{cl})
Fr′	Modified Froud number $(Fr(\rho_G/\rho_L-\rho_G))$
g	Body force, m/s^2
G	Gas (or vapor) phase loading, (kg.mol/s)
G_k	Turbulent kinetic energy production from body forces for phase k

h_{cl}	Clear liquid height, m
h_f	Froth height, m
h_{ow}	Height over weir (h_f - h_w) , m
h_w	Weir height, m
k_k	Turbulent kinetic energy for phase k
$l_{mix,k}$	Mixing length for phase k, m
L	Liquid phase loading, (kg.mol/s)
L_w	Weir length, m
$\mathbf{M_k}$	Interphase momentum interaction for phase k, N/m^3
$\mathbf{M_{ki}}$	Generalized interfacial force, N/m^3
$\mathbf{M_{ki}^B}$	Interfacial body force, N/m^3
$\mathbf{M_{ki}^C}$	Interfacial collision force, N/m^3
$\mathbf{M_{ki}^D}$	Interfacial drag force, N/m^3
$\mathbf{M_{ki}^L}$	Interfacial lift force, N/m^3
$\mathbf{M_{ki}^V}$	Interfacial virtual mass force, N/m^3
$\mathbf{M_{k,k}}$	Interphase turbulent kinetic energy source for phase k
$\mathbf{M_{k,\varepsilon}}$	Interphase turbulent kinetic energy dissipation source for phase k
$\mathbf{M_L}$	Interphase momentum interaction for the liquid phase, N/m^3
p_k	Pressure of phase k, N/m^2
p_{ki}	Pressure of phase k at the phasic interface, N/m^2
P_k	Turbulent kinetic energy production from shear forces for phase k
Q_L	Liquid flow rate, m^3/s

$S_{k,k}$	Source of turbulent kinetic energy for phase k
$S_{k,\varepsilon}$	Source of kinetic energy dissipation for phase k
Sc	Schmidt number ($\mu/\rho\ D_m$), no units
Sc_T	Turbulent Schmidt number ($\mu_{T,L}/\rho_L$ De), no units
t	Tangent to a free surface
t_R	Residence time, s
u_k	x component velocity, m/s
u_s	Superficial vapor velocity, based on bubbling area A_B, m/s
$\mathbf{v}_G$	Gas phase velocity, m/s
$\mathbf{v}_{G,hole}$	Gas phase hole velocity, m/s
v_k	y component velocity, m/s
$\mathbf{v}_k$	Velocity vector for phase k, m/s
$\mathbf{v}_{ki}$	Velocity vector for phase k at the phasic interphase, m/s
$\mathbf{v}_L$	Velocity vector for the liquid phase, m/s
w_k	z component velocity , m/s
W	Weir length, m
x	Cartesian coordinate (m)
$X_{A,L}$	Solute A concentration in the liquid phase, mol/m^3
y	Cartesian coordinate (m)
z	Cartesian coordinate (m)
α_k	Volume fraction of phase k
$\alpha_{L,\,avg}$	Average liquid volume fraction

ε_k	Turbulent energy dissipation for phase k
Γ_k	Interfacial mass transfer, $kg/m^3 s$
μ_k	Laminar viscosity, kg/m s
$\mu_{T,k}$	Turbulent viscosity, kg/m s
ρ_k	Density of phase k, kg/m^3
ρ_G , ρ_L	Gas and liquid phase density, kg/m^3
σ	Surface tension, N/m
σ	Second moment with respect to time, s^2
σ_k	Turbulent Prandtl number for the kinetic energy equation
σ_ε	Turbulent Prandtl number for the dissipation equation
τ_k	Viscous stress of phase k, N/m^2
τ_{ki}	Viscous stress of phase k at the interface, N/m^2
τ_k^T	Reynolds stress of phase k, N/m^2

Subscripts

avg	Average
G	Gas
i	Interface
k	Phase k
L	Liquid

T	Turbulent
V	Vapor

Superscripts

B	Body force
C	Collision force
D	Drag force
L	Lift force
tr	Transpose
T	Turbulent
V	Virtual mass force

1. Introduction

Distillation is one of the most important methods of separation used in the Chemical Processing Industries (CPI). Although energy intensive, the method is typically the first choice among separation technologies because it is not limited by scale and it is highly robust. Distillation towers and equipment can often be the most expensive parts of a chemical plant. Due to the importance and the costs associated with separations, modest improvements in distillation technology can translate into millions of dollars of savings for the CPI.

Modelling distillation tray hydraulics and separation efficiency is extremely important. Over the last 75 years, there has been significant progress in developing distillation models. One of the most important steps forward in distillation modelling was the conceptualization of the equilibrium stage. In 1925, McCabe and Thiele used the concept to develop a method of analyzing distillation systems that is still widely used today. This analysis however assumes that a single tray is a black box. The liquid and vapor streams leaving the tray are assumed to be in equilibrium. The hydrodynamics on the tray was completely neglected. Subsequently, inadequacies in the basic model were handled by using the concept of (a) tray efficiency (Murphree 1925) or (b) non-equilibrium models (Taylor & Krishnamurthy 1985). Currently the most common assumption in distillation models is the concept of the fully mixed, ideal tray - i.e. spatial variations in concentration and velocity are ignored. Yet new tray designs attempt to promote good vapor-liquid contact through clever designs that control the velocity fields.

Predictions of tray hydraulics are largely guided by experience and empirical correlations. In the majority of cases, these methods produce acceptable results. Unfortunately, these methods do have their limitations, particularly with respect to scaling from pilot to large scale systems. The inability to model the hydraulics limits our ability to make reliable predictions in large scale equipment using measured efficiency data on small scale equipment.

Experimentally, it has been observed that there is a significant amount of variation in flow and composition on distillation trays. Maldistribution is the cause of significant losses in separation efficiency on large trays and our inability to predict their performance. The models that have accounted for these maldistributions have typically not incorporated the fundamental concepts of fluid mechanics. In fact, the fluid mechanics have been ignored altogether in several of these modelling efforts. One reason for the reluctance to approach the modelling in a more fundamental way is the difficulty of solving the equations of large and complex three dimensional multiphase flow problems.

The development of powerful computers, advances in numerical techniques, and improvements in multiphase flow models permit the investigation of this type of

complex flow problem that could not be studied in the past. A problem of considerable practical interest is distillation tray modelling. By rigorously applying multiphase flow modelling techniques it may be possible to make predictions and evaluate designs with greater confidence. But such predictions must first be validated against a good set of experimental data. They are still lacking. In the present work we compare liquid phase velocity profiles measured by Solari and Bell (1986) against predictions from our model. We have used Solari and Bell because the data have reasonable accuracy and the data are in a readily usable form. Other data sets are much more inaccurate and/or there are significant flaws in experimental design that have made the data unusable.

2. Literature Review - Fluid Mechanics

2.1 Introduction

In this chapter, the equations and numerical techniques used to solve fluid flow problems are presented. Over the last 25 years, there has been considerable progress made in the analysis of two phase flow from a fundamental standpoint. Coinciding with this time period, there has been an explosive growth in computational power at our disposal. The research area defined as computational fluid mechanics has reached a level of sophistication that will permit the study of complex problems of industrial interest. In the research phase of evaluating such models, particularly from the point of scale invariance there is a need for good experimental data on equipment of different scales.

2.2 Two-Fluid Model

Modelling two phase flow requires the use of appropriate conservation equations that can account for the behavior of each phase and the interactions between them. One very common approach used in this work is the Two-Fluid Model (Ishii 1975).

The foundation for the two-fluid model is the local instantaneous formulation of the momentum and continuity equations on a continuum scale. Two phase flow is visualized as a "number of single phase regions bounded by moving interfaces" (Ishii 1990). In the local instantaneous formulation, single phase conservation equations are implemented in the continuous regions and jump conditions are used to match the phase interfaces. Each of the single phase regions obey the general single phase balance equations for mass, momentum, and energy.

The two-fluid model is developed by taking an Eulerian time and volume average of the instantaneous formulation. High frequency fluctuations in flow are filtered out, leaving only the low frequency effects that are of interest.

The two-fluid model is characterized by two independent velocity fields that specify the motions of each phase. For notational purposes, the velocity of phase k is defined as:

$$\mathbf{v}_k = \begin{bmatrix} u_k \\ v_k \\ w_k \end{bmatrix} \qquad (2\text{-}1)$$

Each phase is also characterized by a volume fraction, α_k. The volume fraction is interpreted as the local concentration of a phase, and is constrained as follows:

$$0 \le \alpha_k \le 1 \qquad (2\text{-}2)$$

The property of saturation defines the relationship between the volume fraction of each phase.

$$\sum_{k=1}^{2} \alpha_k = 1 \qquad (2\text{-}3)$$

Each phase is also constrained by the volume-averaged continuity equation:

$$\frac{\partial}{\partial t}(\alpha_k \rho_k) + \nabla \cdot (\alpha_k \rho_k \mathbf{v}_k) = \Gamma_k \qquad (2\text{-}4)$$

$$k = 1,2$$

The interfacial mass transfer, Γ_k, is constrained by the overall conservation of mass law:

$$\sum_{k=1}^{2} \Gamma_k = 0 \qquad (2\text{-}5)$$

The volume-averaged momentum balance equation can be expressed as follows:

$$\frac{\partial}{\partial t}(\alpha_k \rho_k \mathbf{v}_k) + \nabla \cdot (\alpha_k \rho_k \mathbf{v}_k \mathbf{v}_k) = -\nabla \cdot (\alpha_k p_k) + \nabla \cdot \left(\alpha_k \left(\tau_k + \tau_k^{T}\right)\right) + \alpha_k \rho_k \mathbf{g} + \mathbf{M}_k \qquad (2\text{-}6)$$

$$k = 1,2$$

The terms on the left hand side of equation 2.6 account for the temporal acceleration and the convective acceleration. The terms on the right hand side of the equation

account for the pressure (p_k), the viscous (τ_k) and Reynolds stresses (τ_k^T), body forces ($\mathbf{g}$), and interfacial momentum transfer ($\mathbf{M_k}$), respectively.

2.3 Closure Models for Gas-Liquid Flows

From a mathematical perspective, empirical relationships are required to close the set of equations that are posed in Section 2.1. From a physical perspective, the constitutive relationships describe the fundamental behavior of each phase and interactions between phases. Some of these closure laws are physical laws that are properties of each phase. But generally, these laws must be developed for each flow geometry and flow regime (Boure 1987). The most commonly used closure models for gas-liquid flows are presented below.

2.3.1 Viscous Stress

The viscous stress term, τ_k, is most commonly modelled using the assumption that each phase is a Newtonian fluid:

$$\tau_k = \mu_k\left(\nabla \mathbf{v}_k + \left(\nabla \mathbf{v}_k\right)^{tr}\right) \qquad (2\text{-}7)$$

2.3.2 Reynolds Stress

The Reynolds stress contribution, τ_k^T, is one of the most difficult terms to account for in equation 2-6. The turbulent stress tensor accounts for all of the turbulent fluctuations occurring at small time scales and the convection and diffusion of turbulent structures at length scales smaller than that of the equipment. The primary difficulty with modelling turbulent two phase flow is the lack of adequate models. Almost all of the fundamental studies of turbulence have been conducted for single phase flows. Recently, there has been some work with adapting single phase turbulence models for two phase flows. The k-ε Model (Lauder and Jones 1972) and the Prandtl mixing length model are two turbulence models that have been adapted in this way.

The k-ε model is one of the most widely used turbulence models for single phase flows of industrial importance. The model consists of two scalar transport equations: one for the transport of turbulent kinetic energy and another for the transport of eddy dispersion. The empirical parameters used for these models have been determined from experiments in single phase shear flows. The standard k-ε model has been adapted for some classes of multiphase flows (Neti 1990).

The turbulent stress is evaluated using an equation with the same form as the viscous stress calculation (eqn. 2.7):

$$\tau_k^T = \mu_{T,k}\left(\nabla \mathbf{v}_k + \left(\nabla \mathbf{v}_k\right)^{tr}\right) \qquad (2\text{-}8)$$

In equation 2-8, the turbulent viscosity, μ_k^T, is not a constant but varies as a function of the turbulent kinetic energy and energy dissipation:

$$\mu_{T,k} = C_\mu \rho_L \frac{k_k^2}{\varepsilon_k} \qquad (2\text{-}9)$$

The conservation equation for turbulent kinetic energy, k_k , is evaluated with the following equation:

$$\frac{\partial}{\partial}(\alpha_k \rho_k k_k) + \nabla \cdot (\alpha_k \rho_k \mathbf{v}_k k_k) = \nabla \cdot \left(\alpha_k \left(\mu_k + \frac{\mu_{T,k}}{\sigma_k} \right) \nabla \cdot k_k \right) + \alpha_k S_{k,k} + \mathbf{M}_{k,k}$$

(2-10)

The energy dissipation is calculated using the following equation:

$$\frac{\partial}{\partial}(\alpha_k \rho_k \varepsilon_k) + \nabla \cdot (\alpha_k \rho_k \mathbf{v}_k \varepsilon_k) = \nabla \cdot \left(\alpha_k \left(\mu_k + \frac{\mu_{T,k}}{\sigma_\varepsilon} \right) \nabla \cdot \varepsilon_k \right) + \alpha_k S_{\varepsilon,k} + \mathbf{M}_{\varepsilon,k} \qquad (2\text{-}11)$$

$S_{k,k}$ and $S_{\varepsilon,k}$ are single phase source terms:

$$S_{k,k} = P_k + G_k + \rho_k \varepsilon_k \qquad (2\text{-}12)$$

$$S_{\varepsilon,k} = \frac{\varepsilon_k}{k_k} \left(C_{1\varepsilon} \left(P_k + C_{3\varepsilon} \max(G_k, 0) \right) - C_{2\varepsilon} \rho_k \varepsilon_k \right) \qquad (2\text{-}13)$$

$\mathbf{M}_{k,k}$ and $\mathbf{M}_{k,\varepsilon}$ are source terms that account for the interactions between phases. An example of an interphase turbulent source is a rising bubble inducing turbulence in the surrounding liquid.

The Prandtl mixing length model is an empirical model for turbulence (Wilcox 1990). The model can make reasonable predictions in homogeneous turbulence problems. The turbulent viscosity for two dimensional flows is evaluated with the following formula:

$$\mu_{T,k} = \rho_k l_{mix,k}^2 \left| \frac{\partial u}{\partial y} \right| \qquad (2\text{-}14)$$

This model has been used because of its simplicity and its reasonable accuracy for some types of turbulent flow (Kashiwa 1994).

2.3.3 Interphase Momentum Interaction

The momentum interaction between the phases can be analyzed as a contribution of several different effects (Ishii 1990).

$$\mathbf{M}_k = \Gamma_k \mathbf{v}_{ki} + p_{ki} \nabla \alpha_k + \mathbf{M}_{ik} - \alpha_k \cdot \tau_{ik} \qquad (2\text{-}15)$$

The terms on the right hand side of equation 2-15 account for mass transfer, surface tension effects, generalized interfacial force, and the transport of viscous stress effects of the fluid, respectively. Generally, for gas-liquid flows the only significant effects are the mass transfer and the generalized infacial forces.

The generalized interfacial force is the summed contribution of several effects:

$$\mathbf{M}_{ik} = \mathbf{M}_{ik}^{D} + \mathbf{M}_{ik}^{V} + \mathbf{M}_{ik}^{B} + \mathbf{M}_{ik}^{L} + \mathbf{M}_{ik}^{C} \qquad (2\text{-}16)$$

These effects are the drag (D), virtual mass (V), Basset (B), lift (L), and collision (C) forces, respectively. The drag force is often assumed to be the only significant interphase momentum interaction (Jakobsen 1994, Kashiwa 1994). In these cases, the other forces are assumed to be negligible or some of the forces are lumped with the drag force.

The drag force for any two phase system can often be characterized with two additional models: the interfacial area (A_d/B_d) and the drag coefficient (C_D). For simple two-phase flows, the interfacial area can often be characterized with a characteristic particle(bubble or droplet) size and volume fraction. These types of models have been used in many bubble column and pipe flow simulations (Neti 1990, Jakobsen 1994, Kashiwa 1994). For more complex flows, the models can become more involved, but almost all interfacial area models for gas-liquid systems have been developed exclusively for pipe flows (Ishii 1987). The drag coefficient, C_D, is a parameter that relates the interfacial area concentration and slip velocity to the drag force. Several drag coefficient models have been developed for simple gas-liquid flows and complex pipe flows (Zuber 1979, Wallis 1987). Drag coefficient models are not well developed for other flow geometries, particularly with a free liquid surface where the gas/vapor bubbles can disengage..

2.4 Numerical Methods and Solution Algorithms

The set of equations that are developed in Sections 2.2 and 2.3 are typically solved numerically. Finite volume methods are applied to solve the coupled mass and momentum equations. Finite volume methods are used extensively in commercial software packages such as CFDS-FLOW3D and FLUENT.

In this research work, the program CFDS-FLOW3D is used exclusively. In the following summary, references are provided for the most important algorithms used in the program.

2.4.1 Geometric Transformations, Interpolation, and Discretization Schemes

The techniques developed by Thompson et al. (1982) are used to apply finite volume methods to complex three dimensional geometries. Arbitrary, complicated geometries in the Cartesian coordinate system are mapped onto a simple computational space coordinate system. The flow problem is then solved in this simplified coordinate system.

The discretized flow geometry is a three dimensional grid that has been divided into smaller volume elements or cells. Primitive variables such as u_k , v_k, w_k, p, and α_k are stored at the centroid of each cell in the geometry. The SIMPLE scheme (discussed in Section 2.4.2) for the solution of the momentum and continuity equations requires the use of a staggered grid. In a staggered grid, certain primitive variables must be available at each face of a finite volume cell while others such as pressure, and scalar quantities are used at the cell center. Since the memory cost of storing velocity components at each cell face is prohibitively expensive, the Rhie-Chow interpolation scheme (Rhie and Chow 1983) is implemented. In the Rhie-Chow scheme, the velocity components at cell faces are then interpolated from the centroid values as needed.

The transport equations are discretized using the Hybrid method (Spalding 1972). In this scheme, central differencing is used if the Peclet number is less than 2 and upwind differencing is used if the Peclet number is greater. The Hybrid scheme is very robust yet it has improved accuracy at low speed flows.

2.4.2 SIMPLE, SIMPLEC, and IPSA

The Semi-Implicit Method for Pressure Linked Equations (SIMPLE) (Patankar and Spalding 1972) is the method used in CFDS-FLOW3D to calculate the flow field of single phase flows. The finite difference equations that are produced from discretizing the Navier-Stokes equations are solved in an iterative fashion that accounts for the coupled nature of velocity and the pressure (Patankar 1983).

In CFDS-FLOW3D, a modified version of the SIMPLE algorithm is also implemented. This modified algorithm is commonly known as SIMPLEC (Van Doormal and Raithby 1984) and is used as the default method in CFDS-FLOW3D.

The Inter-Phase Slip Algorithm (IPSA) was developed in order to extend the SIMPLE scheme for multiphase flows (Spalding 1977). In IPSA, the individual phase continuity equations are treated exactly like any other equation in SIMPLE except that the calculated volume fractions are subject to the saturation constraint.

2.5 Conclusions

In this chapter, the generalized equations for two phase flow are introduced. These equations include the Eulerian time and volume averaged continuity and momentum balance equations. These equations will form the basis of the model that will be developed in future chapters. The computational methods used to solve these transport equations have also been outlined.

Some commonly used constitutive relationships for multiphase flow have been extracted from literature. The available turbulence models are primarily designed for single phase flows. There has been some work done with adapting these models for two phases. These two phase studies have primarily concentrated on problems such as pipe and bubble column flow, but nothing as complex as a distillation tray. There are several models available for modelling the interphase momentum interactions, but none are capable of modelling froth regime distillation flows. Thus, from our literature survey we conclude that there are currently no fundamental models that can describe the complex interfacial phenomenon of distillation flows.

3. Literature Review - Distillation

3.1 Introduction

Over the last fifty years, there has been significant progress made in the understanding of distillation tray hydraulics and efficiencies. The goals of these studies have been to improve design and predict performance. This chapter will review some of the current literature regarding sieve tray hydraulics.

Sieve trays are one of the most commonly used and studied internals used in distillation columns. Several authors have written comprehensive books or summaries that focus on sieve tray hydraulics(Lockett 1986, Kister 1990).

3.2 Flow Regimes

Sieve trays can operate in one of five major flow regimes: bubble, cellular foam, froth, spray, and emulsion (Kister 1990). In general, these flow regimes are a function of the physical properties of the fluids, the operating conditions, and the tray geometry. The flow regime characterizes the nature of multiphase flow, mixing, and mass transfer and can be thought of as a qualitative definition of all interfacial phenomenon occurring on the sieve tray. Any hydraulic simulation of distillation must account for the flow regime. Most industrial scale sieve trays operate in the froth and spray regimes. In these flow regimes, both tray efficiency and capacity are maximized. Figure 3.1 shows how the flow regime varies with operating conditions.

The froth regime can be split into two subregimes based on the vapor velocity. The subregimes have different properties. At low vapor velocities, the bubbles have a non-uniform character because some holes will bubble intermittently. At increased vapor rates, holes will begin jetting instead of bubbling. Above the jetting holes, the gas phase is the continuous phase and the liquid is dispersed as droplets in the jet. Between the holes, the liquid is continuous and the vapor phase is dispersed as bubbles.

As the number of jetting holes increase, the spray-froth transition occurs. In the spray regime, the gas phase is the continuous phase and the liquid phase is dispersed as droplets.

3.3 Void Fraction and Liquid Holdup

The study of liquid holdup on sieve trays has been extensively studied in literature. The reason for this is that the liquid holdup will determine the pressure drop, the average liquid phase residence time, and other hydraulic behavior.

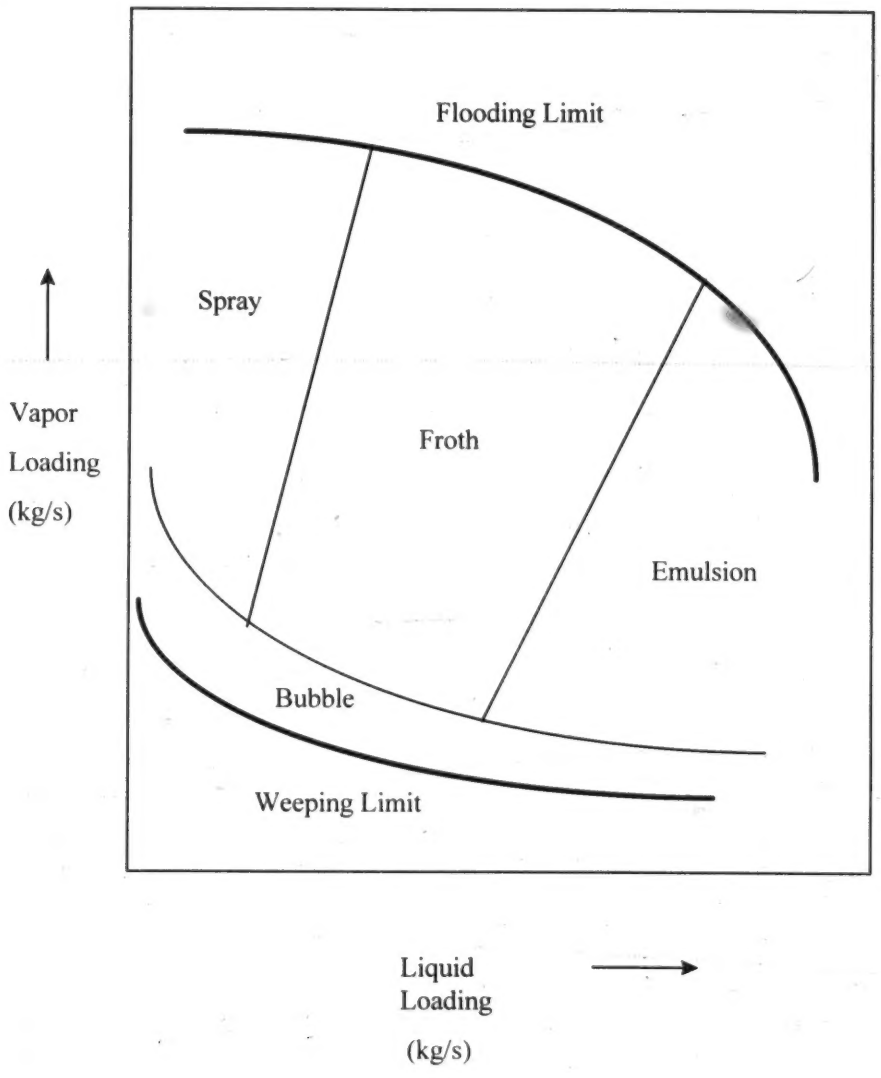

Figure 3.1. Flow Regime Map

3.3.1 Prediction of Liquid Holdup

The clear liquid height, h_{cl}, is a measure of the total amount of liquid holdup on a sieve tray. The relationship between the clear liquid height, the average volume fraction of froth on a tray, and the froth height is:

$$h_{cl} = \alpha_{L,avg} h_f \qquad (3\text{-}1)$$

The following correlation has been developed for evaluating h_{cl} and $\alpha_{L,avg}$ (Bennett 1983):

$$h_{cl} = \alpha_{L,avg}\left[h_w + C\left(\frac{Q_L}{L_w \alpha_{L,avg}}\right)^{0.67}\right] \qquad (3\text{-}2)$$

$$C = 0.50 + 0.438\exp(-137.8 h_w) \qquad (3\text{-}3)$$

The average liquid volume fraction is evaluated using the following correlation:

$$\alpha_{L,avg} = \exp\left[-12.55\left(u_s\left(\frac{\rho_G}{\rho_L - \rho_G}\right)^{0.5}\right)^{0.91}\right] \qquad (3\text{-}4)$$

This correlation is proven to calculate clear liquid height fairly accurately. Unfortunately, the prediction of the average volume fraction is relatively poor.

Colwell has developed an alternative correlation to evaluate clear liquid height and average volume fraction (Colwell 1979). This method does not have the limitations of the Bennett correlation and can predict both the clear liquid height and volume fraction with reasonable accuracy. The clear liquid height is evaluated with the following equation:

$$h_{cl} = \alpha_{L,avg}\left[h_w + 0.527\left(\frac{Q_L}{C_d \alpha_{L,avg}}\right)^{0.67}\right] \qquad (3\text{-}5)$$

$$C_d = \begin{cases} 0.61 + 0.08\dfrac{h_{fow}}{h_w} & \dfrac{h_{fow}}{h_{ow}} < 8.135 \\ 1.06\left(1 + \dfrac{h_w}{h_{fow}}\right)^{1.5} & \dfrac{h_{fow}}{h_{ow}} \geq 8.135 \end{cases} \qquad (3\text{-}6)$$

$$h_{fow} = h_f - h_w \qquad (3\text{-}7)$$

The following equations are used to predict the liquid phase volume fraction:

$$\alpha_{L,avg} = \frac{1}{\eta + 1} \qquad (3\text{-}8)$$

$$\eta = 12.6 Fr'^{0.4} \left(\frac{A_B}{A_h} \right)^{0.25} \qquad (3\text{-}9)$$

$$Fr' = Fr \left(\frac{\rho_G}{\rho_L - \rho_G} \right) \qquad (3\text{-}10)$$

$$Fr = \frac{u_s}{g h_{cl}} \qquad (3\text{-}11)$$

3.3.2 Volume Fraction Profiles

Spatial variation of volume fraction within a sieve tray froth has been reported in several studies (Yongeng et al. 1988, Hofhuis and Zuiderweg 1979). Gamma scan techniques were used to measure the variation in liquid volume fraction on sieve trays. These studies indicate that there is significant variation in liquid phase volume fraction in the vertical direction. The volume fraction profiles vary significantly with different operating conditions. In particular, it was observed that there are distinct differences between froth and spray regime volume fraction profiles.

Hofhuis and Zuiderweg also developed a droplet trajectory model to predict the volume fraction profile on a sieve trays operating in the spray regime. A model for froth regime volume fractions was not developed.

3.4 Eddy Diffusivity

Eddy diffusivities are a commonly used measure of turbulent mixing. They are used to predict tray efficiencies from a known point efficiency on a distillation tray. Several eddy diffusivity correlations have been developed for sieve tray flows. (Gerster et al. 1958, Gilbert 1959, Barker and Self 1962, Sohlo and Kinnunen 1977, Zuiderweg 1982)

Zuiderweg proposed the following eddy diffusivity correlation for spray-mixed froth regime flows:

$$De = \frac{8.3\rho_G u_s^2 h_{cl}^2}{\rho_L\left(\frac{Q_L}{L_w}\right)} \qquad (3\text{-}12)$$

Zuiderweg also proposed a correlation for emulsion regime flows:

$$De = 3.0 u_s h_{cl}\left(\frac{\rho_G}{\rho_L}\right)^{0.5} \qquad (3\text{-}13)$$

3.5 Flow Patterns and Maldistribution

Early studies of distillation internals reported that liquid phase flows on sieve trays are maldistributed. Kirschbaum (1948) observed that liquid crosses large distillation trays in a non-ideal flow pattern. It was predicted that these non-idealities would reduce tray efficiency. These non-idealities were studied in greater detail as more advanced measurement techniques became available and more accurate predictions of tray behavior were required. This detailed study of liquid phase velocity patterns and residence times was primarily directed by two researchers: R. L. Bell and R. B. Solari.

In 1972, Bell studied the residence time distribution of liquid on industrial scale sieve trays (Bell 1972). Residence times were calculated using fluorescent dye tracing techniques. Fluorescent dyes were injected into the inlet downcomer. The concentration of dye was measured at several locations on the sieve tray. Measurements of dye concentration were made using a fiber optic probe and a photomultiplier tube detector. Light from a fiber optic limb would excite the dye on the tray. The fluorescence is transmitted up another fiber optic limb, is amplified using the photomultiplier, and the signal strength is recorded. Residence times were calculated based on the time varying signal profile. Residence time distributions were measured for a variety of operating conditions and two different chemical systems. These two systems could be classified as a non-polar hydrocarbon system (toluene - cyclohexane) and aqueous system (water-isopropyl alcohol).

Techniques were eventually developed to measure liquid phase velocities on sieve trays (Solari et al. 1982). Using multiple exposure photography, it was possible to visually trace the flow of colored dye across the tray. Colored dye would be injected at one location on the tray. The time for the dye to travel an arbitrary distance downstream of the injection point was measured from the photographs. The velocity was calculated by dividing the distance traveled by the travel time. This study was performed with an air-water system at 1 atm. pressure.

Although this method had the advantage of being non-invasive on the tray, it was also highly inaccurate. The convective and diffusive effects could not be differentiated by

the photographs. Repeatability of observations were highly dependent on the judgment of the observer of the photograph.

Further refinements allowed for more accurate measurement of liquid phase velocities (Bell and Solari 1986). The method of velocity calculation was essentially the same as in the 1982 study. This study improved the method used to calculate travel time. The travel time was calculated by determining the difference between residence times at the upstream and downstream points. Residence times were determined using the fluorescent dye injection technique in exactly the same manner as the 1972 studies. The difference in mean residence times is a more accurate estimate of the travel time because both the convective and dispersive effects on dye movement are accounted for. This study was also performed with an air-water system at 1 atm. pressure.

3.6 Liquid Phase Maldistribution Models

Along with the experimental study of liquid phase maldistribution, there has also been an effort to model these phenomenon. A model that can predict the liquid phase flows can be combined with a mass transfer model in order to predict tray efficiency.

3.6.1 Simplified Models

Several models have been proposed for liquid phase flow that are based on highly simplified liquid phase flow assumptions. The Stagnant Regions Model (SRM) is one of the first proposed maldistribution models (Porter et al. 1972). This model assumes that liquid travels across the center of a tray in a plug flow fashion, and the regions on the sides are assumed to be stagnant. Diffusion is the only mechanism of mixing between these two regions.

In their 1986 work, Solari and Bell also proposed a liquid phase flow model. In this model, the tray is divided into forward and backward flow zones. The experimental findings of the study were correlated to develop the required parameters for this model.

The fundamental weakness to each of these models is the fact that the models are inconsistent with the law of momentum conservation. The models are essentially developed by curve fitting the data. Hence they also do not remain scale invariant.

3.6.2 Fundamental Models

Recently, there have been efforts to model the liquid phase flow patterns upon sieve trays using the principles of momentum conservation (Porter et al. 1992). Gas phase flow patterns and the interphase interactions between the gas and liquid phases are specified as part of the model. The model has some success in predicting liquid phase flows but it is clear that the model can be improved.

In this model, the Navier-Stokes equations are applied to the liquid phase flow in two dimensions. The model attempts to capture recirculation and stagnancy phenomenon

but neglects the possibility of any spatial variation in the vertical direction. The model also does not account for the gas phase holdup in the froth. However, the model does account for the gas phase as momentum source to the liquid phase momentum.

Liquid flows are constrained to the froth zone on the distillation tray and liquid spray in the vapor space above the froth is neglected. The sieve tray acts as the lower boundary to flow and the upper boundary is the froth height. This froth height is calculated from hydraulic correlations such as those presented in Section 3.3.1.

Liquid phase turbulence phenomenon is captured using the single phase k-ε equation. The model does not include gas induced turbulence as a source term to the model.

3.7 Conclusions

In this chapter, a literature review is provided for sieve tray hydraulics. Current literature regarding flow regimes, liquid holdup, eddy diffusivity, and liquid phase maldistribution are presented. The model that will be developed in subsequent chapters will rely upon the literature presented in this chapter in several ways.

The model will be based upon the single phase concept initially presented by Porter. The Colwell and Zuiderweg correlations will provide closure equations for the model. These correlations are chosen because of their superior accuracy in predicting phenomenon on sieve trays operating in the froth regime. This model will be validated using the data sets generated by Solari and Bell.

4. Single Phase Flow Model

4.1 Introduction

The goal of this study is to develop a predictive model for sieve tray hydraulics. In theory, a model based on fundamental conservation equations will have a much wider range of applicability than purely empirical models. This flow model can then be applied to mass transfer models in order to predict tray efficiencies.

In Chapter 2, the theoretical basis for the analysis of two phase flow was presented. Both the basic equations and computational methods needed to solve these equations were reviewed. Constitutive relationships were also discussed.

In Chapter 3, the current literature regarding sieve tray hydraulics was reviewed. Several concepts and models that form the basis of our current knowledge regarding sieve trays are presented.

In this chapter, a model is presented for the prediction of liquid phase flows on sieve trays, by combining various elements presented in Chapters 2 and 3.

4.2 Liquid Phase Model

In the two-fluid formulation developed by Ishii (Section 2.2), each phase is described by its own set of mass and momentum conservation equations. This approach has been used extensively, primarily for gas-liquid flows in pipe geometries. Alternatively, in the distillation flow model developed by Porter (Section 3.6.2) only the liquid phase is described by a set of conservation equations. Gas phase flow patterns are specified as part of the model. The latter approach is the basis of the model presented in this thesis. The reasons for this choice are discussed in the following sections.

4.2.1 Simplified Constitutive Relationships and Boundary Conditions

The development of constitutive relationships is not a trivial undertaking. Although a full two fluid formulation would be the most rigorous approach to modelling, it is not practical at this stage. As indicated in Chapter 2, the currently available interphase momentum transfer and turbulence models are not adequate for a two phase distillation flow modelling.

As indicated in Sections 2.3.2 and 2.3.3, turbulence and interphase momentum transfer models have been extensively developed for pipe and bubble column flows. Similar models have not been developed for distillation flows. Fundamental physical phenomenon such as interfacial area, drag coefficients, and turbulent intensities need to be studied. Any models used in predicting distillation tray flows will be restricted because of the absence of this physical data.

By definition, single phase models only have to represent the behavior of one phase. More limited constitutive relationships can be developed based on the available data sets and hydraulic models. Although there is insufficient information for the development of two-fluid models, a single phase model can still be developed with reasonable accuracy.

The specification of boundary conditions is also simplified with a single phase model. It is not a trivial task to ensure that boundary conditions are correctly posed in a two fluid model with multiple flow boundaries. Specifically, the manner in which volume fractions split between multiple outlets is neither predictable nor known from physical description for it to be prescribed in a meaningful manner. The correct specification of single phase boundary conditions is significantly simpler.

4.2.2 Reduced Computational Difficulties

The single phase model has advantages with respect to computational resources and the methods used to obtain solutions.

A rigorous two fluid model requires twice the memory resources as a single phase model. This difference is significant enough to make the full two phase formulation unattractive for a full three dimensional simulation. In addition, the solution of the coupled momentum and continuity equations for each phase is highly computationally expensive. Single phase algorithms such as SIMPLEC are relatively efficient. Problems of reasonable size can be solved quite easily. For multiphase problems, algorithms such as IPSA are not as efficient at solving the coupled set of equations.

In order to evaluate whether it would be feasible to solve a distillation problem using the two fluid approach, a set of simple benchmarking studies of batch gas-liquid systems were conducted. The solution algorithm, IPSA, was tested as implemented in the commercial software package CFDS-FLOW3D. In these studies it was found that excessive floating point operations were required to solve some very simple two phase flow scenarios. More complicated benchmarking studies failed due to convergence difficulties. From these cursory results, it was concluded that the two fluid approach to solving complex distillation problems was currently not feasible from a computational standpoint. The existing codes also neglect some important terms such as the added mass effect and the elastic collision effect in gas/liquid flows. Thus the adequacy of the model used in the present generation of codes is itself questionable. Hence we have settled for the single fluid model in three dimensions with appropriate modelling of the effect of the vapor phase on the liquid.

4.2.3 Data Availability

In order to validate any proposed model, there must be a sufficient amount of experimental data of good quality and spatial resolution. There is a significant amount of data available for liquid phase hydraulics. Several studies of liquid phase velocity profiles and residence time distributions have been conducted, but the gas phase flow patterns have not been studied as thoroughly. The gas phase is typically

assumed to pass through the column in a plug flow fashion. If a two phase model were developed for distillation tray flows, it would be very difficult to validate the gas phase flow patterns, as very little experimental information is available on such patterns.

4.3 Key Model Assumptions

The key assumptions and restrictions behind the proposed model are presented below:

4.3.1 Physical Properties

It is assumed that all gas and liquid physical properties, such as density, viscosity, and surface tension, are constant. The justification of this is that the tray is assumed to be isothermal and pressure variations are assumed to be small.

4.3.2 Froth Regime Flows

This model is restricted only to froth regime flows. The model needs be restricted because each flow regime has very different mixing and hydraulic properties.

4.3.3 Flow Geometry

Froth regime flows (Sec. 4.3.2) are characterized by a well defined interface between the froth (containing both vapor and liquid phases) and the vapor space above the froth. If we assume that the amount of spray in the vapor space is negligible, the flow geometry can be limited to the froth zone on the distillation tray.

Figure 4.1 shows a schematic diagram of a typical sieve tray. The coordinate system presented in this figure will be used in subsequent model development.

4.3.4 Gas Phase Flow Pattern

On industrial size sieve trays, the froth height is typically an order of magnitude smaller than the tray diameter (a typical froth height is in the order of 0.2 m; a typical column diameter is in the order of 2.0 m). Also, the speed of gas rising in the vertical direction is much greater than the speed of the liquid flowing across the tray deck (the vapor phase has a much lower density, and thus will have a higher space velocity). Because of these two factors, the gas phase residence time in the froth zone is much shorter than the liquid phase residence time. Due to the short residence times, it can be assumed that the gas moves through the froth in a plug flow fashion.

4.3.5 Transient Effects

This is a steady state model. There is currently not enough information available on tray dynamics to develop or evaluate a dynamic model.

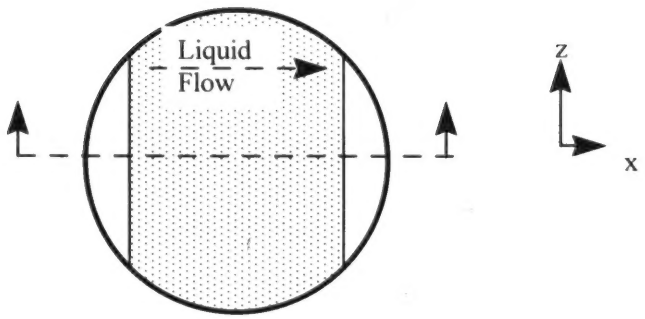

a) Top View

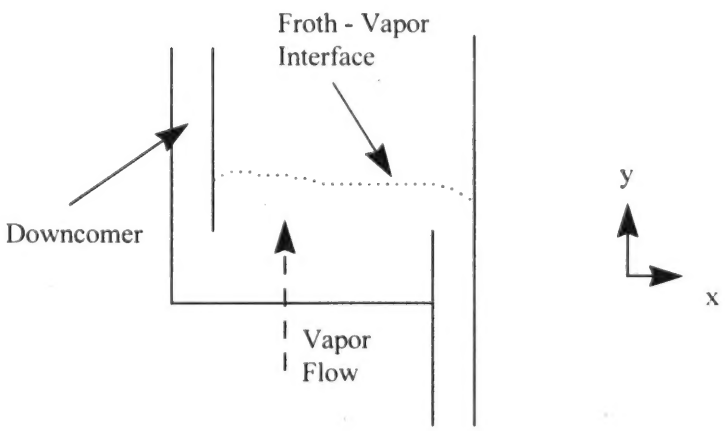

b) Section View

Figure 4.1. Schematic Diagram of a Sieve Tray

4.3.6 Mass Transfer

Interphase mass transfer is neglected and assumed to have a negliglible impact on liquid flow profiles. The modelling of this phenomenon is beyond the scope of this study. Time-dependent mass transfer equations will be used to study liquid phase residence time distributions. These equations will be used to investigate the combined convective and diffusive effects on sieve trays. The steady state velocity fields will be used with these equations.

4.4 Single Phase Transport Equations

The equations used for the single phase formulation are derived from Ishii's two-fluid formulation that is described in Section 2.2.

The phasic continuity equation, equation 2.4, reduces to:

$$\nabla \cdot \left(\alpha_L \rho_L \mathbf{v}_L \right) = 0 \qquad (4\text{-}1)$$

under the conditions of steady state and no interphase mass transfer in the domain. The phasic momentum balance equation, equation 2.6 is combined with equations 2.7 and, 2.8 to give the following equation:

$$\nabla \cdot \left(\alpha_L \rho_L \mathbf{v}_L \mathbf{v}_L \right) = -\nabla \cdot \left(\alpha_L p_L \right) + \nabla \cdot \left(\alpha_L \mu_{\text{effective,L}} \left(\nabla \mathbf{v}_L + \left(\nabla \mathbf{v}_L \right)^{tr} \right) \right) + \alpha_L \rho_L \mathbf{g} + \mathbf{M}_L \qquad (4\text{-}2)$$

where,

$$\mu_{\text{effective,L}} = \mu_L + \mu_{T,L} \qquad (4\text{-}3)$$

The definition of a liquid phase volume fraction, α_L, does not contradict the concept of a single phase model. The model is defined as single phase because the mass and momentum conservation equations are only applied to the liquid phase. The definition of a volume fraction is necessary in order to account for the presence of both gas and liquid phases.

4.5 Constitutive Relationships

Constitutive relationships are required for the interphase momentum transfer (M_L), the liquid phase volume fraction (α_L), and the turbulent viscosity ($\mu_{L,T}$). These effects will be described in the following subsections:

4.5.1 Interphase Momentum Interactions

There are two types of averaged interphase momentum interactions acting on the liquid phase. The first type is the force acting in the vertical (y) direction, parallel to the gravitational force. The second type is the force acting in the horizontal (x and z) direction, parallel to the tray deck.

The vector, $\mathbf{M}_L$, has the following form:

$$\mathbf{M}_L = \begin{bmatrix} M_{L,x} \\ M_{L,y} \\ M_{L,z} \end{bmatrix} \tag{4-4}$$

$M_{L,y}$ is the vertical component force which accounts for the liquid interaction with the rising gas. This contribution is calculated from a mean momentum balance around the froth:

$$M_{L,y} = \frac{\rho_G v_G \left(v_{G,hole} - v_G \right)}{h_f} \tag{4-5}$$

The numerator accounts for the pressure change caused by the change in gas velocity. The constants v_G and $v_{G,hole}$ are the gas phase superficial velocity and the gas phase hole velocity. The interphase momentum transfer is calculated by dividing this force equally throughout the froth.

The forces in the horizontal direction, $M_{L,x}$ and $M_{L,z}$ are evaluated with the following expressions:

$$M_{L,x} = -\rho_G v_G \left(\frac{\partial u_L}{\partial y} \right) \tag{4-6}$$

and,

$$M_{L,z} = -\rho_G v_G \left(\frac{\partial w_L}{\partial y} \right) \tag{4-7}$$

This force is based on the assumption that the rising gas accelerates to the liquid velocity in the x and z directions at all points in the froth.

4.5.2 Froth Height and Liquid Volume Fraction

As a result of the geometry assumption stated in section 4.3.3, the froth height, h_f, establishes the upper boundary of the flow domain. The height is calculated using the Colwell correlation (Equations 3-5 to 3-11). This correlation also determines the

average froth volume fraction, $\alpha_{L,avg}$. It is assumed that the liquid volume fraction does not vary with position:

$$\alpha_L(x,y,z) = \alpha_{L,avg} \tag{4-8}$$

4.5.3 Turbulent Viscosity

All of the turbulence models developed for single and two phase flow have one or more fitted parameters (see Section 2.3.2). These parameters are determined from experimental study. Even the simplest and most limited turbulence model, the Prandtl mixing length model, has a single fitted parameter, l_{mix}. For the distillation system, there is simply not enough data to correlate the required parameters.

A more limited model can be implemented in order to develop a predictive model for turbulent viscosity. In this model, a turbulent Schmidt number is defined:

$$Sc_T = \frac{\mu_{T,L}}{\rho_L De} \tag{4-9}$$

Zuiderweg has proposed equation 3.12 to predict the eddy diffusivity for spray-froth regime flows. If it is assumed that the distillation flows are highly mixed, the turbulent Schmidt number can be assumed to be equal to one. Thus, the turbulent viscosity is equal to the product of density and eddy diffusivity.

4.6 Flow Geometry and Boundary Conditions

Figure 4.2 shows a schematic diagram of the geometry used in simulation. Note that the flow domain consists of only half of the sieve tray because of the symmetry of the geometry. The outer boundaries on all sides are the walls of the column. The liquid enters through the liquid inlet boundary, and leaves the tray through the liquid exit boundary. The gas entry point is the sieve plate. The upper boundary is the froth-vapor boundary. The boundary conditions are specified below:

4.6.1 Walls

All walls and the weir are modelled as free slip walls:

$$\tau_L \cdot \mathbf{t} = 0 \tag{4-10}$$

4.6.2 Symmetry Plane

The centreline symmetry plane is defined as:

$$\frac{\partial v_{L,x}}{\partial z} = \frac{\partial v_{L,y}}{\partial z} = 0 \tag{4-11}$$

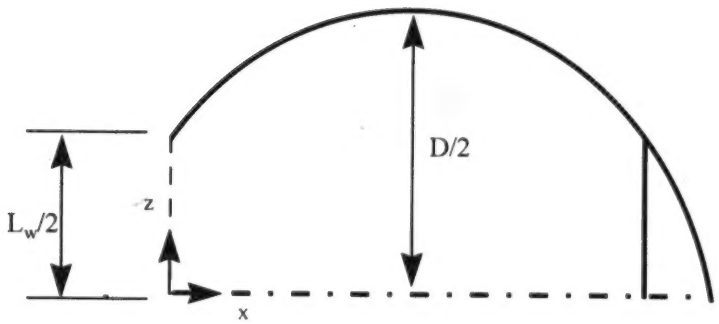

a) Top View

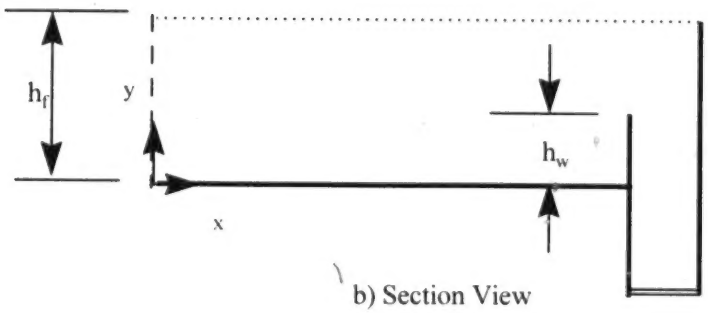

b) Section View

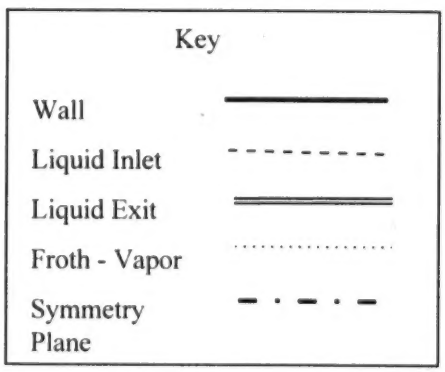

Figure 4.2. Simulation Sieve Tray Geometry

$$v_z = 0 \qquad (4\text{-}12)$$

4.6.3 Liquid Exit

The liquid exit is placed sufficiently far enough down the outlet downcomer in order to assume a fully developed flow profile. A Neumann boundary condition is applied:

$$\frac{\partial v_{L,y}}{\partial y} = K\left(\frac{v_{L,y}}{|v_L|}\right) \qquad (4\text{-}13)$$

The ratio on the right side of the equation is the unit outward normal velocity. The constant, K, is determined by closing the global continuity constraint.

4.6.4 Sieve Plate

The sieve plate is the point of gas inlet. For the liquid, the boundary is modelled as a free slip wall:

$$\tau_L \cdot t = 0 \qquad (4\text{-}14)$$

4.6.5 Liquid Inlet

The overall flow patterns on the distillation tray are sensitive to the inlet boundary conditions. Since the literature provides little quantitative guidance regarding the downcomer flow patterns, the inlet boundary conditions are developed from general observations. The simplest inlet boundary condition approximation is a uniform flow or flat inlet profile:

$$v_L\Big|_{Inlet,Flat} = \begin{bmatrix} \dfrac{Q_L}{h_f L_w} \\ 0 \\ 0 \end{bmatrix} \qquad (4\text{-}15)$$

This boundary condition is based on the assumption that the liquid will enter the tray in a uniform fashion because the flow is highly turbulent. In reality there are higher liquid fluxes near the centre of the tray and lower flows at the edges of the inlet.

A reasonable maldistributed boundary condition is a quadratic inlet flow profile:

$$\mathbf{v}_L(z)\Big|_{Inlet,Quadratic} = \begin{bmatrix} -0.75\left(\frac{Q_L}{h_f}\right)\left(\frac{L_w}{2}\right)^{-3}\left(z^2-\left(\frac{L_w}{2}\right)^2\right) \\ 0 \\ 0 \end{bmatrix} \qquad (4\text{-}16)$$

It is assumed that this quadratic profile is an "upper limit" of the degree of liquid phase flow maldistribution. The true inlet boundary condition will be somewhere between these two extremes and must be measured and characterized from experiments if the data measured downstream are to be interpreted in a meaningful manner.

4.7 Residence Time Distribution

Liquid phase maldistribution is often measured with studies of residence time distribution. In order to validate the proposed model, it is necessary to evaluate the residence time distribution. In this study, concentration profiles are tracked with the following conservation equation:

$$\frac{\partial}{\partial t}\left(\alpha_L \rho_L X_{A,L}\right) + \nabla\cdot\left(\alpha_L \rho_L \mathbf{v}_L X_{A,L}\right) = -\nabla\cdot\left(\alpha_L \rho_L De\left(\nabla\cdot X_{A,L}\right)\right) \qquad (4\text{-}17)$$

This equation uses the eddy diffusivity (De) to characterize the diffusive effects in this equation. De is calculated using Zuiderweg's froth regime correlation, Equation 3-12.

For a pulse introduction of component A at the liquid inlet, the residence time at any point can be calculated as:

$$t_R(x,y,z) = \frac{\int_0^\infty t X_{A,L}(x,y,z,t)dt}{\int_0^\infty X_{A,L}(x,y,z,t)dt} \qquad (4\text{-}18)$$

The tracer is a passive tracer subject to convection-diffusion transport, but no effective mass transfer takes place.

4.8 Conclusions

In this chapter, a unique model for the prediction of liquid flow patterns on sieve trays has been developed. The key feature of this model is that it has only a single set of conservation equations for the liquid phase. Gas phase flows are specified as part of

the model and their effects on the liquid phase motion are captured. In principle the model is similar to that developed by Porter et al. (1992). The main differences are the use of (a) three dimensionality, (b) a more realistic turbulence model, (c) more realistic boundary conditions.

Porter's model was strictly two dimensional. Flow variations in the vertical direction were largely ignored. The model presented in this chapter attempts to account for flow variation in the vertical direction. Porter's model uses the single phase k-ε model. This model does not account for the turbulence generated with liquid - vapor interactions and thus underestimates turbulent intensity. In the model presented here, the turbulence model is more realistic because it is based on experimental data. The last major improvement on Porter's model is the introduction of varying inlet boundary conditions. In Porter's model, the flow maldistributions in the downcomer are ignored. In reality, the variations in downcomer flows have a significant impact on the overall flow patterns on the active area of the sieve tray.

5. Results and Discussion

5.1 Introduction

In this chapter, the proposed model for predicting the liquid flow distribution on sieve trays is evaluated. We will establish both the accuracy and applicability of the model. An additional objective of this chapter is to provide insight and guidance into future experimental techniques used to generate data.

In the previous chapters it was stated that one of the problems facing the development of complete hydraulic models was the lack of adequate fundamental information. The reason for this is that there is great difficulty in obtaining good experimental data. These problems with model development also pose problems with model validation. The data sets used to evaluate models are not always highly accurate. One needs to use judgment in evaluating the quality of the experimental design. In some cases, the data may be meaningless or impossible to interpret because of the limitations in the experimental design. An example would be a case where velocity and residence time distribution over the tray are measured with great care but only mean quantities of liquid and vapor flow are measured.

5.2 Velocity Profiles

5.2.1 Data Sets

The most direct method of evaluating the single phase model is to compare the results with measured velocity profiles. Solari and Bell (1986) provides the best available source of experimental data for an industrial sized distillation tray. (All future references to this publication in the text of this thesis will be abbreviated as: SB-86) The authors measured liquid velocities at four different operating conditions. Velocity profiles were measured at two locations: a) near the center of the 1.22 m. diameter tray and b) closer to the outlet downcomer. The measured velocities are the u or primary flow component velocities. The schematic diagram, Figure 5.1, describes the location of velocity measurements. The technique used to measure the velocities is described in Chapter 3.

Solari et al. (1982) is used as an additional source of velocity data. (All future references to this publication in the text of this thesis will be abbreviated as: SSDB-82) In this experimental work, the velocity profiles at the tray center are measured for several operating conditions. The location of measurements are described in Figure 5.2. As discussed in Section 3.5, the quality of data is low. However, this study does provide useful qualitative information about the overall shape of the flow pattern.

The operating conditions on the sieve tray are characterized using three parameters: F_S , Q_L, and F_{lv}. F_S (or F-factor) is a parameter that describes the vapor loading. It is defined as the square root of vapor phase kinetic energy. Q_L is the volumetric flow

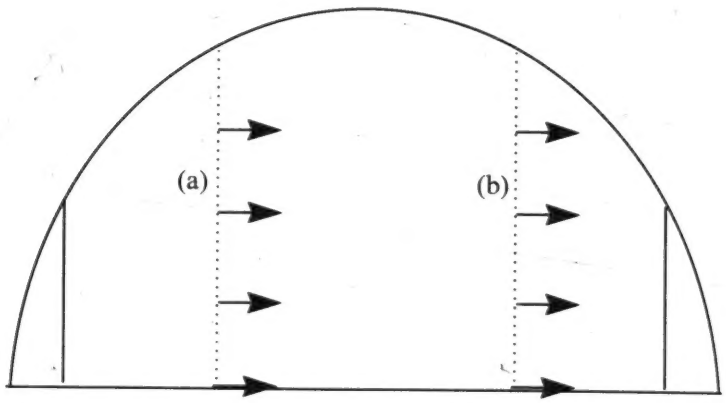

z
W - Component Velocity

x
U - Component Velocity

Notes:

Tray Diameter = 1.213 m

Weir Length = 0.925 m

Upsteam Velocity Profiles are U - Component Velocities (measured along Line a):

0.324 m from the inlet downcomer

Downstream Velocity Profiles are U - Component Velocities (measured along Line b):

0.210 m from the outlet downcomer

Figure 5.1. Location of Velocity Measurements - Solari and Bell, 1986.

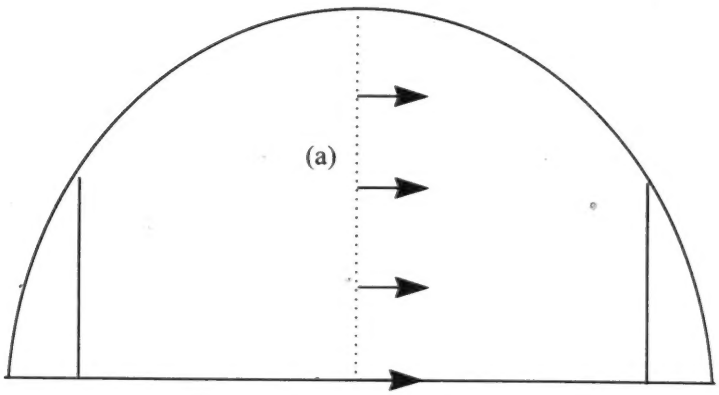

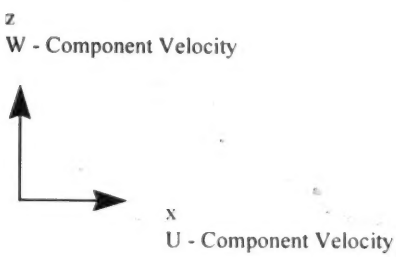

Notes:

Tray Diameter = 1.25m

Weir Length = 0.726 m

Velocity Profiles are U - Component Velocities

measured along Line a : (the tray center)

Figure 5.2. Location of Velocity Measurements - Solari et al., 1982.

rate of liquid. F_{lv} (or flow parameter) is defined as the ratio of liquid to vapor loadings and densities. Usually F_{lv} is used as an indication of pressure because the density of vapor (which is proportional to pressure under ideal conditions) varies to a much larger degree than the ratio of liquid to vapor loading (L/G). Recall that both of the data sets, SB-86 and SSDB-82, are based on an air-water system at 1 atm. pressure. Because the data were collected at these conditions, F_{lv} can be used as a comparison of liquid to vapor loadings ($F_{lv} \alpha$ L/G).

Information regarding the data sets used for model evaluation is summarized in Table 5.1.

5.2.2 Results

The liquid phase model was used to predict the flow patterns for each of the cases listed in Table 5.1.

Data set SB-86 was used for quantitative evaluation of liquid velocities. Results were generated for both of the liquid inlet boundary conditions that were described in Chapter 4: flat and quadratic. The results are tabulated in Table 5.2.

Graphical comparisons of the model with experimental results are also performed. The centerline and downstream velocity profiles for case B1 are compared in Figures 5.3 and 5.4. Similarly, Figures 5.5 and 5.6 compare results from case B2. Figures 5.7 and 5.8 compare results from case B3. Figures 5.9 and 5.10 compare results from case B4. Figure 5.11 shows the predicted centerline velocity profile for case A10. The predictions for case A12, A15, and A17 are shown in Figure 5.12, 5.13, and 5.14, respectively. The velocities reported in Figures 5.3 to 5.10 are the mean u velocities in the y direction.

The predicted flow patterns can be visualized with vector plots. Figures 5.15 and 5.16 show the top and side view predictions for case B2. Figures 5.17 and 5.18 show the top view predictions for cases B3 and A12, respectively.

The flow patterns can also be visualized in a graphical format. For case B2, detailed velocity profiles in three dimensions were extracted. Figure 5.19 shows the variation of the u component velocity in the z direction. Figure 5.20 shows the variation of u component velocities in the y (vertical) direction. Figure 5.21 shows the variation of v component velocities with respect to z. Figure 5.22 shows the variation of w component velocities with respect to z.

Velocity profiles are also presented for case B3. Figure 5.23 shows the variation in u component velocities with respect to z.

Table 5.1. Summary of Data Sets

Case	Operating Conditions	Sieve Tray	Data Set
A10	F_s = 0.649 Q_L= 1.577E-2 m^3/s	d = 1.25 m L_w = 0.726 m h_w = 0.10 m	SSDB-82
A12	F_s = 0.410 Q_L = 1.64E-2 m^3/s	d = 1.25 m L_w = 0.726 m h_w = 0.05 m	SSDB-82
A15	F_s = 0.910 Q_L = 1.64E-2 m^3/s	d = 1.25 m L_w = 0.726 m h_w = 0.05 m	SSDB-82
A17	F_s = 0.910 Q_L = 1.104E-2 m^3/s	d = 1.25 m L_w = 0.726 m h_w = 0.05 m	SSDB-82
B1	F_s = 1.015 Q_L = 6.94E-3 m^3/s	d = 1.213 m L_w = 0.925 m h_w = 0.05 m	SB-86
B2	F_s = 1.464 Q_L = 6.94E-3 m^3/s	d = 1.213 m L_w = 0.925 m h_w = 0.05 m	SB-86
B3	F_s = 0.462 Q_L = 1.78E-2 m^3/s	d = 1.213 m L_w = 0.925 m h_w = 0.05 m	SB-86
B4	F_s = 0.801 Q_L = 1.78E-2 m^3/s	d = 1.213 m L_w = 0.925 m h_w = 0.05 m	SB-86

Table 5.2. Standard Error of Model Predictions

Case	Operating Conditions	Standard Error - Flat Inlet Boundary *		Standard Error - Quadratic Inlet Boundary *	
		(m/s)	(percent)	(m/s)	(percent)
B1	F_s = 1.015 Q_L = 6.94E-3 m^3/s F_{lv} = 0.25	0.05030	25.6	0.05034	25.8
B2	F_s = 1.464 Q_L = 6.94E-3 m^3/s F_{lv} = 0.17	0.0268	10.9	0.0647	26.3
B3	F_s = 0.462 Q_L = 1.78E-2 m^3/s F_{lv} = 1.39	0.2189	83.5	0.1430	54.5
B4	F_s = 0.801 Q_L = 1.78E-2 m^3/s F_{lv} = 0.80	0.1024	32.8	0.0818	26.2

* Standard Error defined in Appendix III

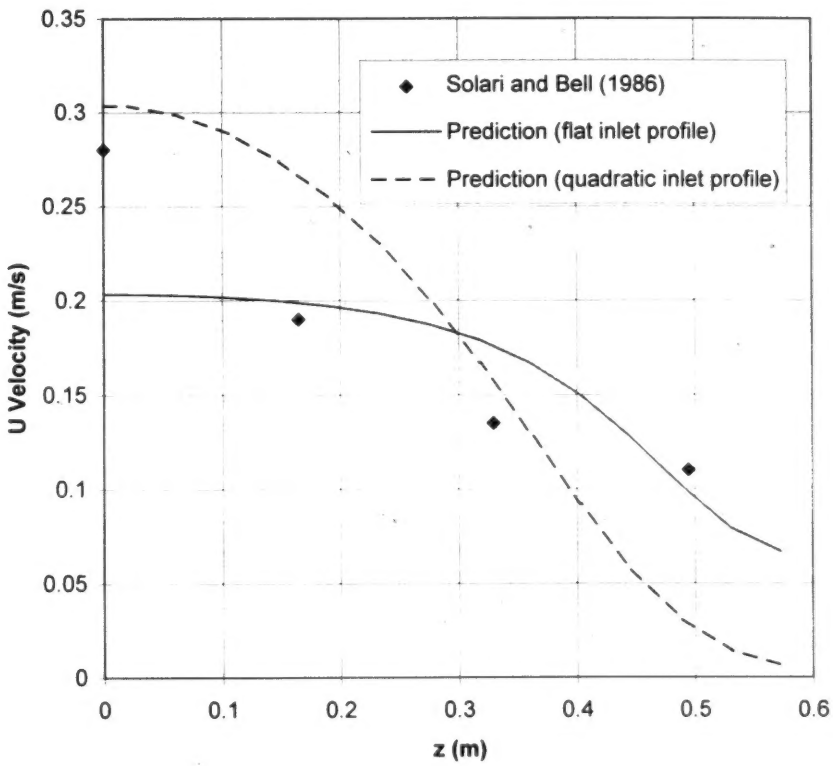

Figure 5.3. Centerline U Velocity Versus Radial Position - Case B1

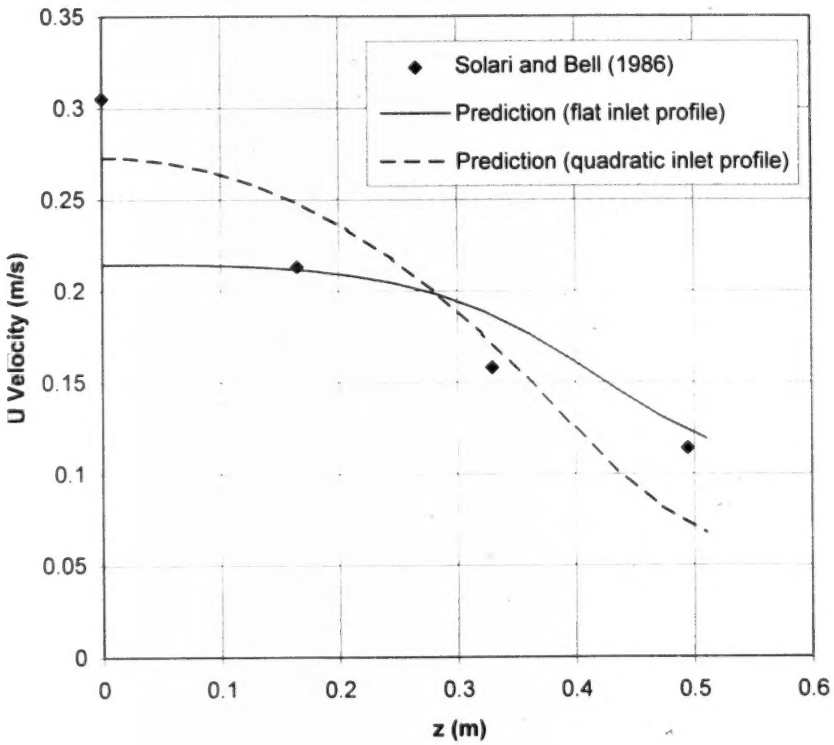

Figure 5.4. Downstream U Velocity Versus Radial Position - Case B1

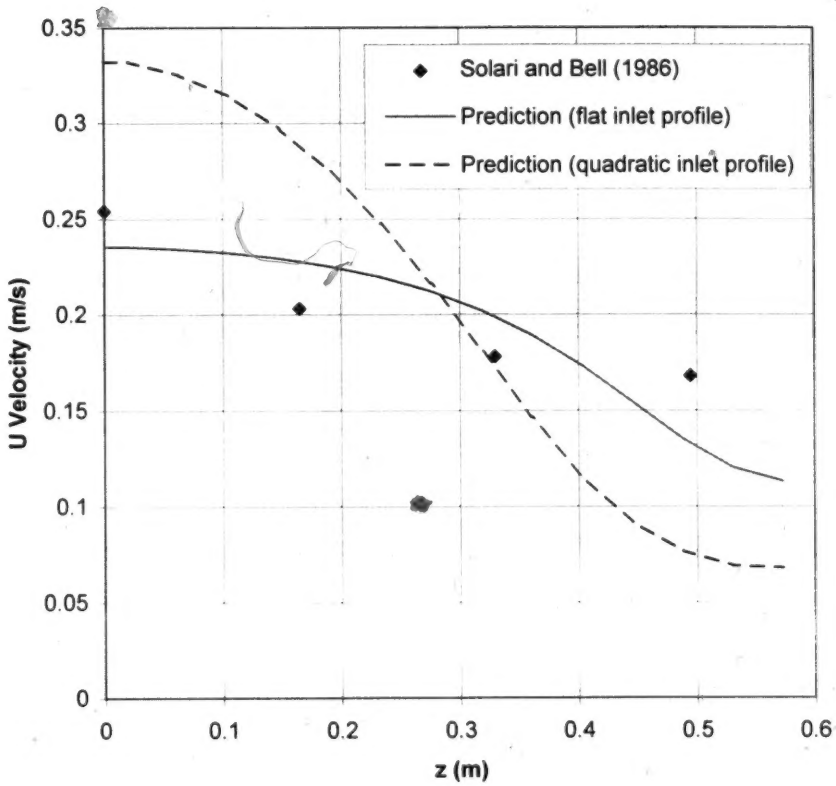

Figure 5.5 Centerline U Velocity Versus Radial Position - Case B2

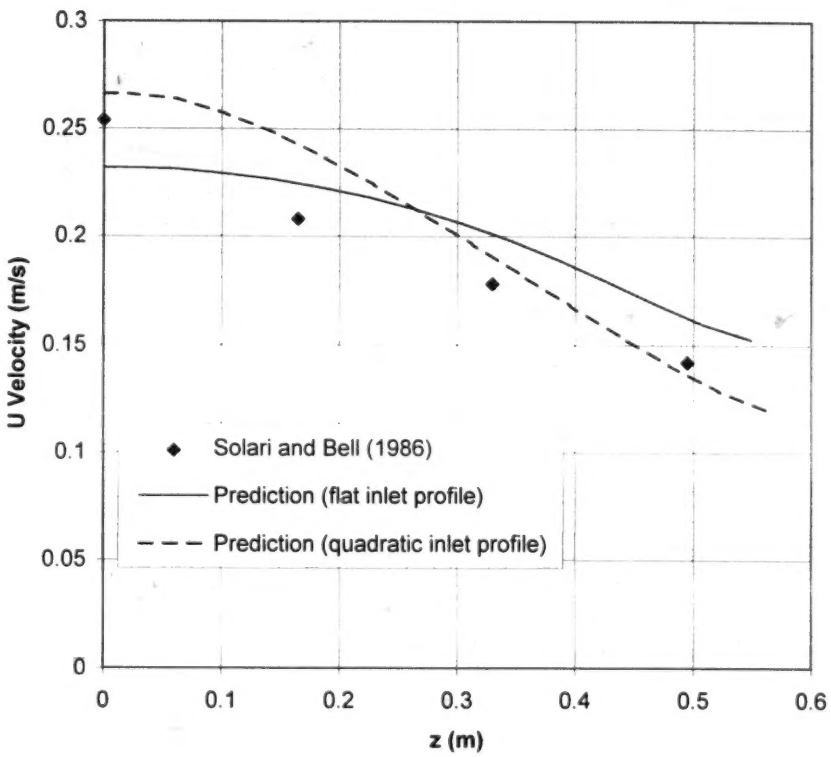

Figure 5.6. Downstream U Velocity Versus Radial Position- Case B2

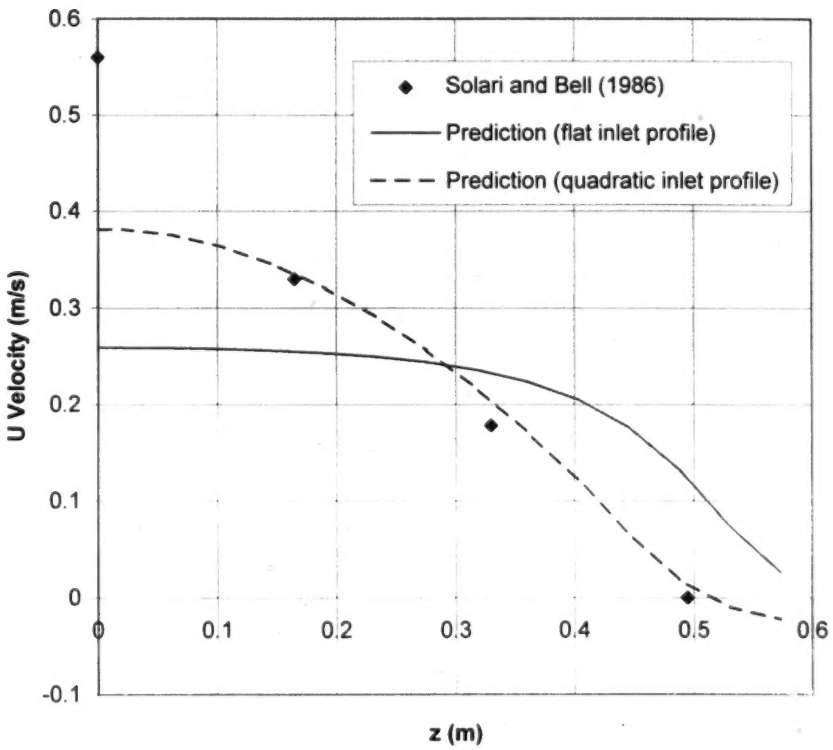

Figure 5.7. Centerline U Velocity Versus Radial Position - Case B3

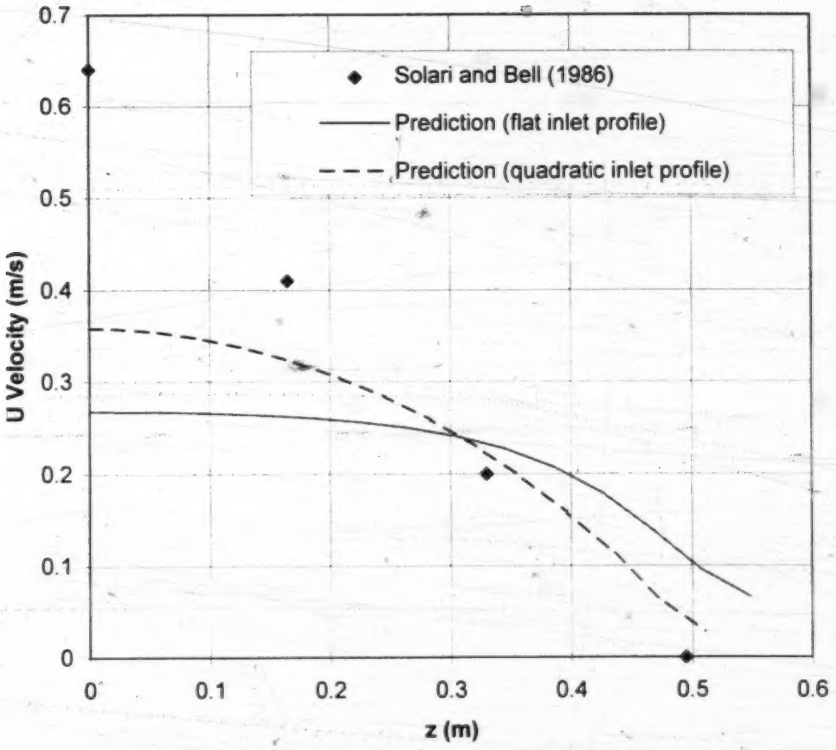

Figure 5.8. Downstream U Velocity Versus Radial Position - Case B3

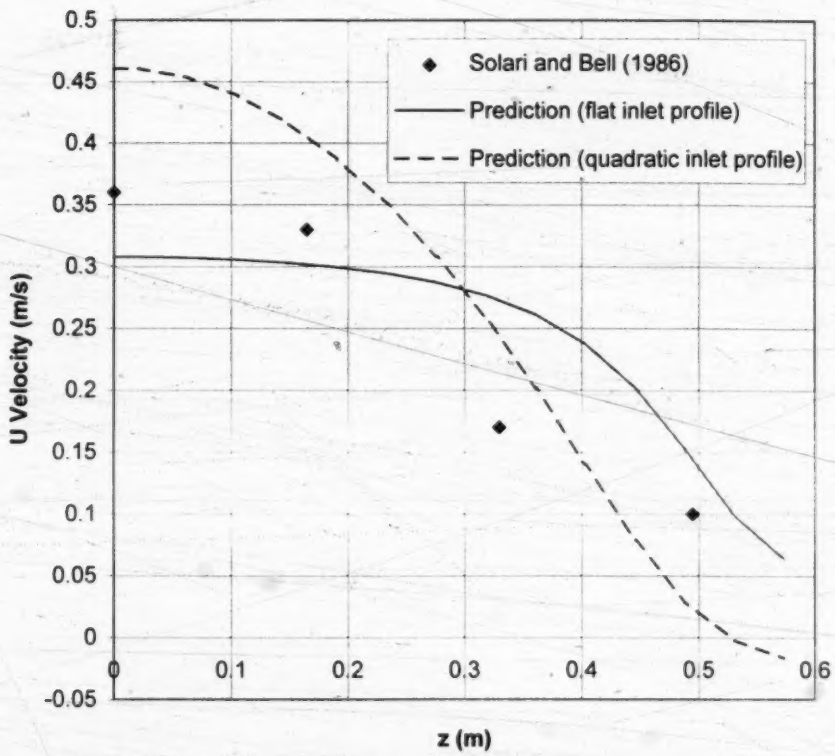

Figure 5.9. Centerline U Velocity Versus Position - Case B4

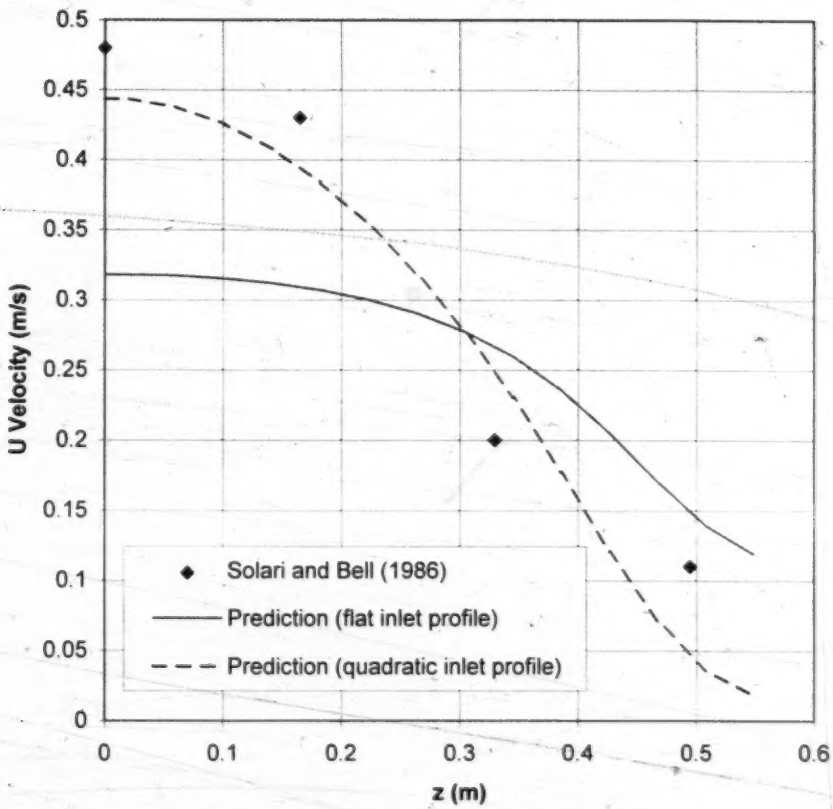

Figure 5.10. Downstream U Velocity Versus Position - Case B4

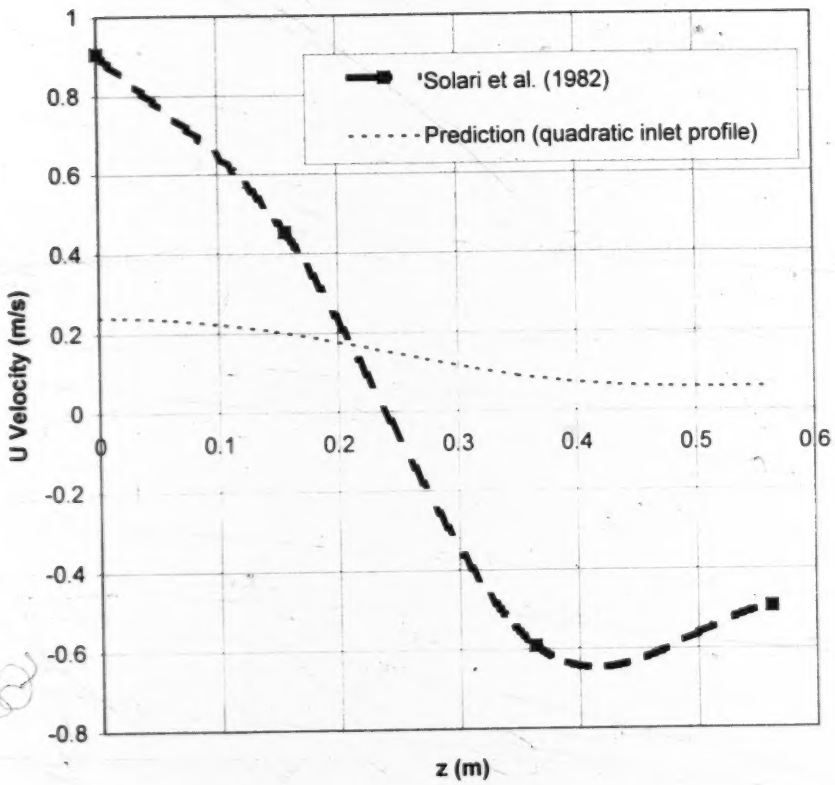

Figure 5.11. Centerline U Velocity Versus Position - Case A10

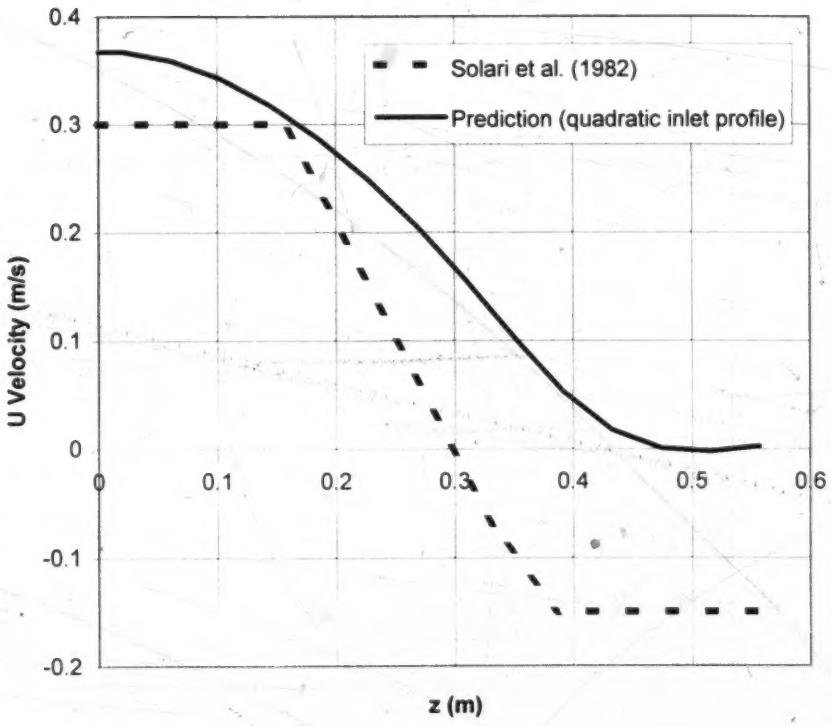

Figure 5.12. Centreline U Velocity Versus Radial Position - Case A12

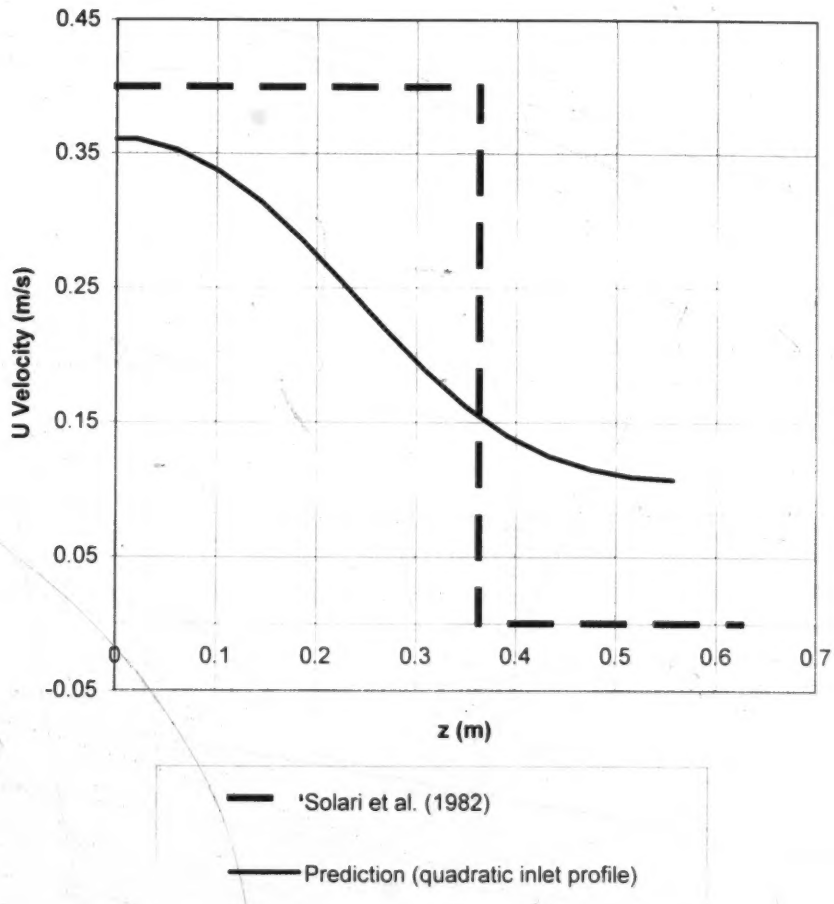

Figure 5.13. Centerline U Velocity Versus Radial Position - Case A15

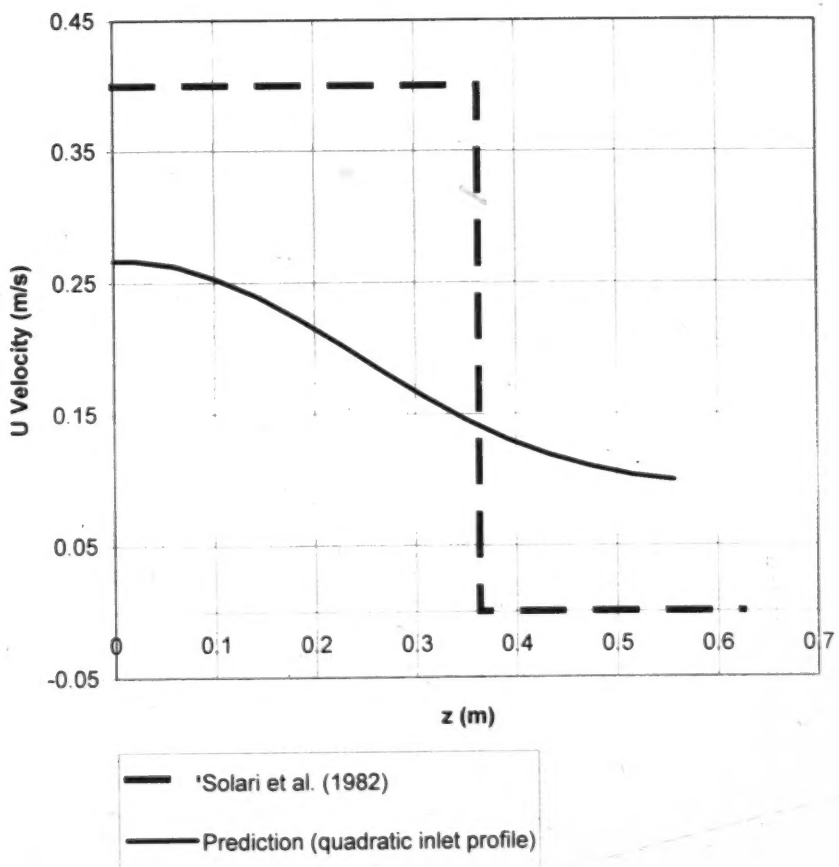

Figure 5.14. Centerline U Velocity Versus Radial Position - Case A17

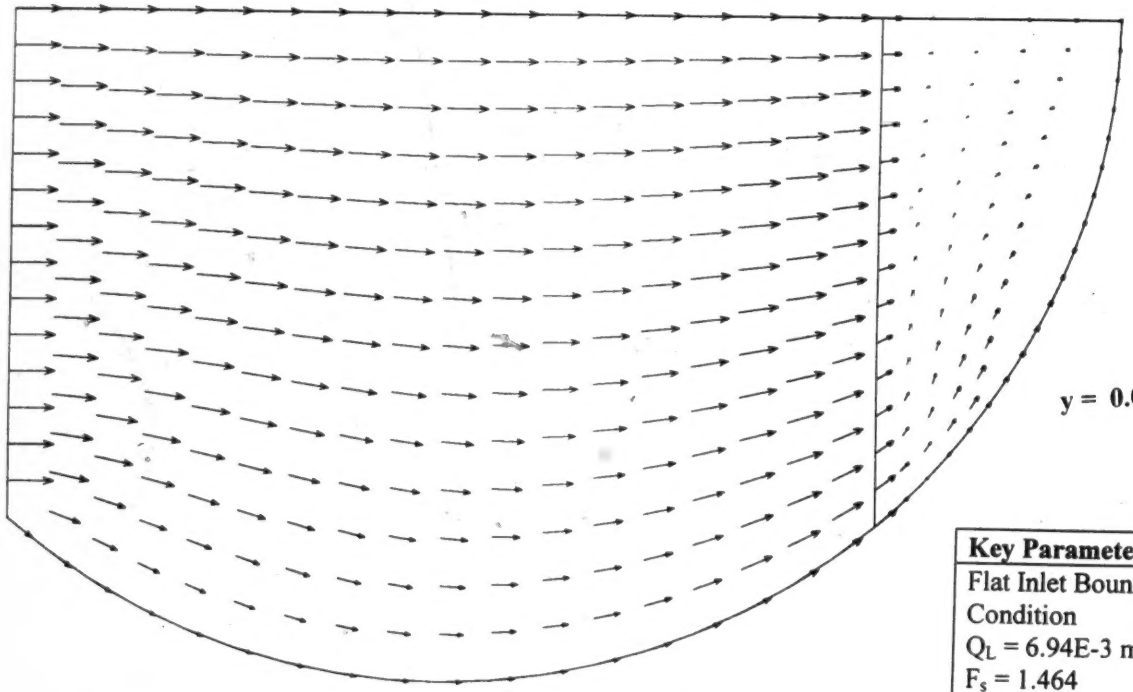
y = 0.06 m
Key Parameters
Flat Inlet Boundary Condition
Q_L = 6.94E-3 m^3/s
F_s = 1.464
d = 1.213 m
L_w = 0.925 m
h_w = 0.05 m
Scale: 1.0 m in Geometry = 5.86 m/s

Figure 5.15. Top View of the Liquid Phase Flow Pattern - Case B2

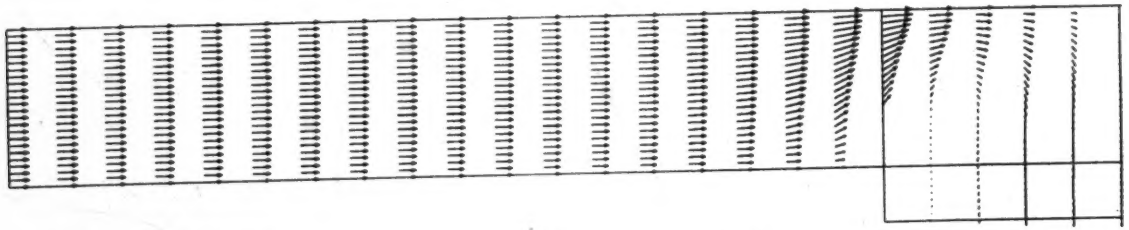

z = 0 m

Key Parameters
Flat Inlet Boundary Condition
Q_L = 6.94E-3 m^3/s
F_s = 1.464
d = 1.213 m
L_w = 0.925 m
h_w = 0.05 m

Scale: 1.0 m in Geometry = 13.5 m/s

Figure 5.16. Side View of the Liquid Phase Flow Pattern - Case B2

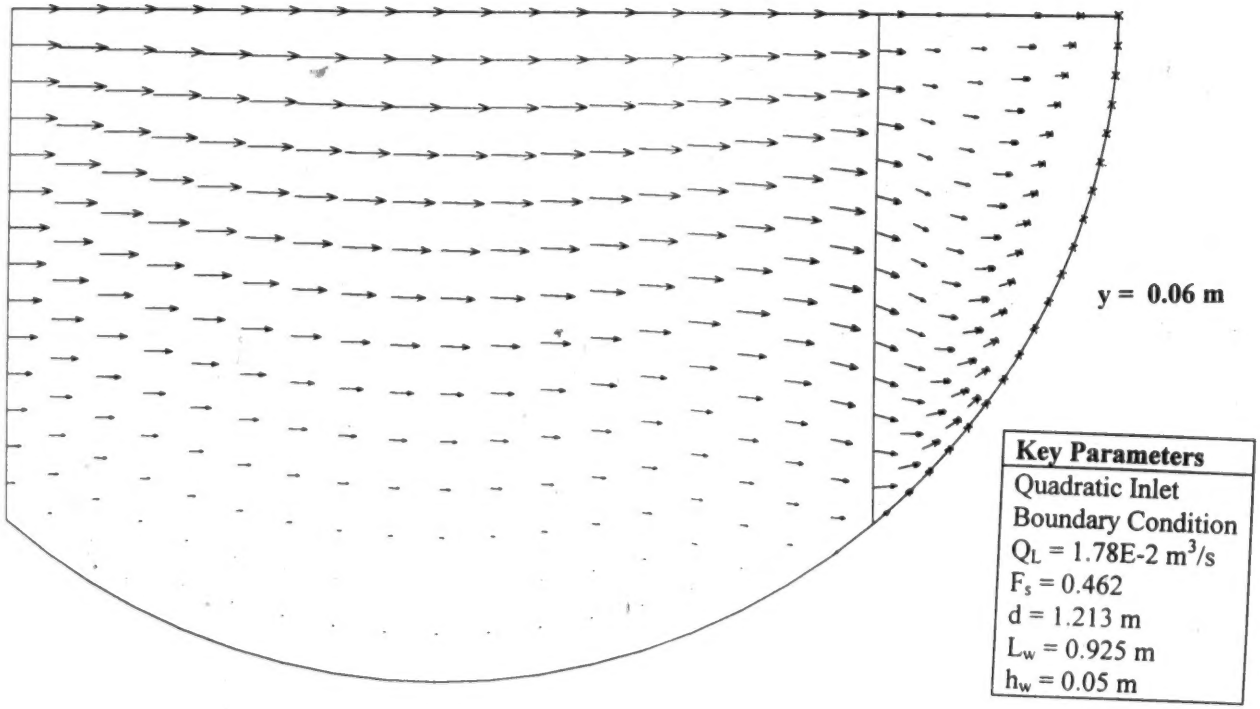

Figure 5.17. Top View of the Liquid Phase Flow Pattern - Case B3

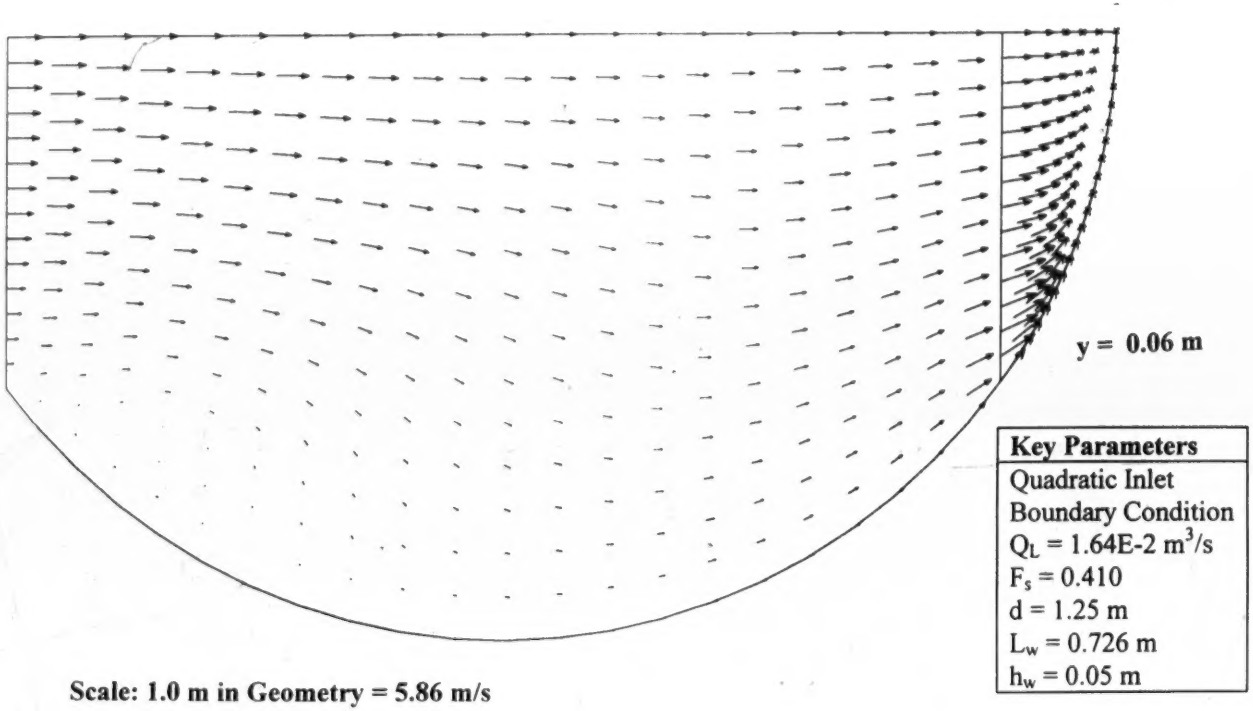

Figure 5.18. Top View of the Liquid Phase Flow Pattern - Case A12

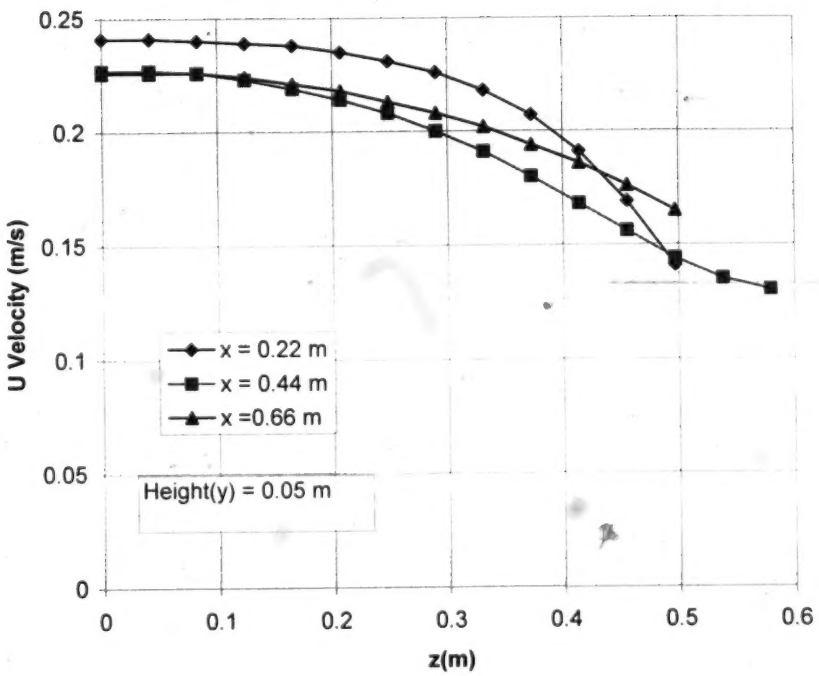

Figure 5.19. U Velocity Versus Radial Position (Z) - Case B2

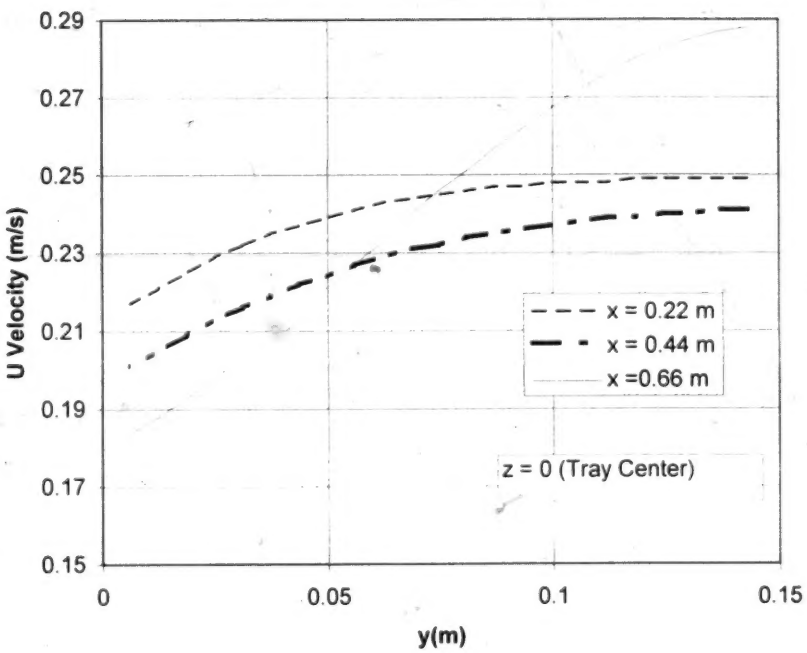

Figure 5.20. U Velocity Versus Height (y) - Case B2

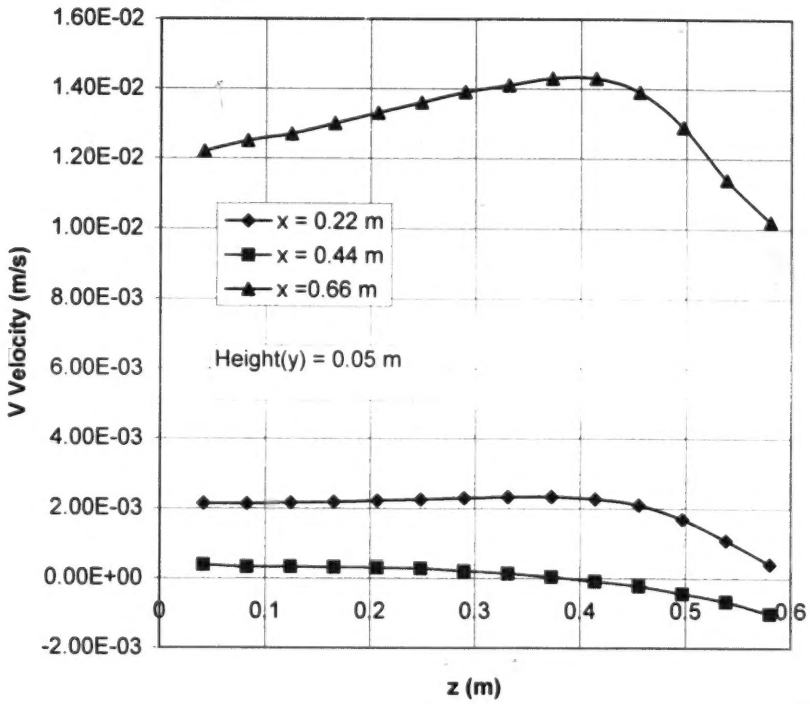

Figure 5.21. V Velocity Versus Radial Position (z) - Case B2

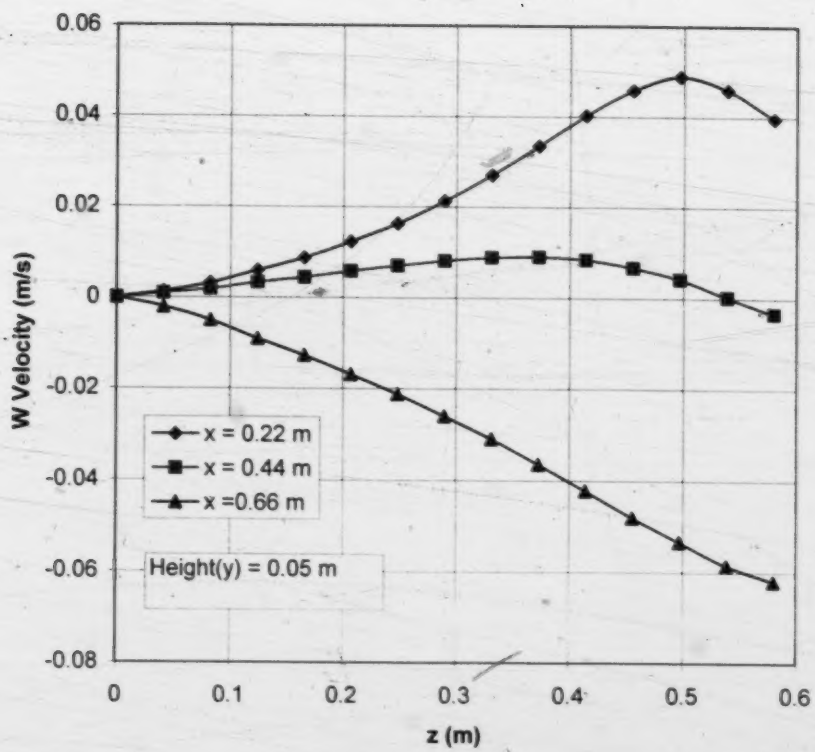

Figure 5.22. W Velocity Versus Radial Position (Z) - Case B2

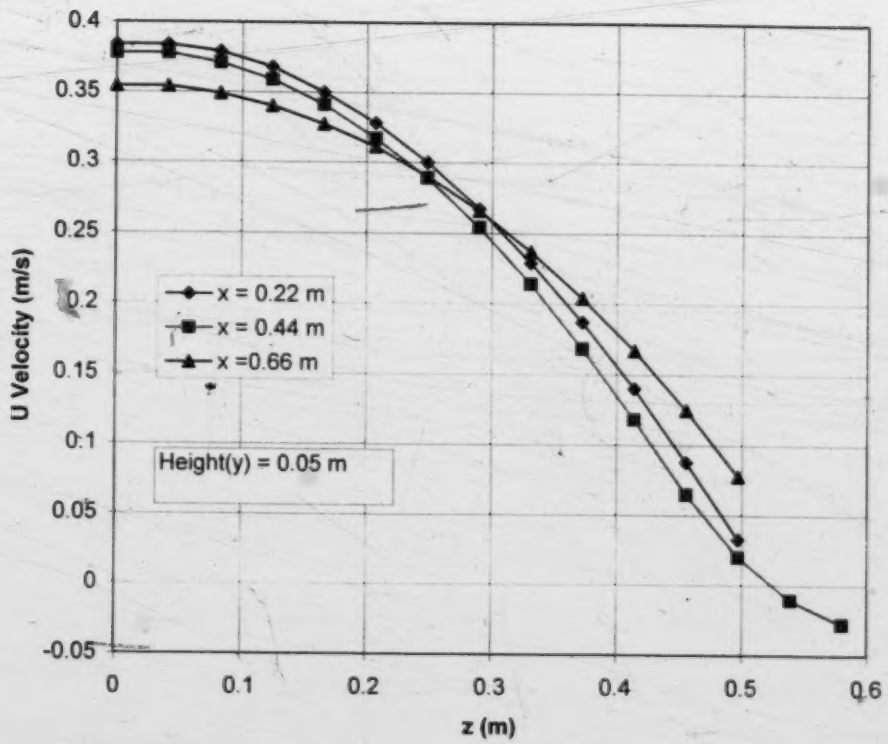

Figure 5.23. U Velocity Versus Radial Position(z) - Case B3

5.2.3 Evaluation of Model Performance

Overall, the model shows very good agreement with experimental results.

As indicated in Table 5.2, the best agreement with the experimental results occur with case B2 - flat inlet profile (see Figures 5.5 and 5.6). The standard prediction error is only 10.9%. This is excellent agreement considering that the data has errors in the order of 10%.

For case B1, the agreement with experiments are virtually the same for either boundary condition (see Table 5.2, Figure 5.3, Figure 5.4). Both the flat and quadratic cases have errors of approximately 26%. As mentioned in Section 4.6.5, the inlet boundary conditions are approximations. The operating conditions for case B1 are likely at the transition point between the two extremes for inlet flow. This will be discussed in greater detail in Section 5.2.4.

For cases B3 and B4, the quadratic inlet profile has more agreement with experimental results. This would suggest that at higher ratios of liquid to vapor loadings (high F_{lv}), the quadratic inlet profile is more valid. Note that B3 has the highest prediction error of any of the 4 cases studied in SB-86. The reasons for this will be discussed in Section 5.2.6.

Overall, the model has performed well in predicting liquid flows on sieve trays. It must be noted that the constitutive relationships have been developed from empirical correlations that were never intended for this modelling purpose. It is also important to note that this model is purely predictive; the data sets used for model evaluation are not used for model development in any way. The only variable parameter in the model is the choice of liquid inlet boundary condition.

5.2.4 Liquid Inlet Boundary Conditions

Figures 5.3 to 5.10 clearly show that the predicted flow patterns are highly sensitive to variations in inlet boundary conditions. The nature of mathematical modelling is such that the equations governing the phenomena must be solved over a domain of interest by isolating the domain from the surrounding through the proper choice of boundary conditions. The model is not complete unless the conditions on the boundary are specified. Unfortunately, experimentalists who go to great extent in measuring detailed profiles in the domain often fail to characterize the conditions on the boundary. Without such characterization of boundary data, the data in the interior are of questionable value. We are faced precisely with this problem in the distillation literature. Hence we have chosen to use the effect of inlet flow condition as a parameter and study its effect on the prediction of the interior flow.

The literature survey provided only qualitative guidance regarding the nature of downcomer flow. The flow out of the downcomer onto the sieve tray is a function of the tray geometry, the system physical properties, and the operating conditions. These three variables will affect how the froth flows over the weir into the downcomer, how

the gas disengages from the liquid, how long the liquid spends in the downcomer (residence time), and ultimately how liquid flows onto the sieve tray below.

When selecting an inlet boundary condition, there is a great deal of flexibility. The only constraint on any proposed boundary condition is mass balance closure:

$$Q_L = \iint_{\text{Inlet}} u(y,z)dydz$$

There are an infinite number of different boundary conditions that can satisfy this constraint. Because there is insufficient and inadequate data, the proposed model uses both flat and quadratic inlet boundary conditions as approximations for the actual inlet boundary conditions. The justification for these selections were presented in Section 4.6.5.

The flat inlet boundary is clearly the best boundary condition for case B2. This case is characterized by low liquid flows and higher vapor flows. The liquid will spend more time in the downcomer and thus enters the tray in a more even fashion. Furthermore, the higher vapor flows will result in more even liquid phase flows on the sieve tray. This even flow will result in more even downcomer flows and a more flattened inlet flow profile on the downstream tray.

Comparison of results for cases B3 and B4 (Table 5.2 and Figures 5.7 to 5.10) shows that the quadratic boundary condition is most appropriate. The higher liquid flows and lower vapor flows result in more maldistributed flows through the downcomer. As stated earlier, either boundary condition is acceptable for case B1.

The flow parameter is a useful parameter providing the ratio of liquid and vapor loadings. A low F_{lv} as in case B2 indicates a relatively low liquid loading and a relatively high vapor loading. These operating conditions are best modelled with a flat inlet boundary condition. In contrast, a high F_{lv}, as in case B3 and B4 are best modelled with quadratic boundary conditions. Since either boundary condition performed well in case B1, the transition point is likely near these operating conditions.

Based on cases B1 to B4, quadratic inlet boundary conditions will be most appropriate at flow parameters greater than 0.25. Flat inlet profiles can be applied at lower flow parameters. Caution must be applied when using this criterion. Further study will be required in order to establish the boundary conditions more definitively.

It has been demonstrated by simulation that the tray flow patterns are highly sensitive to inlet boundary conditions. Future experimentalists must be aware of this and they must characterize the phenomenon at the downcomer more rigorously. If the boundary flows are characterized, the internal flows can be predicted with more confidence.

5.2.5 Prediction of Flow Patterns

The single phase model can make predictions that will help us develop insights into the physics of sieve tray flow.

It is useful to study the overall flow patterns with vector plots. Figure 5.15 shows the top view flow patterns for case B2. Note that the overall flow pattern is fairly balanced. This contrasts significantly with case B3 (see Figure 5.17) The predicted flow pattern has a large stagnancy zone because most of the flow channels near the center of the tray. The channeling and resulting stagnancy zone will likely cause a significant reduction in tray efficiency.

We can also compare the flow patterns by studying the u velocity profiles in Figures 5.19 and 5.23. The flow patterns are very different in these two cases. For case B2 (Figure 5.19), there is a significant liquid phase flow across the entire tray cross-section. There are no large stagnant flow regions. This again contrasts with case B3 (Figure 5.23), where there is a stagnant region at the edges of the tray.

We can also gain insights into the physics of flow by studying the variations in the other component velocities with respect to position.

Figure 5.22 shows the variation of w component velocities in the z direction for case B2. Note that the w velocities deviate from zero as we move away from the tray center. The liquid sweeps outward towards the wall near the inlet downcomer and then sweeps back inward as the flow approaches the outlet downcomer.

The non-fundamental sieve tray models, such as SRM (Porter et al. 1972), have assumed that the liquid flows in the z direction are zero at all points in the tray. The simulations have shown that these velocities are not insignificant. With the available experimental techniques, z component velocities are extremely difficult to measure. The development of more advanced experimental methods would allow us to measure these flows.

One of the most common assumptions used in distillation tray analysis is that the velocity variations in the y direction are negligible. Even in Porter's fundamental model (1992), the simulations were conducted in two dimensions. The single phase model presented in this work can predict variations in the third dimension. Figures 5.16 and 5.20 shows the variation in u component velocities with respect to height (y) at the tray center.

For most of the active region of the tray, this two dimensional assumption is acceptable. From Figure 5.20, it can be seen that the variation of u velocity with position is relatively small. At x = 0.22m and x = 0.44 m, the velocity near the sieve tray (y = 0) is 85% of the velocity at the froth surface. Near the bottom of the tray, the rising gas has a dampening effect on the liquid. As the flow moves closer to the outlet downcomer, the vertical variations become much more significant. The flow

near the sieve tray drops to only 62% of the velocity at the froth surface. The effect of geometry, such as the weir, has a significant impact on the predicted flow.

Figure 5.21 shows the spatial variations of the v component velocity. Note that the predicted velocities are about an order of magnitude smaller than the w component velocities and two orders of magnitude smaller than the u component velocities. It is important to remember that these reported velocities are both volume and time averaged. The instantaneous effects are averaged out and only the net flow is predicted. Thus the predicted velocities in the active area of the tray (x = 0.22 m and 0.44 m) are very small - there is almost no net flow in the vertical direction. Near the outlet downcomer, there is an increase of flow in the vertical direction as the liquid motion is affected by the weir.

It is imperative that the next generation of experimentalists develop more sophisticated measurement techniques to confirm the phenomena that are predicted in these models. The flow of liquid on sieve trays appears to be much more complex than what the existing models have assumed. These complex flow patterns will contribute to bulk phenomenon such as tray efficiency.

5.2.6 Prediction of Recirculation and Large Flow Maldistributions

As discussed in the Section 5.2.1, data set SSDB-82 is used for qualitative comparisons. Because of the accuracy of their experimental techniques, the authors do not report detailed velocity profiles. Velocity profiles are reported in the form of simplified step or ramp functions. The purpose of using SSDB-82 is to determine how well the model predicts the overall flow patterns for an alternative geometry. The tray diameter used in SSDB-82 is approximately the same size as that for SB-86, but the weir length is 27% shorter. Thus the flow path is longer and the proportion of the tray area that is not in the direct flow path is larger.

Cases A15 and A17 were selected for study in order to confirm whether the model can predict "U-Shaped" flow patterns, similar to those in SB-86, for a different tray geometry. For these cases Solari et al. report fairly constant velocities in the tray center and essentially stagnant flow at the sides of the tray. From this data we can infer that the flow pattern is actually "U-Shaped".

Figures 5.13 and 5.14 compare the data with simulations for these two cases. The model does predict the flow pattern and it also predicts velocities within the same order of magnitude as the experimental findings.

Case A12 was selected for study because a recirculating flow pattern was observed. This flow pattern is characterized by reverse flows of liquid near the outer walls of the tray. The shape of the flow pattern is reported to be a ramp type function. Figures 5.12 and 5.18 show that although the predicted velocities are of the same order of magnitude as the experimental results, the recirculating flow pattern is not captured. Instead the model predicts a "U-Shaped" flow pattern.

In order to understand the reasons why the recirculating flow pattern is not predicted in case A12, it is useful to revisit our observations for case B3.

Case B3 has the highest prediction error of all the cases studied in SB-86. Cases B1, B2, and B4 all have errors of 26.3% or less; case B3 has an error of 54.5%. Figures 5.7 and 5.8 show that most of the error is concentrated at the tray center (x = 0 m). The model under-predicts the tray center u velocities by nearly 50%. Not only is the degree of maldistribution much greater than predicted by simulation, but it is also much greater than the other case with the same liquid loading (B4). The average tray center velocity for case B3 is 30% higher than that for case B4.

A fundamental assumption in the development of the model is that the vapor flows through the active area of the sieve tray are uniform. Based on this assumption, the liquid phase volume fraction and the turbulent viscosity are assumed invariant with position. At relatively high gas flow rates this assumption is most valid. As gas flow rates decrease, it has been observed that this uniform bubbling assumption is less valid (Lockett 1986).

In SSDB-82 it was observed that at lower gas flow rates, there is preferential bubbling through the sides of the tray. In contrast, Chuang (1996) has observed the opposite effect. He has observed that gas primarily channels through the tray center and there is reduced bubbling in the stagnant zone. Chuang's observations are more consistent with the principles of fluid dynamics. If the column is viewed as a large pipe, one would intuitively expect the highest vapor velocities at the tray center.

The positional variance in vapor flow will also result in positional variation in volume fractions and turbulent viscosity. These variations will contribute to the flow maldistributions that are not captured in the model. The next generation of modelling attempts should include the dynamics of the vapor phase and hence should be able to predict spatial variations in these. However lack of experimental data takes away the impetus for carrying out such a detailed simulation. At the current lower level of modelling such data can be used as inputs.

This breakdown of the assumption of uniform bubbling may also be a reasonable explanation for the results of case A12 (see Figure 5.12 and 5.18). In this case the recirculation pattern was not captured by the model. Both cases have F-factors (F_S) less than 0.5. The only major difference between the two cases is the ratio of weir length to column diameter. Case A12 has a lower ratio and thus a larger portion of the tray is outside of the direct flow path of the liquid. Under the same operating conditions, the large flow maldistribution manifests itself as recirculating flow. Because it is assumed that the vapor flow is uniform, the recirculation pattern is not captured.

Although these results indicate that the model may have difficulty in predicting the recirculation phenomenon, there is insufficient evidence to state that the model is unable to predict it altogether. Further experimental work will be required in order to

understand the complex effects of vapor phase hydraulics and to define the limitations of the model.

5.2.7 Prediction of Flow with High Weir Heights

Case A17 was selected for simulation because recirculation was observed and the weir height in this case is 0.10 m. All other cases that have been studied have used 0.05 m weirs. Figure 5.11 compares the model with experimental results. In this case, the predicted velocities are almost an order of magnitude less than experimental, and the large recirculation is not predicted. Both the Colwell and Zuiderweg constitutive relationships have lower accuracy at higher weir heights. The prediction error from these correlations are the most likely cause for the poor flow predictions. If the experimentalist had measured the vapor holdup and turbulence intensities, they could not only be used to tune correlations such as Colwell and Zuiderweg, but they could also be used directly in detailed simulation in order to get better predictions of the flow field.

5.3 Residence Time Distribution

5.3.1 Data Sets

Most of the literature reporting liquid flow and mixing on distillation tray present the experimental data in the form of residence time distributions in the liquid phase by introducing a tracer in that phase. The reason for this is that the experimental method is simple, accurate, and repeatable. (Bell 1972, Solari and Bell 1986). Data have been collected for several tray geometries and chemical systems.

The equipment used to determine residence time on sieve trays are essentially the same as the apparatus used for SB-86. Fluorescent dye is injected at a single point in the inlet downcomer. An array of detectors on the tray are used to measure the dye signal over time. Mean residence times are calculated from the time varying dye signal.

Unfortunately, the authors of the above research probably did not imagine that their work would be used to evaluate models such as the one presented in this thesis. The data were not collected in a fashion that will allow for detailed quantitative analysis. From the residence time distribution plots, it is clear that that the dye spends several seconds in the downcomer prior to entering the tray. During this time, the dye will be dispersed. Dye will enter the tray over a large area and as a dispersed wave. Thus the dye does not enter the active region on the tray as a simple mathematical function (pulse, square wave, step, etc.) that can be easily modelled. Instead the dye enters as an unknown complex distribution function.

Figure 5.24 shows a typical residence time distribution plot that was reported in SB-86. The operating conditions for this case are: Q_l = 6.94E-2 m^3/s , F_s = 1.105. The

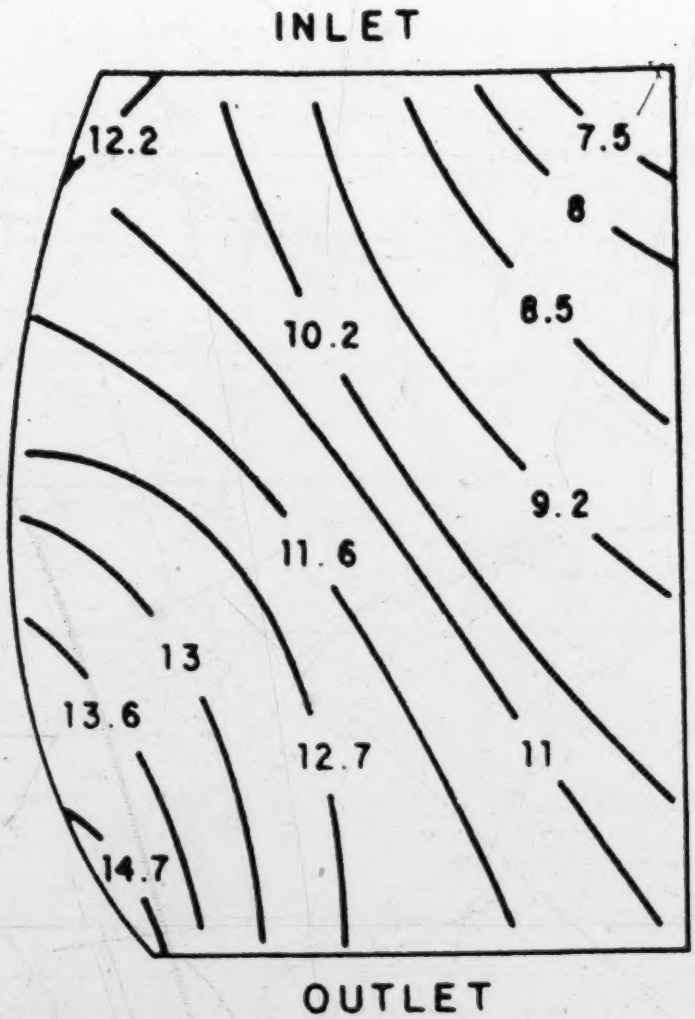

Key Parameters
Q_L = 6.94E-3 m^3/s
F_s = 1.015
d = 1.213 m
L_w = 0.925 m
h_w = 0.05 m

All Contour Values in Seconds

Note: Figure copied from Solari and Bell 1986

Figure 5.24. Experimentally Determined Residence Time Distribution - Case B5

contours are interpolated from data taken at only 18 points on the active area of the tray.

5.3.2 Simulations

In order to calculate the residence time distribution using the proposed model, equation 4-17 is implemented as an additional transport equation. All of the variables in the equation are defined. Equation 4-18 is used to calculate the mean residence time at each point in the model geometry. The integrals are evaluated by numerical integration.

Table 5.3 summarizes the transient boundary conditions used to model the injection of tracer dye onto the tray.

Note that the dye is assumed to enter the tray at a time of zero. The experimental results shown in Figure 5.24 indicates that the dye first emerges onto the sieve tray between 0 and 7.5 seconds. When comparing the measured and the simulated residence time distributions the contour shape and the relative distances between contours become relevant. The precise times have less meaning because we do not know the exact time of dye entry.

Table 5.3. Transient Inlet Boundary Conditions

Time (seconds)	Location (y and z coordinates on the Liquid Inlet Boundary)	Dye Concentration (mol/L)
$t < 0$	$0 \le z \le L_w/2$ $0 \le y \le h_f$	0
$0 \le t \le 0.1$	$0 \le z \le L_w/28$ $0 \le y \le h_f$	1
	$L_w/28 \le z \le L_w/2$ $0 \le y \le h_f$	0
$t \ge 0.1$	$0 \le z \le L_w/2$ $0 \le y \le h_f$	0

The resulting residence time distribution plot for a case with Q_L = 6.94E-2 m^3/s and F_s = 1.015 is shown in Figure 5.25. Note that the model does predict contours that are similar in shape and spacing to those in Figures 5.24. Because of the limitations imposed by the uncertainties of boundary conditions, a more quantitative analysis cannot be performed.

There would be merit in revisiting the residence time distribution experiments performed in the past. By changing the location of dye injection, we will be able to

INLET

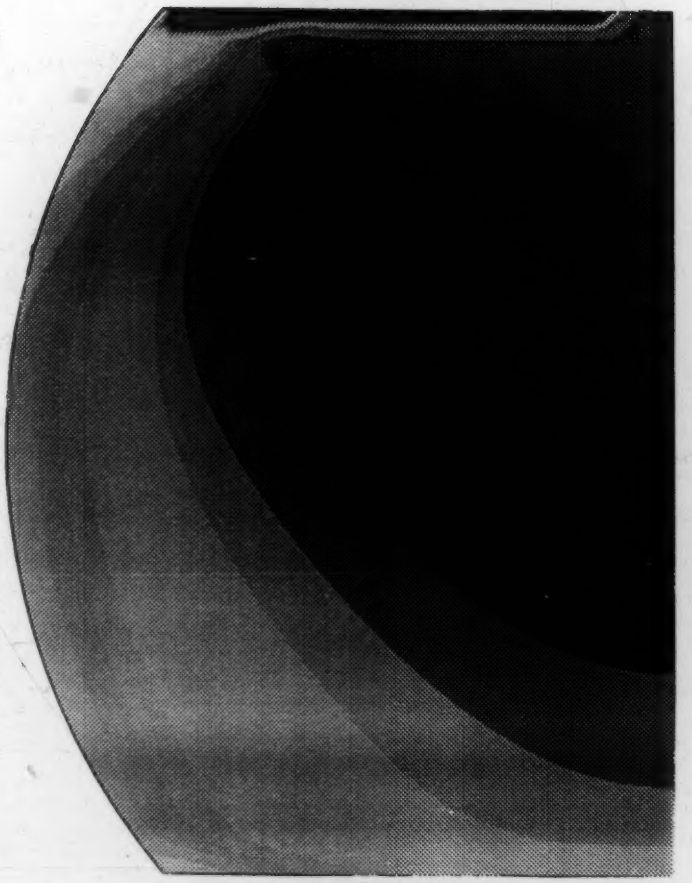

OUTLET

Key Parameters
Q_L = 6.94E-3 m^3/s
F_s = 1.105
d = 1.213 m
L_w = 0.925 m
h_w = 0.05 m

Contour Values (s)

> 1.0000E+01
8.6667E+00
6.8333E+00
5.0000E+00
3.1667E+00
1.3333E+00
< 0.0000E+00

Figure 5.25. Predicted Residence Time Distribution - Case B5

make better use of the data. If the tracer dye pulse is injected at the inlet of the tray's active area, then the problems with boundary conditions will be reduced significantly. The data from the experiments can then be compared with the model.

5.4 Conclusions

Overall, the model has made excellent predictions of liquid phase flows on sieve trays operating in the froth regime. For most cases, the predicted flows are within 26.3% of the measured values.

It is clear that the flow patterns on the active area of the sieve tray are highly sensitive to the inlet boundary conditions. The results indicate that the following criteria be used to determine the appropriate boundary condition:

$F_{lv} < 0.25$ Flat Boundary Condition (Equation 4-15)

$F_{lv} \geq 0.25$ Quadratic Boundary Condition (Equation 4-16)

Further experimental work is necessary in order to obtain better understanding of the inlet boundary conditions and downcomer flows. It is necessary to characterize the phenomenon in the downcomer in order to analyze what is actually occurring on the active area of the tray.

Caution must be used when applying this model at low gas flow rates (F-factors less than 0.5). At these operating conditions, the assumption of uniform gas phase bubbling breaks down and the degree of liquid phase flow maldistribution breaks down. Since these are precisely the operating conditions where recirculation is observed, it is not clear whether this phenomenon will be predicted. Further study is required in order to clarify this.

In order to improve the predictions at low gas flow rates, further study of gas flows through distillation towers will be required. Liquid phase maldistribution has been recognized to be significant for several years. Gas phase maldistributions are typically assumed to be negligible. The error in the simulations at low F-factors indicate that the effect of gas phase flow on the liquid flow patterns may be more significant than previously thought.

The model predicts the variations in liquid phase flow in three dimensions. The simulations indicate that many of the common assumptions regarding the liquid phase flow patterns may not necessarily be valid. The simulations indicate that there are significant variations in flow across the active area of the tray as well as in the vertical direction through the froth. Experimentalists must now attempt to measure the phenomena that are predicted by this model.

6. Conclusions and Future Work

6.1 Introduction

The scope of this research work was to develop a model to predict liquid phase flow patterns on sieve trays. The purpose for this model was to provide insight into distillation tray performance and design.

A complete two phase flow model is currently not practical. Although the two fluid model equations have been available for over a decade, we still need to understand the mechanisms of vapor-liquid momentum transfer and turbulence. Fundamental experimental studies of these phenomenon must be conducted. Until the fundamental interactions are understood, the truly multiphase model must wait.

There is still considerable merit in attempting to develop more limited models of distillation tray flows. It has been recognized for many years that liquid phase flow patterns have a direct relationship with tray efficiency. If the liquid phase flow patterns can be predicted, we have improved our overall predictive ability for distillation tray performance.

The single phase model that has been developed in Chapter 4 can predict the liquid phase flow patterns in the froth regime. The model is most accurate at liquid loads less than 1.65E-3 m^3/s and at F-factors of greater than 1.0.

The model predictions show a greater error at low vapor flow conditions because the key assumption of uniform gas flow is no longer valid. It is important to note that recirculation is typically observed at these operating conditions. Although there are no limitations in the model that would explicitly prevent the prediction of recirculation, it is not clear whether the recirculation phenomenon can be predicted at all.

6.2 Future Modelling Work

The model presented in this thesis is simply a first step towards the development of more fundamental distillation tray models. Several future projects can extend the work.

6.2.1 Mass Transfer Models

The prediction of tray efficiency is extremely important from both a design and performance assessment standpoint. Tray efficiency can be predicted if a mass transfer model is superimposed upon the flow model. This can be done at two levels: (a) using the velocity distribution from a single fluid model along with the convective diffusion equation . We need to assume that the mass transfer resistance in the liquid phase is dominant Under such conditions, the convective diffusion equation can

predict concentration distribution. (b) use of the velocity field from the two fluid model will be necessary if mass transfer resistance in both phases is of comparable magnitude.

6.2.2 Two Fluid Model

A long term modelling goal will be to capture the effects of both gas and liquid phase flow. This type of model will use the two fluid equations and will require fundamental models for constitutive relationships. This type of model will certainly have a wider range of applicability than the current model.

6.3 *Future Experimental Work*

The relationship between experimental and modelling work is unique. The experiment allows us to further our understanding of physical systems. The model allows us to predict the behavior of these systems. As the model is applied, we begin to understand its limitations. These limitations will focus the direction of further experimental study.

6.3.1 Further Model Evaluation

The model has performed remarkably well against the available data. To fully understand the limitations of the model, more data will be required. The experimental technique used in Solari and Bell 1986, is fairly accurate. If this experimental method can be applied to a wider range of operating conditions, we will be able to establish firmer boundaries of model applicability. Additional data characterizing the state of the boundary, spatial variation of velocity, holdup and concentration field would be helpful in validating the model before it can be used in scaleup operations

An area of study that should be revisited is the measurement of residence time distribution. Due to the choice of experimental technique, it is virtually impossible to quantitatively evaluate the model with the available data. With slight modifications of the experimental apparatus and procedure, the model's residence time distribution predictions can be evaluated. If the injection point of the tracer dye is moved to the liquid inlet plane that was used in the model, the dye injection can be described with a simple mathematical function and the inlet boundary conditions can be characterized correctly.

6.3.2 Downcomer Hydraulics

The liquid phase flow patterns are highly sensitive to the selection of inlet boundary conditions. This would suggest that the downcomer flow patterns have a significant impact on the overall tray performance. There is very little quantitative information available regarding the liquid phase flow patterns in downcomers. Further experimental study of downcomer hydraulics is essential for greater understanding of tray hydraulics in general.

6.3.3 Vapor Phase Flow Patterns

Vapor phase flow must be studied in order to get a more complete picture of distillation flow. As demonstrated in this model, as the vapor phase flow rates became very low, the assumptions of uniform flow distribution becomes invalid. At the length scale of the column, there can be significant flow maldistributions.

The changes in vapor flow rates also become relevant at much smaller length scales. At the length scale of a sieve tray hole, one can observe intermittent bubbling, regular bubbling, and jetting phenomenon. Each of these different types of flow will affect the local flow and mass transfer in different ways.

6.3.4 Vapor-Liquid Interactions

To ultimately have a fully predictive model that is not limited by flow regime, chemical system, or geometry, we must have constitutive relationships with a fundamentally sound basis. As indicated in Chapter 2, interphase momentum transfer and turbulence models for distillation systems are simply not available. Once fundamental constitutive relationships are developed we will be able to develop more robust and rigorous models.

6.4 Conclusions

A model has been proposed that can predict the liquid phase flow patterns on sieve trays operating in the froth regime. This model is based on the fundamental concepts of fluid dynamics and clearly has promise as an alternative means of predicting sieve tray hydraulics. As any model, this one has its limitations but overall, it is a excellent first step towards a more detailed look at flow in distillation systems.

Bibliography

"Bubble Tray Design Manual", AIChE, New York, 1958.

Bell, R.L. and Solari, R.B., "Effect of Nonuniform Velocity Fields and Retrograde Flow on Distillation Tray Efficiency", AIChE J, **20**, p. 688, 1974.

Bell, R.L., "Experimental Determination of Residence Time Distributions on Commercial-Scale Distillation Trays Using a Fiber Optic Technique", AIChE J, **18**, p. 491, 1972.

Bell, R.L., "Residence time and fluid mixing on commercial-scale sieve trays", AIChE J, **18**, p. 498, 1972.

Bennett, D. L., Agrawal, R. and Cook, P. J., "New pressure drop correlation for sieve tray distillation columns", AIChE J. **29**, No. 3, p. 434, 1983.

Boure, J.A., "Two-phase flow models: the closure issue", Multiphase Science and Technology, **3**, p.1, Hemisphere Publishing Corporation, New York, 1987.

CFDS-FLOW3D, Harwell Laboratory, Oxfordshire, UK.

Chen J.J.J., Jamialahmadi M. and Li M., "Effect of Liquid Depth on Circulation in Bubble Columns: A Visual Study", Chem. Eng. Res. Des., **67**, p. 203, 1989.

Chuang, K. T., Personal Communication, University of Alberta, 1994.

Chuang, K.T, "Lecture Notes - ChE 615 Separation Processes", University of Alberta, 1994.

Colwell, C. J., "Clear liquid height and froth density on sieve trays", Ind. Eng. Chem. Proc. Des. Dev., **20**, p. 298, 1979.

Distillation Trays Using a Fiber Optic Technique", AIChE J, **18**, p. 491, 1972.

Gerster, J. A. , Hill, A. B.,Hochgraf, N. N., and Robinson, D. G., "Tray efficiencies in distillation columns. Final Report", AIChE, University of Delaware, 1958.

Glasgow L.A. and Rainbolt R., "Interfacial Velocities in the Vicinity of a Sieve Plate Sparger", AIChE J, **40**, p. 178, 1994.

Hofhuis, P.A.M. and Zuiderweg, F.J., "Sieve Plates: Dispersion Density and Flow Regimes", IChemE Symposium Series, Vol. 1, No. 56, 2.2-1, 1979.

Ishii, M. and Zuber, N., "Drag Coefficient and Relative Velocity in Bubbly, Droplet or Particulate Flows", AIChE J, **25**, p. 843, 1979.

Ishii, M., "Interfacial Area Modeling", Multiphase Science and Technology, **3**, p. 31, Hemisphere Publishing Corporation, New York, 1987.

Ishii, M., "Thermo-Fluid Dynamic Theory of Two-Phase Flow", Eyrolles, Paris, 1975.

Ishii, M., "Two-Fluid Model for Two Phase Flow", Multiphase Science and Technology , **5**, p. 1, Hemisphere Publishing Corporation, New York, 1990.

Jakobsen, H.A., Svendsen H.F., and Hjarbo K.W., "On the prediction of local flow structures in internal loop and bubble column reactors using a two fluid model", European Symposium on Computer Aided Engineering, No. 2, p. S531, 1994.

Jones, W.P. and Lauder, B.E., "The Prediction of Laminarization with a Two-Equation Model of Turbulence", International Journal of Heat and Mass Transfer, **15**, p. 301, 1972.

Kashiwa, B.A., Padial N.T., Rauenzahn R. M., and VanderHeyden W.B., "A Cell-Centred ICE Method for Multiphase Flow Simulations", Los Almos National Laboratory, Vol: LA-UR-93-3922, p. 1, 1994.

Kirschbaum, E., "Distillation and Rectification",Chemical Publishing Co.,New York..

Kister, H. , "Distillation Design", Mcgraw-Hill, New York, 1992.

Lockett, M.J. "Distillation Tray Fundamentals", Cambridge University Press, Cambridge, 1986.

Lockett, M.J. and Dhulesia, H.A., Chem. Eng. J., **19**, p. 183, 1980.

Murphree, E. V., "Rectifying column calculations with particular reference to N component mixtures", Ind. Engng. Chem., **17**, No. 7, p. 747, 1925.

Neti, S. and Mohamed, O. E. E., "Numerical simulation of turbulent two-phase flows", Int. J. Heat and Fluid Flow, **11**, No. 3., p. 204, 1990.

Patankar, S.V. and Spalding, D.B., "Calculation procedure for heat, mass and momentum transfer in three dimensional parabolic flows", International Journal of Heat and Mass Transfer, **15**, p.1787, 1972.

Patankar, S.V., "Numerical heat transfer and fluid flow", Hemisphere Publishing Corporation, New York, 1983.

Porter, K.E., Davies, B., Ani, C.C. and Enjugu, B. A., "Investigating the effect of the liquid flow pattern on sieve tray performance by means of the water cooling technique", IChemE Symposium Series, No. 104, p. A569, 1988.

Porter, K.E., Yu, K.T., Chambers, S. and Zhang, M.Q., "Flow Patterns and Temperature Profiles on a 2.44 m. Diameter Sieve Tray", IChemE Symposium Series, V. 1, No. 128, p. A2571, 1992.

Prado, M. , Johnson, K.J. and Fair J.R., Chem. Eng. Prog., **83**, p. 32, 1987.

Prado, M. and Fair, J.R., "Fundamental model for the prediction of sieve tray efficiency", Ind. Eng. Chem., **29**, p. 1031, 1990.

Rhie, C.M and Chow, W.L., "Numerical study of the turbulent flow past an airfoil with trailing edge separation", AIAA J1, **21**, p. 1527, 1983.

Solari, R. B. and Bell, R. L., "Fluid Flow Patterns and Velocity Distribution on Commercial-Scale Sieve Trays", AIChE J, **32**, p. 640, 1986.

Solari, R. B., Saez, E., D'Apollo, I. and Bellet, A., "Velocity Distribution and Liquid Flow Patterns on Industrial Sieve Trays", Chem. Eng. Commun., **13**, p. 369, 1982.

Spalding, D.B., "A novel finite difference formulation for differential expressions involving both first and second derivatives", Int. J. Num. Meth. Engng, **4**, p. 551, 1972.

Spalding, D.B., "The calculation of free-convection phenomenon in gas-liquid mixtures", ICHMT Seminar, Dubrovnik, p. 569, 1976.

Taylor, R. and Krishnamurthy, R., Am. Inst. Chem. Engrs. J., **31**, p. 449, 1985.

Thompson, J. F., Warsi, Z. U., and Mastin, C. W., "Boundary-fitted coordinate systems for numerical solution of partial differential equations", J. Comp. Phys., **47**, p. 1, 1982.

Van Doormal, J.P. and Raithby, G.D., "Enhancements of the SIMPLE method for predicting incompressible fluid flows", Numerical Heat Transfer, **7**, p.147, 1984.

Wallis, G.B., "Interfacial Friction Modeling", Multiphase Science and Technology, **3**, p. 63, Hemisphere Publishing Corporation, New York, 1987.

Wilcox, D.C., "Turbulence Modeling for CFD", DCW Industries, La Cañada, CA., 1993.

Yanagi, T., "Inside a trayed distillation column", Chemical Engineering, No. 11, p. 120, 1990.

Yongheng, Ye, Zhirong, Fang, and Jifen, Shi, "The vertical density profiles of two-phase mixture and the flow regime transition on sieve trays", Journal of Chemical Industry and Engineering (China), **3**, No. 2, p. 229, 1988.

Zuiderweg, F.J., "Sieve trays - a view on the state of the art", Chemical Engineering Science, **37**, No. 10, p. 1441, 1982.

Appendix I

Simulation Code

CFDS-FLOW3D Command Files:

The Computational Fluid Dynamics software package: CFDS-FLOW3D is used to conduct all of the simulations performed in this work.

For additional information on CFDS-FLOW3D contact :

CFDS-FLOW3D
Building 8.19
Harwell Laboratory
Oxfordshire, UK
0X11 0RA

There are typically three types of files used as inputs for the simulation:

a) Command File - a keyword based text file listing most of the model specifications
b) User FORTRAN File - if a keyword is not available in the model to perform special tasks (i.e. Define a special boundary condition) then a FORTRAN subroutine can be programmed
c) Geometry File - The vertices of the cells in the finite volume grid are reported in a text file.

In this Appendix, samples of the Command and the User FORTRAN files are provided. See Appendix II for more detail regarding the generation of the grid file.

I. CFDS-FLOW3D Sample Command File:

```
>>FLOW3D
/* Allocation of Memory and Filespace for Simulation*/
 >>SET LIMITS
  TOTAL INTEGER WORK SPACE 1000000
  TOTAL CHARACTER WORK SPACE 3000
  TOTAL REAL WORK SPACE 3500000
  MAXIMUM NUMBER OF BLOCKS 4
  MAXIMUM NUMBER OF PATCHES 40
  END
 >>OPTIONS
/* 3D Simulation */
  THREE DIMENSIONS
/* Porous Flow option allows for the specification of a volume fraction without
implementing a second set of conservation equations*/
  POROUS FLOW
  END
/* User Fortran Code:  These routines will be called during the simulation*/
 >>USER FORTRAN
  USRBCS       /*Inlet Boundary Conditions*/
  USRBF        /*Body Forces - interphase momentum transfer */
  USRPOR       /*Volume Fraction*/
  USRVIS       /*Turbulent Viscosity*/
  END
 >>VARIABLE NAMES
  U VELOCITY 'U VELOCITY'
  V VELOCITY 'V VELOCITY'
  W VELOCITY 'W VELOCITY'
  PRESSURE 'PRESSURE'
  VOLUME FRACTION 'VOLUME FRACTION'
  DENSITY 'DENSITY'
  VISCOSITY 'VISCOSITY'
  END
>>MODEL TOPOLOGY
/*********************************************
* Definition of Sieve Tray Geometry
*********************************************/
 >>CREATE BLOCK
  BLOCK NAME 'BLOCK-NUMBER-1'
  BLOCK DIMENSIONS 18 23 14
  END
 >>CREATE BLOCK
```

```
 BLOCK NAME 'BLOCK-NUMBER-2'
 BLOCK DIMENSIONS 5 23 14
 END
>>CREATE BLOCK
 BLOCK NAME 'BLOCK-NUMBER-3'
 BLOCK DIMENSIONS 5 8 14
 END
>>CREATE PATCH
 PATCH NAME 'LIQINLET'
 PATCH TYPE 'INLET'
 BLOCK NAME 'BLOCK-NUMBER-1'
 LOW I
 END
>>CREATE PATCH
 PATCH NAME 'LIQEXIT'
 PATCH TYPE 'MASS FLOW BOUNDARY'
 BLOCK NAME 'BLOCK-NUMBER-3'
 LOW J
>>CREATE PATCH
 PATCH NAME 'WEIR1'
 PATCH TYPE 'THIN SURFACE'
 BLOCK NAME 'BLOCK-NUMBER-1'
 PATCH LOCATION 18 18  1 8 1 14
 HIGH I
 END
>>CREATE PATCH
 PATCH NAME 'WEIR2'
 PATCH TYPE 'WALL'
 BLOCK NAME 'BLOCK-NUMBER-2'
 PATCH LOCATION 1 1 1 8 1 14
 LOW I
 END
>>CREATE PATCH
 PATCH NAME 'CENTRE-LINE1'
 PATCH TYPE 'SYMMETRY PLANE'
 BLOCK NAME 'BLOCK-NUMBER-1'
 PATCH LOCATION 1 18 1 23 1 1
 LOW K
 END
>>CREATE PATCH
 PATCH NAME 'CENTRE-LINE2'
 PATCH TYPE 'SYMMETRY PLANE'
 BLOCK NAME 'BLOCK-NUMBER-2'
 PATCH LOCATION 1 5 1 23 1 1
 LOW K
```

```
 END
>>CREATE PATCH
 PATCH NAME 'CENTRE-LINE3'
 PATCH TYPE 'SYMMETRY PLANE'
 BLOCK NAME 'BLOCK-NUMBER-3'
 PATCH LOCATION 1 5 1 8 1 1
 LOW K
 END
>>CREATE PATCH
 PATCH NAME 'GASEXIT1'
 PATCH TYPE 'WALL'
 BLOCK NAME 'BLOCK-NUMBER-1'
 PATCH LOCATION 1 18 23 23 1 14
 HIGH J
 END
>>CREATE PATCH
 PATCH NAME 'GASEXIT2'
 PATCH TYPE 'WALL'
 BLOCK NAME 'BLOCK-NUMBER-2'
 PATCH LOCATION 1 5 23 23 1 14
 HIGH J
 END
>>CREATE PATCH
 PATCH NAME 'GASINLET'
 PATCH TYPE 'WALL'
 BLOCK NAME 'BLOCK-NUMBER-1'
 PATCH LOCATION 1 18 1 1 1 14
 LOW J
 END
>>CREATE PATCH
 PATCH NAME 'LIQ_VF'
 PATCH TYPE 'POROUS REGION'
 BLOCK NAME 'BLOCK-NUMBER-1'
 PATCH LOCATION 1 18 1 23 1 14
 PATCH GROUP NUMBER 1
 END
>>CREATE PATCH
 PATCH NAME 'CONNECT12-1'
 PATCH TYPE 'INTER BLOCK BOUNDARY'
 BLOCK NAME 'BLOCK-NUMBER-1'
 HIGH I
 END
>>CREATE PATCH
 PATCH NAME 'CONNECT12-2'
 PATCH TYPE 'INTER BLOCK BOUNDARY'
```

```
  BLOCK NAME 'BLOCK-NUMBER-2'
  LOW I
  END
 >>CREATE PATCH
  PATCH NAME 'CONNECT23-1'
  PATCH TYPE 'INTER BLOCK BOUNDARY'
  BLOCK NAME 'BLOCK-NUMBER-2'
  LOW J
  END
 >>CREATE PATCH
  PATCH NAME 'CONNECT23-2'
  PATCH TYPE 'INTER BLOCK BOUNDARY'
  BLOCK NAME 'BLOCK-NUMBER-3'
  HIGH J
  END
>>GLUE PATCHES
  FIRST PATCH NAME 'CONNECT12-1'
  SECOND PATCH NAME 'CONNECT12-2'
  ORIENTATION CHANGE 'HIGH I' 'HIGH J' 'HIGH K'
  END
 >>GLUE PATCHES
  FIRST PATCH NAME 'CONNECT23-1'
  SECOND PATCH NAME 'CONNECT23-2'
  ORIENTATION CHANGE 'HIGH I' 'HIGH J' 'HIGH K'
  END
>>MODEL DATA
 >>WALL TREATMENTS
  SLIP          /* All Walls are Free Slip Boundaries */
  END
 >>TITLE
  PROBLEM TITLE '3D DISTILLATION TRAY - 1 phase simulation'
  END
 #CALC
 rhol = 1000.0;
 rhog = 1.36;
 Vs = 1.255;
 Vliq = -20.;  /*Dummy Value to pass the error check*/
#ENDCALC
>>PHYSICAL PROPERTIES
 >>POROUS REGION PARAMETERS
  PATCH GROUP NUMBER 1
  VOLUME POROSITY 1.0        /* Dummy Value to pass the error check*/
  END
/* Physical Properties */
  >>FLUID PARAMETERS
```

```
    VISCOSITY    1.0E-03
    DENSITY      #rhol
    END
* /*Solver Control Parameters*/
 >>SOLVER DATA
  >>PROGRAM CONTROL
   MAXIMUM NUMBER OF ITERATIONS 4000
   MINIMUM NUMBER OF ITERATIONS 1
   OUTPUT MONITOR BLOCK 'BLOCK-NUMBER-1'
   OUTPUT MONITOR POINT 10 8 1
   MASS SOURCE TOLERANCE 5.0000E-03
   END
  >>UNDER RELAXATION FACTORS
   U VELOCITY 0.4
   V VELOCITY 0.4
   W VELOCITY 0.4
 /* Input of Grid from a Separate File*/
 >>CREATE GRID
  >>INPUT GRID
   READ GRID FILE
   END
 >>MODEL BOUNDARY CONDITIONS
  >>SET VARIABLES
   PATCH NAME 'LIQINLET'
   U VELOCITY #Vliq          /*Dummy Value to Pass the Error Check*/
   END
 >>STOP
```

II. CFDS-FLOW3D USER FORTAN FILES

```
      SUBROUTINE USRBCS(VARBCS,VARAMB,A,B,C,ACND,BCND,CCND,FLOUT,NLABEL,
     +                  NSTART,NEND,NCST,NCEN,U,V,W,P,VFRAC,DEN,VIS,TE,
     +                  ED,RS,T,H,RF,SCAL,XP,YP,ZP,VOL,AREA,VPOR,ARPOR,
     +                  WFACT,IPT,IBLK,IPVERT,IPNODN,IPFACN,IPNODF,
     +                  IPNODB,IPFACB,WORK,IWORK,CWORK)
C
C***********************************************************************
C
C  USER ROUTINE TO SET REALS AT BOUNDARIES.
C
C  >>> IMPORTANT                                <<<
C  >>>                                          <<<
C  >>> USERS MAY ONLY ADD OR ALTER PARTS OF THE SUBROUTINE WITHIN  <<<
C  >>> THE DESIGNATED USER AREAS                <<<
C
C***********************************************************************
C
C  THIS SUBROUTINE IS CALLED BY THE FOLLOWING SUBROUTINE
C   CUSR  SRLIST
C
C***********************************************************************
C  CREATED
C    30/11/88 ADB
C  MODIFIED
C    08/09/90 ADB  RESTRUCTURED FOR USER-FRIENDLINESS.
C    10/08/91 IRH  FURTHER RESTRUCTURING ADD ACND BCND CCND
C    22/09/91 IRH  CHANGE ICALL TO IUCALL + ADD /SPARM/
C    10/03/92 PHA  UPDATE CALLED BY COMMENT, ADD RF ARGUMENT,
C             CHANGE LAST DIMENSION OF RS TO 6 AND IVERS TO 2
C    03/06/92 PHA  ADD PRECISION FLAG AND CHANGE IVERS TO 3
C    30/06/92 NSW  INCLUDE FLAG FOR CALLING BY ITERATION
C             INSERT EXTRA COMMENTS
C    03/08/92 NSW  MODIFY DIMENSION STATEMENTS FOR VAX
C    21/12/92 CSH  INCREASE IVERS TO 4
C    02/08/93 NSW  INCORRECT AND MISLEADING COMMENT REMOVED
C    05/11/93 NSW  INDICATE USE OF FLOUT IN MULTIPHASE FLOWS
C    23/11/93 CSH  EXPLICITLY DIMENSION IPVERT ETC.
C    01/02/94 NSW  SET VARIABLE POINTERS IN WALL EXAMPLE.
C             CHANGE FLOW3D TO CFDS-FLOW3D.
C             MODIFY MULTIPHASE MASS FLOW BOUNDARY TREATMENT.
C    03/03/94 FHW  CORRECTION OF SPELLING MISTAKE
C
C***********************************************************************
C
C  SUBROUTINE ARGUMENTS
C
C    VARBCS - REAL BOUNDARY CONDITIONS
C    VARAMB - AMBIENT VALUE OF VARIABLES
C    A      - COEFFICIENT IN WALL BOUNDARY CONDITION
C    B      - COEFFICIENT IN WALL BOUNDARY CONDITION
C    C      - COEFFICIENT IN WALL BOUNDARY CONDITION
C    ACND   - COEFFICIENT IN CONDUCTING WALL BOUNDARY CONDITION
```

```
C   BCND  - COEFFICIENT IN CONDUCTING WALL BOUNDARY CONDITION
C   CCND  - COEFFICIENT IN CONDUCTING WALL BOUNDARY CONDITION
C   FLOUT  - MASS FLOW/FRACTIONAL MASS FLOW
C   NLABEL - NUMBER OF DISTINCT OUTLETS
C   NSTART - ARRAY POINTER
C   NEND  - ARRAY POINTER
C   NCST  - ARRAY POINTER
C   NCEN  - ARRAY POINTER
C   U     - U COMPONENT OF VELOCITY
C   V     - V COMPONENT OF VELOCITY
C   W     - W COMPONENT OF VELOCITY
C   P     - PRESSURE
C   VFRAC  - VOLUME FRACTION
C   DEN   - DENSITY OF FLUID
C   VIS   - VISCOSITY OF FLUID
C   TE    - TURBULENT KINETIC ENERGY
C   ED    - EPSILON
C   RS    - REYNOLD STRESSES
C   T     - TEMPERATURE
C   H     - ENTHALPY
C   RF    - REYNOLD FLUXES
C   SCAL  - SCALARS (THE FIRST 'NCONC' OF THESE ARE MASS FRACTIONS)
C   XP    - X COORDINATES OF CELL CENTRES
C   YP    - Y COORDINATES OF CELL CENTRES
C   ZP    - Z COORDINATES OF CELL CENTRES
C   VOL   - VOLUME OF CELLS
C   AREA  - AREA OF CELLS
C   VPOR  - POROUS VOLUME
C   ARPOR  - POROUS AREA
C   WFACT  - WEIGHT FACTORS
C
C   IPT   - 1D POINTER ARRAY
C   IBLK  - BLOCK SIZE INFORMATION
C   IPVERT - POINTER FROM CELL CENTERS TO 8 NEIGHBOURING VERTICES
C   IPNODN - POINTER FROM CELL CENTERS TO 6 NEIGHBOURING CELLS
C   IPFACN - POINTER FROM CELL CENTERS TO 6 NEIGHBOURING FACES
C   IPNODF - POINTER FROM CELL FACES TO 2 NEIGHBOURING CELL CENTERS
C   IPNODB - POINTER FROM BOUNDARY CENTERS TO CELL CENTERS
C   IPFACB - POINTER TO NODES FROM BOUNDARY FACES
C
C   WORK  - REAL WORKSPACE ARRAY
C   IWORK  - INTEGER WORKSPACE ARRAY
C   CWORK  - CHARACTER WORKSPACE ARRAY
C
C  SUBROUTINE ARGUMENTS PRECEDED WITH A '*' ARE ARGUMENTS THAT MUST
C  BE SET  BY THE USER IN THIS ROUTINE.
C
C  NOTE THAT OTHER DATA MAY BE OBTAINED FROM CFDS-FLOW3D USING THE
C  ROUTINE GETADD, FOR FURTHER DETAILS SEE THE RELEASE 3
C  USER MANUAL.
C
C*************************************************************************
      DOUBLE PRECISION VARBCS
      DOUBLE PRECISION VARAMB
      DOUBLE PRECISION A
```

```
      DOUBLE PRECISION B
      DOUBLE PRECISION C
      DOUBLE PRECISION ACND
      DOUBLE PRECISION BCND
      DOUBLE PRECISION CCND
      DOUBLE PRECISION FLOUT
      DOUBLE PRECISION U
      DOUBLE PRECISION V
      DOUBLE PRECISION W
      DOUBLE PRECISION P
      DOUBLE PRECISION VFRAC
      DOUBLE PRECISION DEN
      DOUBLE PRECISION VIS
      DOUBLE PRECISION TE
      DOUBLE PRECISION ED
      DOUBLE PRECISION RS
      DOUBLE PRECISION T
      DOUBLE PRECISION H
      DOUBLE PRECISION RF
      DOUBLE PRECISION SCAL
      DOUBLE PRECISION XP
      DOUBLE PRECISION YP
      DOUBLE PRECISION ZP
      DOUBLE PRECISION VOL
      DOUBLE PRECISION AREA
      DOUBLE PRECISION VPOR
      DOUBLE PRECISION ARPOR
      DOUBLE PRECISION WFACT
      DOUBLE PRECISION WORK
      DOUBLE PRECISION SMALL
      DOUBLE PRECISION SORMAX
      DOUBLE PRECISION TIME
      DOUBLE PRECISION DT
      DOUBLE PRECISION DTINVF
      DOUBLE PRECISION TPARM
      LOGICAL LDEN,LVIS,LTURB,LTEMP,LBUOY,LSCAL,LCOMP,LRECT,LCYN,LAXIS,
     +     LPOROS,LTRANS
C
      CHARACTER*(*) CWORK
C
C+++++++++++++++++ USER AREA 1 +++++++++++++++++++++++++++++++++++++++++
C---- AREA FOR USERS EXPLICITLY DECLARED VARIABLES
C
      DOUBLE PRECISION VF_AVG, HTCL, HTFR
      DOUBLE PRECISION dia,areat, weirln, weirht, holearea, dcarea, dcclear
      DOUBLE PRECISION rhol, rhog, visl
      DOUBLE PRECISION ug, Ql
C
      DOUBLE PRECISION  coef, zloc, n, nfrac
C
C+++++++++++++++++ END OF USER AREA 1 +++++++++++++++++++++++++++++++++++
C
      COMMON /ALL/NBLOCK,NCELL,NBDRY,NNODE,NFACE,NVERT,NDIM,
     +     /ALLWRK/NRWS,NIWS,NCWS,IWRFRE,IWIFRE,IWCFRE,/ADDIMS/NPHASE,
     +     NSCAL,NVAR,NPROP,NDVAR,NDPROP,NDXNN,NDGEOM,NDCOEF,NILIST,
```

```
     +     NRLIST,NTOPOL,/BCSOUT/IFLOUT,/CHKUSR/IVERS,IUCALL,IUSED,
     +     /DEVICE/NREAD,NWRITE,NRDISK,NWDISK,/IDUM/ILEN,JLEN,
     +     /IMFBMP/IMFBMP,/LOGIC/LDEN,LVIS,LTURB,LTEMP,LBUOY,LSCAL,
     +     LCOMP,LRECT,LCYN,LAXIS,LPOROS,LTRANS,/MLTGRD/MLEVEL,NLEVEL,
     +     ILEVEL,/SGLDBL/IFLGPR,ICHKPR,/SPARM/SMALL,SORMAX,NITER,
     +     INDPRI,MAXIT,NODREF,NODMON,/TRANSI/NSTEP,KSTEP,MF,INCORE,
     +     /TRANSR/TIME,DT,DTINVF,TPARM,/UBCSFL/IUBCSF
C
C+++++++++++++++++ USER AREA 2 ++++++++++++++++++++++++++++++++++++++++++++
C---- AREA FOR USERS TO DECLARE THEIR OWN COMMON BLOCKS
C    THESE SHOULD START WITH THE CHARACTERS 'UC' TO ENSURE
C    NO CONFLICT WITH NON-USER COMMON BLOCKS
C
     COMMON /UCFROTH/VF_AVG, HTCL, HTFR
     COMMON /UCTRAY/dia,areat,weirln, weirht, holearea,dcarea,dcclear
     COMMON /UCPHYS/rhol, rhog, visl
     COMMON /UCOPCOND/ug, Ql
C
C+++++++++++++++++ END OF USER AREA 2 ++++++++++++++++++++++++++++++++++++++
C
    DIMENSION VARBCS(NVAR,NPHASE,NCELL+1:NNODE),VARAMB(NVAR,NPHASE),
     +     A(4+NSCAL,NPHASE,NSTART:*),B(4+NSCAL,NPHASE,NSTART:*),
     +     C(4+NSCAL,NPHASE,NSTART:*),FLOUT(*),ACND(NCST:*),
     +     BCND(NCST:*),CCND(NCST:*)
C
     DIMENSION U(NNODE,NPHASE),V(NNODE,NPHASE),W(NNODE,NPHASE),
     +     P(NNODE,NPHASE),VFRAC(NNODE,NPHASE),DEN(NNODE,NPHASE),
     +     VIS(NNODE,NPHASE),TE(NNODE,NPHASE),ED(NNODE,NPHASE),
     +     RS(NNODE,NPHASE,6),T(NNODE,NPHASE),H(NNODE,NPHASE),
     +     RF(NNODE,NPHASE,4),SCAL(NNODE,NPHASE,NSCAL)
C
     DIMENSION XP(NNODE),YP(NNODE),ZP(NNODE),VOL(NCELL),AREA(NFACE,3),
     +     VPOR(NCELL),ARPOR(NFACE,3),WFACT(NFACE),IPT(*),
     +     IBLK(5,NBLOCK),IPVERT(NCELL,8),IPNODN(NCELL,6),
     +     IPFACN(NCELL,6),IPNODF(NFACE,4),IPNODB(NBDRY,4),
     +     IPFACB(NBDRY),IWORK(*),WORK(*),CWORK(*)
C
C+++++++++++++++++ USER AREA 3 ++++++++++++++++++++++++++++++++++++++++++++
C---- AREA FOR USERS TO DIMENSION THEIR ARRAYS
C
C---- AREA FOR USERS TO DEFINE DATA STATEMENTS
C
C+++++++++++++++++ END OF USER AREA 3 ++++++++++++++++++++++++++++++++++++++
C
C---- STATEMENT FUNCTION FOR ADRESSING
     IP(I,J,K) = IPT((K-1)*ILEN*JLEN+ (J-1)*ILEN+I)
C
C----VERSION NUMBER OF USER ROUTINE AND PRECISION FLAG
C
     IVERS = 4
     ICHKPR = 2
C
C+++++++++++++++++ USER AREA 4 ++++++++++++++++++++++++++++++++++++++++++++
C---- TO USE THIS USER ROUTINE FIRST SET IUSED=1
C    AND SET IUBCSF FLAG:
```

```
C    BOUNDARY CONDITIONS NOT CHANGING                  IUBCSF=0
C    BOUNDARY CONDITIONS CHANGING WITH ITERATION       IUBCSF=1
C    BOUNDARY CONDITIONS CHANGING WITH TIME            IUBCSF=2
C    BOUNDARY CONDITIONS CHANGING WITH TIME AND ITERATION  IUBCSF=3
C
     IUSED = 1
     IF (IUSED.EQ.0) RETURN
     IUBCSF = 0
C++++++++++++++++++ END OF USER AREA 4 +++++++++++++++++++++++++++++++++
C
C---- FRONTEND CHECKING OF USER ROUTINE
     IF (IUCALL.EQ.0) RETURN
C
C++++++++++++++++++ USER AREA 5 +++++++++++++++++++++++++++++++++++++++
C
C---- AREA FOR SETTING VALUES AT INLETS, PRESSURE BOUNDARIES
C    AND OUTLETS. (NOTE THAT THE MASS FLOW AT OUTLETS IS
C    SPECIFIED IN USER AREA 7)
C
C    IF USING A REYNOLDS STRESS OR FLUX MODEL, NOTE THAT AT INLETS
C    IT IS IMPORTANT THAT THE USER SETS ALL COMPONENTS OF THE
C    REYNOLDS STRESS AND FLUX AND THE TURBULENT KINETIC ENERGY
C    AS WELL AS THE ENERGY DISSIPATION RATE.
C
C    SET THE VALUES IN VARBCS(NVAR,NPHASE,ILEN,JLEN,KLEN)
C
C--Set inlet velocity profile as LIQINLET
C
     coef = Ql/(weirln*HTFR)
C
C--  INTERROGATE GETVAR FOR VARIABLE NUMBERS.
C
     CALL GETVAR('USRBCS','U     ',IU)
C
C  SET IPHS = 1 FOR SINGLE PHASE FLOW.
C
     IPHS = 1
C
C  USE IPREC TO FIND ADDRESSES
C
     CALL IPREC('LIQINLET','PATCH','CENTRES',IPT,ILEN,JLEN,KLEN,
    +          CWORK,IWORK)
C
C
C
C  LOOP OVER PATCH
     DO 103 K = 1, KLEN
       DO 102 J = 1, JLEN
         DO 101 I = 1, ILEN
C  USE STATEMENT FUNCTION IP TO GET ADDRESSES
       INODE = IP(I,J,K)
C  SET VARBCS
C
           zloc = ZP(INODE)
       VARBCS(IU,IPHS,INODE) =  coef/VF_AVG
```

```
C
 101     CONTINUE
 102   CONTINUE
 103  CONTINUE
C
C----END OF EXAMPLE
C
C+++++++++++++++++ END OF USER AREA 5 +++++++++++++++++++++++++++++++++
C
C+++++++++++++++++ USER AREA 6 +++++++++++++++++++++++++++++++++++++++
C
C---- AREA FOR SETTING VALUES AT WALLS
C
C+++++++++++++++++ END OF USER AREA 6 +++++++++++++++++++++++++++++++++
C
C
C+++++++++++++++++ USER AREA 7 +++++++++++++++++++++++++++++++++++++++
C
C----- DEFINE FLOW AT OUTLETS (MASS FLOW BOUNDARIES)
C
C+++++++++++++++++ END OF USER AREA 7 +++++++++++++++++++++++++++++++++
C
   RETURN
C
   END



   SUBROUTINE USRBF(IPHASE,BX,BY,BZ,BPX,BPY,BPZ,U,V,W,P,VFRAC,DEN,
  +            VIS,TE,ED,RS,T,H,RF,SCAL,XP,YP,ZP,VOL,AREA,VPOR,
  +            ARPOR,WFACT,IPT,IBLK,IPVERT,IPNODN,IPFACN,IPNODF,
  +            IPNODB,IPFACB,WORK,IWORK,CWORK)
C
C*************************************************************************
C
C  UTILITY SUBROUTINE FOR USER-SUPPLIED BODY FORCES
C
C  >>> IMPORTANT                                <<<
C  >>>                                  <<<
C  >>> USERS MAY ONLY ADD OR ALTER PARTS OF THE SUBROUTINE WITHIN  <<<
C  >>> THE DESIGNATED USER AREAS                        <<<
C
C*************************************************************************
C
C  THIS SUBROUTINE IS CALLED BY THE FOLLOWING SUBROUTINES
C    BFCAL
C
C*************************************************************************
C  CREATED
C    24/01/92  ADB
C  MODIFIED
C    03/06/92  PHA  ADD PRECISION FLAG AND CHANGE IVERS TO 2
C    23/11/93  CSH  EXPLICITLY DIMENSION IPVERT ETC.
C    03/02/94  PHA  CHANGE FLOW3D TO CFDS-FLOW3D
```

```
C    03/03/94  FHW  CORRECTION OF SPELLING MISTAKE
C    23/03/94  FHW  EXAMPLES COMMENTED OUT
C*********************************************************************
C
C  SUBROUTINE ARGUMENTS
C
C   IPHASE - PHASE NUMBER
C  * BX    - X-COMPONENT OF VELOCITY-INDEPENDENT BODY FORCE
C  * BY    - Y-COMPONENT OF VELOCITY-INDEPENDENT BODY FORCE
C  * BZ    - Z-COMPONENT OF VELOCITY-INDEPENDENT BODY FORCE
C  * BPX   -
C  * BPY   - COMPONENTS OF LINEARISABLE BODY FORCES.
C  * BPZ   -
C
C  N.B. TOTAL BODY-FORCE IS GIVEN BY:
C
C      X-COMPONENT = BX + BPX*U
C      Y-COMPONENT = BY + BPY*V
C      Z-COMPONENT = BZ + BPZ*W
C
C   U     - U COMPONENT OF VELOCITY
C   V     - V COMPONENT OF VELOCITY
C   W     - W COMPONENT OF VELOCITY
C   P     - PRESSURE
C   VFRAC  - VOLUME FRACTION
C   DEN    - DENSITY OF FLUID
C   VIS    - VISCOSITY OF FLUID
C   TE     - TURBULENT KINETIC ENERGY
C   ED     - EPSILON
C   RS     - REYNOLD STRESSES
C   T      - TEMPERATURE
C   H      - ENTHALPY
C   SCAL   - SCALARS (THE FIRST 'NCONC' OF THESE ARE MASS FRACTIONS)
C   XP     - X COORDINATES OF CELL CENTRES
C   YP     - Y COORDINATES OF CELL CENTRES
C   ZP     - Z COORDINATES OF CELL CENTRES
C   VOL    - VOLUME OF CELLS
C   AREA   - AREA OF CELLS
C   VPOR   - POROUS VOLUME
C   ARPOR  - POROUS AREA
C   WFACT  - WEIGHT FACTORS
C
C   IPT    - 1D POINTER ARRAY
C   IBLK   - BLOCK SIZE INFORMATION
C   IPVERT - POINTER FROM CELL CENTERS TO 8 NEIGHBOURING VERTICES
C   IPNODN - POINTER FROM CELL CENTERS TO 6 NEIGHBOURING CELLS
C   IPFACN - POINTER FROM CELL CENTERS TO 6 NEIGHBOURING FACES
C   IPNODF - POINTER FROM CELL FACES TO 2 NEIGHBOURING CELL CENTERS
C   IPNODB - POINTER FROM BOUNDARY CENTERS TO CELL CENTERS
C   IPFACB - POINTER FROM BOUNDARY CENTERS TO BOUNDARY FACESS
C
C   WORK   - REAL WORKSPACE ARRAY
C   IWORK  - INTEGER WORKSPACE ARRAY
C   CWORK  - CHARACTER WORKSPACE ARRAY
C
```

```
C  SUBROUTINE ARGUMENTS PRECEDED WITH A '*' ARE ARGUMENTS THAT MUST
C  BE SET  BY THE USER IN THIS ROUTINE.
C
C  NOTE THAT OTHER DATA MAY BE OBTAINED FROM CFDS-FLOW3D USING THE
C  ROUTINE GETADD, FOR FURTHER DETAILS SEE THE RELEASE 3
C  USER MANUAL.
C
C*************************************************************************
C
      DOUBLE PRECISION BX
      DOUBLE PRECISION BY
      DOUBLE PRECISION BZ
      DOUBLE PRECISION BPX
      DOUBLE PRECISION BPY
      DOUBLE PRECISION BPZ
      DOUBLE PRECISION U
      DOUBLE PRECISION V
      DOUBLE PRECISION W
      DOUBLE PRECISION P
      DOUBLE PRECISION VFRAC
      DOUBLE PRECISION DEN
      DOUBLE PRECISION VIS
      DOUBLE PRECISION TE
      DOUBLE PRECISION ED
      DOUBLE PRECISION RS
      DOUBLE PRECISION T
      DOUBLE PRECISION H
      DOUBLE PRECISION RF
      DOUBLE PRECISION SCAL
      DOUBLE PRECISION XP
      DOUBLE PRECISION YP
      DOUBLE PRECISION ZP
      DOUBLE PRECISION VOL
      DOUBLE PRECISION AREA
      DOUBLE PRECISION VPOR
      DOUBLE PRECISION ARPOR
      DOUBLE PRECISION WFACT
      DOUBLE PRECISION WORK
      DOUBLE PRECISION SMALL
      DOUBLE PRECISION SORMAX
      DOUBLE PRECISION TIME
      DOUBLE PRECISION DT
      DOUBLE PRECISION DTINVF
      DOUBLE PRECISION TPARM
      LOGICAL LDEN,LVIS,LTURB,LTEMP,LBUOY,LSCAL,LCOMP,LRECT,LCYN,LAXIS,
     +     LPOROS,LTRANS
C
      CHARACTER*(*) CWORK
C
C+++++++++++++++++ USER AREA 1 ++++++++++++++++++++++++++++++++++++++++
C---- AREA FOR USERS EXPLICITLY DECLARED VARIABLES
C
C-- Global variables
      DOUBLE PRECISION VF_AVG, HTCL, HTFR
      DOUBLE PRECISION dia, areat,weirln, weirht, holearea,dcarea,dcclear
```

```
      DOUBLE PRECISION rhol, rhog, visl
      DOUBLE PRECISION ug, Ql
C
C-- Local variables
C
      DOUBLE PRECISION GRAV
      DOUBLE PRECISION VHOLE, Qgas,  GDRAG
      DOUBLE PRECISION COEF_XZ,TEMPX,TEMPZ
C
C
C+++++++++++++++++ END OF USER AREA 1 +++++++++++++++++++++++++++++++++++
C
      COMMON /ALL/NBLOCK,NCELL,NBDRY,NNODE,NFACE,NVERT,NDIM,
     +     /ALLWRK/NRWS,NIWS,NCWS,IWRFRE,IWIFRE,IWCFRE,/ADDIMS/NPHASE,
     +     NSCAL,NVAR,NPROP,NDVAR,NDPROP,NDXNN,NDGEOM,NDCOEF,NILIST,
     +     NRLIST,NTOPOL,/CHKUSR/IVERS,IUCALL,IUSED,/DEVICE/NREAD,
     +     NWRITE,NRDISK,NWDISK,/IDUM/ILEN,JLEN,/LOGIC/LDEN,LVIS,
     +     LTURB,LTEMP,LBUOY,LSCAL,LCOMP,LRECT,LCYN,LAXIS,LPOROS,
     +     LTRANS,/MLTGRD/MLEVEL,NLEVEL,ILEVEL,/SGLDBL/IFLGPR,ICHKPR,
     +     /SPARM/SMALL,SORMAX,NITER,INDPRI,MAXIT,NODREF,NODMON,
     +     /TRANSI/NSTEP,KSTEP,MF,INCORE,/TRANSR/TIME,DT,DTINVF,TPARM
C
C+++++++++++++++++ USER AREA 2 +++++++++++++++++++++++++++++++++++++++++
C---- AREA FOR USERS TO DECLARE THEIR OWN COMMON BLOCKS
C    THESE SHOULD START WITH THE CHARACTERS 'UC' TO ENSURE
C    NO CONFLICT WITH NON-USER COMMON BLOCKS
C
      COMMON /UCFROTH/VF_AVG, HTCL, HTFR
      COMMON /UCTRAY/dia, areat, weirln, weirht, holearea, dcarea,dcclear
      COMMON /UCPHYS/rhol, rhog, visl
      COMMON /UCOPCOND/ug, Ql
C
C+++++++++++++++++ END OF USER AREA 2 +++++++++++++++++++++++++++++++++++
C
      DIMENSION BX(NCELL),BY(NCELL),BZ(NCELL),BPX(NCELL),BPY(NCELL),
     +     BPZ(NCELL)
C
      DIMENSION U(NNODE,NPHASE),V(NNODE,NPHASE),W(NNODE,NPHASE),
     +     P(NNODE,NPHASE),VFRAC(NNODE,NPHASE),DEN(NNODE,NPHASE),
     +     VIS(NNODE,NPHASE),TE(NNODE,NPHASE),ED(NNODE,NPHASE),
     +     RS(NNODE,NPHASE,*),T(NNODE,NPHASE),H(NNODE,NPHASE),
     +     RF(NNODE,NPHASE,4),SCAL(NNODE,NPHASE,NSCAL)
C
      DIMENSION XP(NNODE),YP(NNODE),ZP(NNODE),VOL(NCELL),AREA(NFACE,3),
     +     VPOR(NCELL),ARPOR(NFACE,3),WFACT(NFACE),IPT(*),
     +     IBLK(5,NBLOCK),IPVERT(NCELL,8),IPNODN(NCELL,6),
     +     IPFACN(NCELL,6),IPNODF(NFACE,4),IPNODB(NBDRY,4),
     +     IPFACB(NBDRY),IWORK(*),WORK(*),CWORK(*)
C
C+++++++++++++++++ USER AREA 3 +++++++++++++++++++++++++++++++++++++++++
C---- AREA FOR USERS TO DIMENSION THEIR ARRAYS
C
C---- AREA FOR USERS TO DEFINE DATA STATEMENTS
C
C+++++++++++++++++ END OF USER AREA 3 +++++++++++++++++++++++++++++++++++
```

```
C
C---- STATEMENT FUNCTION FOR ADRESSING
      IP(I,J,K) = IPT((K-1)*ILEN*JLEN+ (J-1)*ILEN+I)
C
C----VERSION NUMBER OF USER ROUTINE AND PRECISION FLAG
C
      IVERS = 2
      ICHKPR = 2
C
C+++++++++++++++++ USER AREA 4 ++++++++++++++++++++++++++++++++++++++++
C---- TO USE THIS USER ROUTINE FIRST SET IUSED=1
C
      IUSED = 1
      IF (IUSED.EQ.0) RETURN
C
C+++++++++++++++++ END OF USER AREA 4 +++++++++++++++++++++++++++++++++
C
C---- FRONTEND CHECKING OF USER ROUTINE
      IF (IUCALL.EQ.0) RETURN
C
C+++++++++++++++++ USER AREA 5 ++++++++++++++++++++++++++++++++++++++++
C---Note that gravity is included as an effect in this routine.
C---Do not include buoyancy as a keyword in the command file
C
C
C--Constants
      GRAV = -9.81*rhol
C
C--Y Direction Body Force Calculations
C
C----BLOCK-NUMBER-1
C----INTERPHASE DRAG IS CALCULATED ONLY IN BLOCK-NUMBER-1 (ACTIVE REGION)
C
C--Calculate hole velocities
C
      Qgas = areat*ug*(1-dcarea)
      VHOLE = Qgas/(areat*holearea)
      GDRAG = ug*rhog*(VHOLE-ug)/HTCL
C
      CALL IPREC('BLOCK-NUMBER-1','BLOCK','CENTRES',IPT
     +           ,ILEN,JLEN,KLEN,CWORK,IWORK)
C
C----Y MOMENTUM EQUATION
C
      DO 313 K = 1, KLEN
        DO 312 J = 1, JLEN
          DO 311 I = 1, ILEN
C
          INODE = IP(I,J,K)
          BY(INODE) = BY(INODE) + GRAV + GDRAG
C
311       CONTINUE
312     CONTINUE
313   CONTINUE
C
```

```
C----BLOCK-NUMBER-2
C
      CALL IPREC('BLOCK-NUMBER-2','BLOCK','CENTRES',IPT
     +           ,ILEN,JLEN,KLEN,CWORK,IWORK)
C
      DO 403 K = 1, KLEN
        DO 402 J = 1, JLEN
          DO 401 I = 1, ILEN
C
          INODE = IP(I,J,K)
          BY(INODE) = BY(INODE) + GRAV
C
 401      CONTINUE
 402    CONTINUE
 403  CONTINUE
C
C----BLOCK-NUMBER-3
C
      CALL IPREC('BLOCK-NUMBER-3','BLOCK','CENTRES',IPT
     +           ,ILEN,JLEN,KLEN,CWORK,IWORK)
C
      DO 503 K = 1, KLEN
        DO 502 J = 1, JLEN
          DO 501 I = 1, ILEN
C
          INODE = IP(I,J,K)
          BY(INODE) = BY(INODE) + GRAV
C
 501      CONTINUE
 502    CONTINUE
 503  CONTINUE
C
C
C
C----X,Z MOMENTUM EQUATIONS (ONLY FOR BLOCK 1)
C
      CALL IPREC('BLOCK-NUMBER-1','BLOCK','CENTRES',IPT
     +           ,ILEN,JLEN,KLEN,CWORK,IWORK)
C
      DO 623 K = 1,KLEN
        DO 622 I = 1,ILEN
          DO 621 J = 1,JLEN
C
          INODE = IP(I,J,K)
          IBEL  = IP(I,J-1,K)
          IFACE = IPFACN(INODE,5)
C
          COEF_XZ = -rhog*ug*AREA(IFACE,2)/VPOR(INODE)
C
          IF (J.EQ.1) THEN
            TEMPX = 0.0
            TEMPZ = 0.0
          ELSE
            TEMPX = -COEF_XZ*U(IBEL,1)
            TEMPZ = -COEF_XZ*W(IBEL,1)
```

```
          END IF
C
          BX(INODE) =  BX(INODE) + TEMPX
          BPX(INODE) = BPX(INODE) + COEF_XZ
C
          BZ(INODE) =BZ(INODE) + TEMPZ
          BPZ(INODE) = BPZ(INODE) + COEF_XZ
C
 621       CONTINUE
 622     CONTINUE
 623    CONTINUE
C
C
C
C+++++++++++++++++ END OF USER AREA 5 +++++++++++++++++++++++++++++++++++
C
    RETURN
C
    END



    SUBROUTINE USRPOR(PORV,PORA,XP,YP,ZP,VOL,AREA,VPOR,ARPOR,WFACT,
   +              IPT,IBLK,IPVERT,IPNODN,IPFACN,IPNODF,IPNODB,
   +              IPFACB,WORK,IWORK,CWORK)
C
C**********************************************************************
C
C  UTILITY SUBROUTINE FOR USER-SUPPLIED VOLUME POROSITIES
C
C  >>> IMPORTANT                                  <<<
C  >>>                                            <<<
C  >>> USERS MAY ONLY ADD OR ALTER PARTS OF THE SUBROUTINE WITHIN  <<<
C  >>> THE DESIGNATED USER AREAS                          <<<
C
C**********************************************************************
C
C  THIS SUBROUTINE IS CALLED BY THE FOLLOWING SUBROUTINES
C    SETPOR
C
C**********************************************************************
C  CREATED
C    24/01/92  ADB
C  MODIFIED
C    03/06/92  PHA  ADD PRECISION FLAG AND CHANGE IVERS TO 2
C    23/11/93  CSH  EXPLICITLY DIMENSION IPVERT ETC.
C    03/02/94  PHA  CHANGE FLOW3D TO CFDS-FLOW3D
C    23/03/94  FHW  EXAMPLES COMMENTED OUT
C**********************************************************************
C
C  SUBROUTINE ARGUMENTS
C
C  * PORV   - VOLUME POROSITY (GAMMA)
```

```
C  * PORA   - AREA POROSITY (KIJ)
C
C                          1  = KXX
C                          2  = KYY
C   PORV(INODE) = GAMMA,     PORA(INODE,3) = KZZ
C                          4  = KXY
C                          5  = KYZ
C                          6  = KZX
C
C    XP    - X COORDINATES OF CELL CENTRES
C    YP    - Y COORDINATES OF CELL CENTRES
C    ZP    - Z COORDINATES OF CELL CENTRES
C    VOL   - VOLUME OF CELLS
C    AREA  - AREA OF CELLS
C    VPOR  - POROUS VOLUME
C    ARPOR - POROUS AREA
C    WFACT - WEIGHT FACTORS
C
C    IPT   - 1D POINTER ARRAY
C    IBLK  - BLOCK SIZE INFORMATION
C    IPVERT - POINTER FROM CELL CENTERS TO 8 NEIGHBOURING VERTICES
C    IPNODN - POINTER FROM CELL CENTERS TO 6 NEIGHBOURING CELLS
C    IPFACN - POINTER FROM CELL CENTERS TO 6 NEIGHBOURING FACES
C    IPNODF - POINTER FROM CELL FACES TO 2 NEIGHBOURING CELL CENTERS
C    IPNODB - POINTER FROM BOUNDARY CENTERS TO CELL CENTERS
C    IPFACB - POINTER FROM BOUNDARY CENTERS TO BOUNDARY FACESS
C
C    WORK  - REAL WORKSPACE ARRAY
C    IWORK - INTEGER WORKSPACE ARRAY
C    CWORK - CHARACTER WORKSPACE ARRAY
C
C  SUBROUTINE ARGUMENTS PRECEDED WITH A '*' ARE ARGUMENTS THAT MUST
C  BE SET  BY THE USER IN THIS ROUTINE.
C
C  NOTE THAT OTHER DATA MAY BE OBTAINED FROM CFDS-FLOW3D USING THE
C  ROUTINE GETADD, FOR FURTHER DETAILS SEE THE RELEASE 3
C  USER MANUAL.
C
C*************************************************************************
C
      DOUBLE PRECISION PORV
      DOUBLE PRECISION PORA
      DOUBLE PRECISION XP
      DOUBLE PRECISION YP
      DOUBLE PRECISION ZP
      DOUBLE PRECISION VOL
      DOUBLE PRECISION AREA
      DOUBLE PRECISION VPOR
      DOUBLE PRECISION ARPOR
      DOUBLE PRECISION WFACT
      DOUBLE PRECISION WORK
      DOUBLE PRECISION SMALL
      DOUBLE PRECISION SORMAX
      DOUBLE PRECISION TIME
      DOUBLE PRECISION DT
```

```
      DOUBLE PRECISION DTINVF
      DOUBLE PRECISION TPARM
      LOGICAL LDEN,LVIS,LTURB,LTEMP,LBUOY,LSCAL,LCOMP,LRECT,LCYN,LAXIS,
     +     LPOROS,LTRANS
C
      CHARACTER*(*) CWORK
C
C+++++++++++++++++ USER AREA 1 +++++++++++++++++++++++++++++++++++++++++
C---- AREA FOR USERS EXPLICITLY DECLARED VARIABLES
      DOUBLE PRECISION COEF
C
      DOUBLE PRECISION VF_AVG, HTCL, HTFR
      DOUBLE PRECISION dia,areat, weirln, weirht, holearea, dcarea, dcclear
      DOUBLE PRECISION rhol, rhog, visl
      DOUBLE PRECISION ug, Ql
C
C+++++++++++++++++ END OF USER AREA 1 +++++++++++++++++++++++++++++++++++
C
      COMMON /ALL/NBLOCK,NCELL,NBDRY,NNODE,NFACE,NVERT,NDIM,
     +     /ALLWRK/NRWS,NIWS,NCWS,IWRFRE,IWIFRE,IWCFRE,/ADDIMS/NPHASE,
     +     NSCAL,NVAR,NPROP,NDVAR,NDPROP,NDXNN,NDGEOM,NDCOEF,NILIST,
     +     NRLIST,NTOPOL,/CHKUSR/IVERS,IUCALL,IUSED,/DEVICE/NREAD,
     +     NWRITE,NRDISK,NWDISK,/IDUM/ILEN,JLEN,/LOGIC/LDEN,LVIS,
     +     LTURB,LTEMP,LBUOY,LSCAL,LCOMP,LRECT,LCYN,LAXIS,LPOROS,
     +     LTRANS,/MLTGRD/MLEVEL,NLEVEL,ILEVEL,/SGLDBL/IFLGPR,ICHKPR,
     +     /SPARM/SMALL,SORMAX,NITER,INDPRI,MAXIT,NODREF,NODMON,
     +     /TRANSI/NSTEP,KSTEP,MF,INCORE,/TRANSR/TIME,DT,DTINVF,TPARM
C
C+++++++++++++++++ USER AREA 2 +++++++++++++++++++++++++++++++++++++++++
C---- AREA FOR USERS TO DECLARE THEIR OWN COMMON BLOCKS
C    THESE SHOULD START WITH THE CHARACTERS 'UC' TO ENSURE
C    NO CONFLICT WITH NON-USER COMMON BLOCKS
C
      COMMON /UCFROTH/VF_AVG, HTCL, HTFR
      COMMON /UCTRAY/dia,areat,weirln, weirht, holearea,dcarea, dcclear
      COMMON /UCPHYS/rhol, rhog, visl
      COMMON /UCOPCOND/ug, Ql
C
C+++++++++++++++++ END OF USER AREA 2 +++++++++++++++++++++++++++++++++++
C
      DIMENSION PORV(NCELL),PORA(NCELL,6)
C
      DIMENSION XP(NNODE),YP(NNODE),ZP(NNODE),VOL(NCELL),AREA(NFACE,3),
     +     VPOR(NCELL),ARPOR(NFACE,3),WFACT(NFACE),IPT(*),
     +     IBLK(5,NBLOCK),IPVERT(NCELL,8),IPNODN(NCELL,6),
     +     IPFACN(NCELL,6),IPNODF(NFACE,4),IPNODB(NBDRY,4),
     +     IPFACB(NBDRY),IWORK(*),WORK(*),CWORK(*)
C
C+++++++++++++++++ USER AREA 3 +++++++++++++++++++++++++++++++++++++++++
C---- AREA FOR USERS TO DIMENSION THEIR ARRAYS
C
C---- AREA FOR USERS TO DEFINE DATA STATEMENTS
C
C+++++++++++++++++ END OF USER AREA 3 +++++++++++++++++++++++++++++++++++
C
```

```
C---- STATEMENT FUNCTION FOR ADRESSING
      IP(I,J,K) = IPT((K-1)*ILEN*JLEN+ (J-1)*ILEN+I)
C
C----VERSION NUMBER OF USER ROUTINE AND PRECISION FLAG
C
      IVERS = 2
      ICHKPR = 2
C
C+++++++++++++++++ USER AREA 4 ++++++++++++++++++++++++++++++++++++++++++
C---- TO USE THIS USER ROUTINE FIRST SET IUSED=1
C
      IUSED = 1
      IF (IUSED.EQ.0) RETURN
C
C+++++++++++++++++ END OF USER AREA 4 ++++++++++++++++++++++++++++++++++
C
C---- FRONTEND CHECKING OF USER ROUTINE
      IF (IUCALL.EQ.0) RETURN
C
C+++++++++++++++++ USER AREA 5 ++++++++++++++++++++++++++++++++++++++++++
C---Sept 10/95  - specify constant avg por.
C---Sept 13/95  - setup so all model data will be input in this subroutine
C               with common blocks
C---Nov 4/95    - remove Bennett correlation; results from colwell are used
C
C
C---Initialize variables
C
      dia = 1.213
      weirln = 0.925
      weirht = 0.05
C---frac hole area based on total area
      holearea = 0.05
C---frac dc area based on total area
      dcarea = 0.2381
C---downcomer clearance
      dcclear = 0.05
C
      areat = 3.14*dia*dia/4.0
C
      rhog = 1.36
      rhol = 1000.0
      visl = 0.001
C
      Ql = 6.94E-3
      ug = 1.255
C
C
C---Specify average void fraction and froth height (Colwell Correlation)
C
      VF_AVG = 0.2129
      HTFR = 0.143
      HTCL = HTFR*VF_AVG
C
C
```

```
C---Loop through the nodes of block 1
C
      CALL IPREC('BLOCK-NUMBER-1','BLOCK','CENTRES',IPT
     +           ,ILEN,JLEN,KLEN,CWORK,IWORK)
C
C
      DO 103 K = 1, KLEN
        DO 102 J = 1, JLEN
          DO 101 I = 1, ILEN
C
            INODE = IP(I,J,K)
C
            PORV(INODE) = VF_AVG
C
            PORA(INODE,1) = VF_AVG
            PORA(INODE,2) = VF_AVG
            PORA(INODE,3) = VF_AVG
            PORA(INODE,4) = 0.0
            PORA(INODE,5) = 0.0
            PORA(INODE,6) = 0.0
C
 101      CONTINUE
 102    CONTINUE
 103  CONTINUE
C
C++++++++++++++++++ END OF USER AREA 5 +++++++++++++++++++++++++++++++++++
C
      RETURN
C
      END



      SUBROUTINE USRVIS(VISN,U,V,W,P,VFRAC,DEN,VIS,TE,ED,RS,T,H,RF,SCAL,
     +                  XP,YP,ZP,VOL,AREA,VPOR,ARPOR,WFACT,DIFLAM,
     +                  URFVAR,IPT,IBLK,IPVERT,IPNODN,IPFACN,IPNODF,
     +                  IPNODB,IPFACB,WORK,IWORK,CWORK)
C
C**********************************************************************
C
C  USER SUBROUTINE TO PROVIDE VARIABLE LAMINAR VISCOSITY, IF REQUIRED.
C
C  >>> IMPORTANT                                  <<<
C  >>>                                        <<<
C  >>> USERS MAY ONLY ADD OR ALTER PARTS OF THE SUBROUTINE WITHIN  <<<
C  >>> THE DESIGNATED USER AREAS                          <<<
C
C**********************************************************************
C
C  THIS SUBROUTINE IS CALLED BY THE FOLLOWING SUBROUTINES
C    CUSR  CVIS
C
C**********************************************************************
C  CREATED
```

```
C    22/11/89  ADB
C  MODIFIED
C    08/08/91  IRH  NEW STRUCTURE
C    03/09/91  IRH  CORRECT ARGUMENT LIST AND /CHKUSR/
C    25/09/91  IRH  ADD USEFUL COMMON BLOCKS
C    29/11/91  PHA  UPDATE CALLED BY COMMENT, INCLUDE RF ARGUMENT,
C              CHANGE LAST DIMENSION OF RS TO 6 AND IVERS TO 2
C    03/06/92  PHA  ADD PRECISION FLAG AND CHANGE IVERS TO 3
C    03/07/92  DSC  CORRECT COMMON MLTGRD.
C    02/08/93  NSW  INCLUDE DIMENSIONING FOR URFVAR
C    21/09/93  NSW  MODIFY FOR USER TO SET NEW VALUE OF VISCOSITY
C              TO BE UNDER-RELAXED. CHANGE IVERS TO 4
C    23/11/93  CSH  EXPLICITLY DIMENSION IPVERT ETC.
C    03/02/94  PHA  CHANGE FLOW3D TO CFDS-FLOW3D
C    03/03/94  FHW  CORRECTION OF SPELLING MISTAKE
C
C*************************************************************************
C
C  SUBROUTINE ARGUMENTS
C
C * VISN   - NEW VALUE OF VISCOSITY
C   U      - U COMPONENT OF VELOCITY
C   V      - V COMPONENT OF VELOCITY
C   W      - W COMPONENT OF VELOCITY
C   P      - PRESSURE
C   VFRAC  - VOLUME FRACTION
C   DEN    - DENSITY OF FLUID
C   VIS    - OLD VALUE OF VISCOSITY
C   TE     - TURBULENT KINETIC ENERGY
C   ED     - EPSILON
C   RS     - REYNOLD STRESSES
C   T      - TEMPERATURE
C   H      - ENTHALPY
C   RF     - REYNOLD FLUXES
C   SCAL   - SCALARS (THE FIRST 'NCONC' OF THESE ARE MASS FRACTIONS)
C   XP     - X COORDINATES OF CELL CENTRES
C   YP     - Y COORDINATES OF CELL CENTRES
C   ZP     - Z COORDINATES OF CELL CENTRES
C   VOL    - VOLUME OF CELLS
C   AREA   - AREA OF CELLS
C   VPOR   - POROUS VOLUME
C   ARPOR  - POROUS AREA
C   DIFLAM - LAMINAR DIFFUSIVITY
C   URFVAR - UNDER RELAXATION FACTORS
C
C   IPT    - 1D POINTER ARRAY
C   IBLK   - BLOCK SIZE INFORMATION
C   IPVERT - POINTER FROM CELL CENTERS TO 8 NEIGHBOURING VERTICES
C   IPNODN - POINTER FROM CELL CENTERS TO 6 NEIGHBOURING CELLS
C   IPFACN - POINTER FROM CELL CENTERS TO 6 NEIGHBOURING FACES
C   IPNODF - POINTER FROM CELL FACES TO 2 NEIGHBOURING CELL CENTERS
C   IPNODB - POINTER FROM BOUNDARY CENTERS TO CELL CENTERS
C   IPFACB - POINTER FROM BOUNDARY CENTERS TO BOUNDARY FACES
C
C   WORK   - REAL WORKSPACE ARRAY
```

```
C    IWORK  - INTEGER WORKSPACE ARRAY
C    CWORK  - CHARACTER WORKSPACE ARRAY
C
C  SUBROUTINE ARGUMENTS PRECEDED WITH A '*' ARE ARGUMENTS THAT MUST
C  BE SET  BY THE USER IN THIS ROUTINE.
C
C  NOTE THAT THE USER SHOULD SET THE VALUE REQUIRED FOR THE
C  NEW VISCOSITY. THIS WILL BE UNDER-RELAXED WITH REGARD TO THE OLD
C  VALUE OF VISCOSITY AUTOMATICALLY BY THE PROGRAM.
C
C  NOTE THAT OTHER DATA MAY BE OBTAINED FROM CFDS-FLOW3D USING THE
C  ROUTINE GETADD, FOR FURTHER DETAILS SEE THE RELEASE 3
C  USER MANUAL.
C
C*************************************************************************
C
      DOUBLE PRECISION VISN
      DOUBLE PRECISION U
      DOUBLE PRECISION V
      DOUBLE PRECISION W
      DOUBLE PRECISION P
      DOUBLE PRECISION VFRAC
      DOUBLE PRECISION DEN
      DOUBLE PRECISION VIS
      DOUBLE PRECISION TE
      DOUBLE PRECISION ED
      DOUBLE PRECISION RS
      DOUBLE PRECISION T
      DOUBLE PRECISION H
      DOUBLE PRECISION RF
      DOUBLE PRECISION SCAL
      DOUBLE PRECISION XP
      DOUBLE PRECISION YP
      DOUBLE PRECISION ZP
      DOUBLE PRECISION VOL
      DOUBLE PRECISION AREA
      DOUBLE PRECISION VPOR
      DOUBLE PRECISION ARPOR
      DOUBLE PRECISION WFACT
      DOUBLE PRECISION DIFLAM
      DOUBLE PRECISION URFVAR
      DOUBLE PRECISION WORK
      DOUBLE PRECISION SMALL
      DOUBLE PRECISION SORMAX
      DOUBLE PRECISION TIME
      DOUBLE PRECISION DT
      DOUBLE PRECISION DTINVF
      DOUBLE PRECISION TPARM
      LOGICAL LDEN,LVIS,LTURB,LTEMP,LBUOY,LSCAL,LCOMP,LRECT,LCYN,LAXIS,
     +        LPOROS,LTRANS
C
      CHARACTER*(*) CWORK
C
C+++++++++++++++++ USER AREA 1 +++++++++++++++++++++++++++++++++++++++++
C---- AREA FOR USERS EXPLICITLY DECLARED VARIABLES
```

```
C
      DOUBLE PRECISION LK, LKSQ, ABGRAD
C
C+++++++++++++++++ END OF USER AREA 1 +++++++++++++++++++++++++++++++++++
C
      COMMON /ALL/NBLOCK,NCELL,NBDRY,NNODE,NFACE,NVERT,NDIM,
     +      /ALLWRK/NRWS,NIWS,NCWS,IWRFRE,IWIFRE,IWCFRE,/ADDIMS/NPHASE,
     +      NSCAL,NVAR,NPROP,NDVAR,NDPROP,NDXNN,NDGEOM,NDCOEF,NILIST,
     +      NRLIST,NTOPOL,/CHKUSR/IVERS,IUCALL,IUSED,/DEVICE/NREAD,
     +      NWRITE,NRDISK,NWDISK,/IDUM/ILEN,JLEN,/LOGIC/LDEN,LVIS,
     +      LTURB,LTEMP,LBUOY,LSCAL,LCOMP,LRECT,LCYN,LAXIS,LPOROS,
     +      LTRANS,/MLTGRD/MLEVEL,NLEVEL,ILEVEL,/SGLDBL/IFLGPR,ICHKPR,
     +      /SPARM/SMALL,SORMAX,NITER,INDPRI,MAXIT,NODREF,NODMON,
     +      /TRANSI/NSTEP,KSTEP,MF,INCORE,/TRANSR/TIME,DT,DTINVF,TPARM
C
C+++++++++++++++++ USER AREA 2 +++++++++++++++++++++++++++++++++++++++++
C---- AREA FOR USERS TO DECLARE THEIR OWN COMMON BLOCKS
C    THESE SHOULD START WITH THE CHARACTERS 'UC' TO ENSURE
C    NO CONFLICT WITH NON-USER COMMON BLOCKS
C
C+++++++++++++++++ END OF USER AREA 2 +++++++++++++++++++++++++++++++++++
C
      DIMENSION DIFLAM(NVAR,NPHASE),URFVAR(NVAR,NPHASE)
C
      DIMENSION VISN(NNODE,NPHASE),U(NNODE,NPHASE),V(NNODE,NPHASE),
     +      W(NNODE,NPHASE),P(NNODE,NPHASE),VFRAC(NNODE,NPHASE),
     +      DEN(NNODE,NPHASE),VIS(NNODE,NPHASE),TE(NNODE,NPHASE),
     +      ED(NNODE,NPHASE),RS(NNODE,NPHASE,6),T(NNODE,NPHASE),
     +      H(NNODE,NPHASE),RF(NNODE,NPHASE,4),
     +      SCAL(NNODE,NPHASE,NSCAL)
C
      DIMENSION XP(NNODE),YP(NNODE),ZP(NNODE),VOL(NCELL),AREA(NFACE,3),
     +      VPOR(NCELL),ARPOR(NFACE,3),WFACT(NFACE),IPT(*),
     +      IBLK(5,NBLOCK),IPVERT(NCELL,8),IPNODN(NCELL,6),
     +      IPFACN(NCELL,6),IPNODF(NFACE,4),IPNODB(NBDRY,4),
     +      IPFACB(NBDRY),IWORK(*),WORK(*),CWORK(*)
C
C+++++++++++++++++ USER AREA 3 +++++++++++++++++++++++++++++++++++++++++
C---- AREA FOR USERS TO DIMENSION THEIR ARRAYS
C
C---- AREA FOR USERS TO DEFINE DATA STATEMENTS
C
C+++++++++++++++++ END OF USER AREA 3 +++++++++++++++++++++++++++++++++++
C
C---- STATEMENT FUNCTION FOR ADDRESSING
      IP(I,J,K) = IPT((K-1)*ILEN*JLEN+ (J-1)*ILEN+I)
C
C----VERSION NUMBER OF USER ROUTINE AND PRECISION FLAG
C
      IVERS = 4
      ICHKPR = 2
C
C+++++++++++++++++ USER AREA 4 +++++++++++++++++++++++++++++++++++++++++
C---- TO USE THIS USER ROUTINE FIRST SET IUSED=1
C
```

```
      IUSED = 1
      IF (IUSED.EQ.0) RETURN
C+++++++++++++++++ END OF USER AREA 4 ++++++++++++++++++++++++++++++++++
C
C---- FRONTEND CHECKING OF USER ROUTINE
      IF (IUCALL.EQ.0) RETURN
C
C+++++++++++++++++ USER AREA 5 ++++++++++++++++++++++++++++++++++++++++
C
C-----CALCULATION OF TURBULENT VISCOSITY
C     PRANDTL'S MIXING LENGTH RULE
C     DEFINED BY AN EDDY DIFFUSIVITY CALCULATION
C     AVERAGE 0F ZUIDERWEG'S CORRELATIONS FOR SPRAY-FROTH AND EMULSION
REGIMES
C
C----- Note that the calcs are done elsewhere and the final value is used.
C
C---initialize variables
      IPHASE = 1
C
C----get all cell centres
      CALL IPALL('*','*','BLOCK','CENTRES',IPT,NPT,CWORK,IWORK)
C
C
C---compute velocity gradients for IPHASE
C
C----loop over interior cells set viscosity = turbvis
      DO 200 I=1,NPT
C
       INODE=IPT(I)
C
       VISN(INODE,IPHASE) = 2.2086
C
 200  CONTINUE
C
C
C
C
C+++++++++++++++++ END OF USER AREA 5 ++++++++++++++++++++++++++++++++++
C
      RETURN
C
      END
```

Appendix II

Grid Generation

Geometry File:

CFDS-FLOW3D uses a finite volume method to solve the partial differential equations that are posed in the model. In this method, the flow geometry is discretized into finite volume cells in a three dimensional grid. The shape of the cells and the grid is established by specifying the coordinates of each of the cell's 8 vertices.

The C++ program presented in this Appendix is used to generate the geometry file. The geometry file will contain the coordinates of all the cell vertices in the geometry grid. Figures A2-1 and A2-2 show the top and side views of a typical geometry generated using this program.

Grid Refinement:

The grid resolution determines the accuracy of the predictions. Obviously, the finer the grid resolution, the more accurate the solution. The number of cells in a geometry is limited by the computational limits of run time and memory constraints. The size of a cell in the grid was chosen to be:

Coordinate Direction	Length (m)
x	0.04500
y	0.00625
z	0.04500

To test the adequacy of this grid size, a single simulation (B2) was conducted with each of the coordinate lengths halved. Thus the number of cells increased by a factor of 8.

Case	Number of Cells
Base	7966
Test Grid	63728

The average difference in results was only 0.6%. The coarser grid size has sufficient resolution for this model.

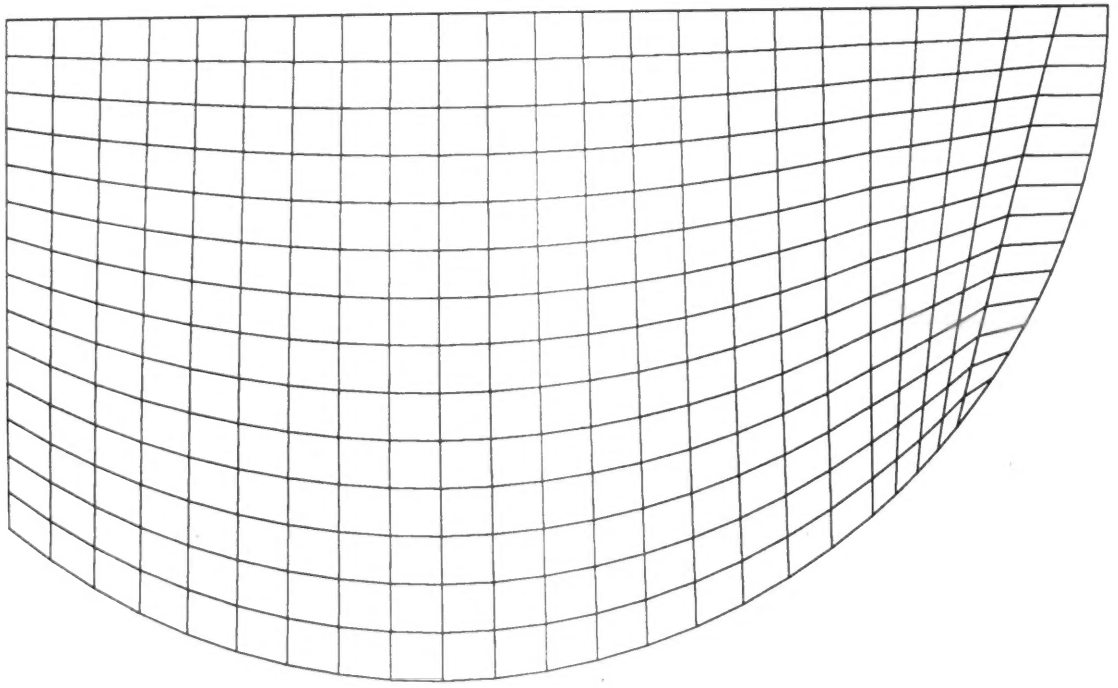

Figure A2-1. Simulation Geometry - Top View

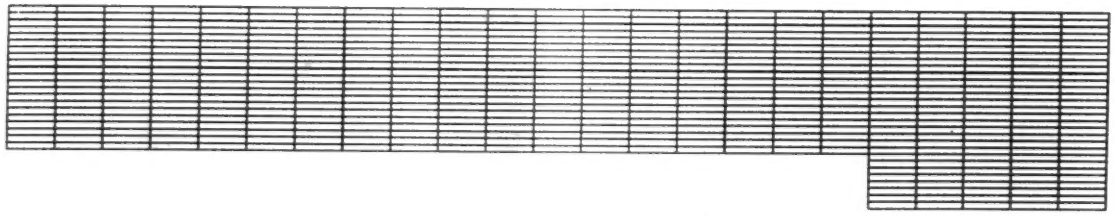

Figure A2-2. Simulation Geometry - Side View

```
/*****************************************************
* Distillation Tray Geometry Creation Program
* Nov 5/95: UNIX version - xlC compiled
*
* Bemal Mehta
* MSc Student
* University of Alberta
*
*
* This program creates an output file that contains the
* geometry information for a sieve tray simulation.
* This geometry file will then be used in a CFDS-FLOW3D
* Simulation.
*****************************************************/

#include <fstream.h>
#include <math.h>
#define MAXSIZE  100

/*****************************************************
* Class Vertex
*****************************************************/

class Vertex
{
        double x,y,z;
public:
        Vertex();
        Vertex(double a, double b, double c);
        void print(ofstream& outfile);
        Vertex operator+(Vertex);
        Vertex operator-(Vertex);
        Vertex operator=(Vertex);
        void curvept(double radius, double phi, double ht);
        void set(double a, double b, double c);
        void inter_vect(Vertex a, Vertex b, int n);
};

Vertex::Vertex()
{
        x = 0.0;
        y = 0.0;
        z = 0.0;
}
```

```
Vertex::Vertex(double a, double b, double c)
{
        x = a;
        y = b;
        z = c;
}

void Vertex::print(ofstream& outfile)
{
        outfile << "    " <<x;
        outfile << "    " <<y;
        outfile << "    " <<z << "\n";

}

Vertex Vertex::operator+ (Vertex a)
{
        Vertex Temp;
        Temp.x = x + a.x;
        Temp.y = y + a.y;
        Temp.z = z + a.z;
        return Temp;
}

Vertex Vertex::operator- (Vertex a)
{
        Vertex Temp;
        Temp.x = x - a.x;
        Temp.y = y - a.y;
        Temp.z = z - a.z;
        return Temp;
}

Vertex Vertex::operator= (Vertex a)
{
        x = a.x;
        y = a.y;
        z = a.z;
        return *this;
}

void Vertex::curvept(double radius, double phi, double ht)
{
        x = radius*cos(phi);
        y = ht;
```

```
        z = radius*sin(phi);
}

void Vertex::set(double a, double b, double c)
{
        x = a;
        y = b;
        z = c;
}

void Vertex::inter_vect(Vertex a, Vertex b, int n)
{
        *this = a - b;
        x = x/n;
        y = y/n;
        z = z/n;
}

int main(void)
{
// INPUT DATA  - Tray

        double radius= 0.6065;
        double weirlength = 0.925;
        double downcomer = 0.10;
        double weir_ht = 0.05;

        int NR = 20 ;
      int NC = 8;  //NC is declared here because dc is too small
        int NW = 8;

//  INPUT DATA  - Operating Conditions

        double Us = 0.9475;
        double Ql = 6.94E-3;
        double rhol = 1000.0;
        double rhog = 1.36;

// Declare Variables

        int NA, NAW, NLD,NI,NK;

        double froth_ht,A, C, theta, phi,del_theta;
        int i,j,k;
```

```
        double vf_l;

        Vertex del_ik, del_centrept, del_j, point;
        Vertex jdisp;

        Vertex matrix[MAXSIZE][MAXSIZE];


// Colwell Corrlation results (Calculated separately)

        vf_l = 0.2631 ;
        froth_ht = 0.1323 ;

// Calculate dimensional info

        A = sqrt( pow(radius,2.0) - pow((weirlength/2),2.0))  ;
        C = radius -A;
        theta = acos(A/radius);

// Calculate cell discetization information

        NA = int(floor(NR*A/radius));

        NI = 2*NA;
        NK = NR;

        NAW = int( ceil(NW*(froth_ht - weir_ht)/weir_ht));
        NLD = int( floor(NW*downcomer/weir_ht));


// File and Print Format Management
        ofstream file;
        ofstream ofile;

// Flow3D geometry file name - m09.geo
        ofile.open("m09.geo");
        ofile.setf(ios::scientific);

// Data File - for reference purposes only
        file.open("geo09.data");

//Write geometry data

          file << "Block1: "
```

```
  << NI <<"  " << (NW+NAW) <<"  " << NK <<"\n" ;
 file << "Block2: "
  << NC <<"  " << (NW+NAW) <<"  " << NK <<"\n" ;
 file << "Block3: "
  << NC <<"  " << NLD <<"  " << NK <<"\n" ;
 file << froth_ht << "  "<< vf_l << "\n" ;


/*****************************************
* Calculate Block-Number-1 -active area *
*****************************************/


        ofile << "/* VERTEX CO-ORDS(X,Y,Z) FOR BLOCK    1 */\n" ;

//Calculate active area constants

        del_centrept.set(A/NA, 0., 0.);
        del_theta = ( M_PI_2 - theta)/NA;
        phi = M_PI-theta;

// Calculate and Initialize a Block 1 plane (matrix)

        for (i= 0; i<=NI; i++)
         {
           if (i == 0)
                {
                 matrix[0][0].set(-A, 0., 0.);
                }
           else
                {
                 phi = phi - del_theta;

                 matrix[i][0] = matrix[i-1][0] + del_centrept;
                }

           matrix[i][NK].curvept(radius,phi,0.0);
           del_ik.inter_vect(matrix[i][NK],matrix[i][0],NK);

         for (k = 1; k<=(NK-1); k++)
          {
           matrix[i][k] = matrix[i][k-1] + del_ik;
          }

          }
```

```
// Calculate and Print Block 1

        for (k=0; k<=NK; k++)
         {
          jdisp.set(0., 0., 0.);

        for (j=0; j<=(NW+NAW); j++)
            {

             for (i=0; i<=NI; i++)
                 {
                        point = matrix[i][k] + jdisp;
                        point.print(ofile);
                 }

                if (j<=NW)
                 del_j.set(0., weir_ht/NW, 0.);
                else
                 del_j.set(0., (froth_ht-weir_ht)/NAW, 0.);

                jdisp = jdisp + del_j;
            }
      }
/*****************************************************
* Calculate Block-Number-2 and 3  -downcomer area *
*****************************************************/


        ofile << "/* VERTEX CO-ORDS(X,Y,Z) FOR BLOCK   2 */\n" ;

//Calculate active area constants

        del_centrept.set(C/NC, 0., 0.);
        del_theta = theta/(NC+NK);
        phi = theta;

// Calculate and Initialize a Block 2 and 3 plane (matrix)

        for (i= 0; i<=NC; i++)
         {
           if (i == 0)
               {
                matrix[0][0].set(A, 0., 0.);
               }
```

```
        else
            {
             phi = phi - del_theta;

             matrix[i][0] = matrix[i-1][0] + del_centrept;
            }

        matrix[i][NK].curvept(radius,phi,0.0);
        del_ik.inter_vect(matrix[i][NK],matrix[i][0],NK);

        //do last line - mapped on the curve
        if (i==NC)
            phi = 0;

      for (k = 1; k<=(NK-1); k++)
       {
        if (i==NC)
            {
             phi = phi+del_theta;
             matrix[i][k].curvept(radius,phi,0.);
            }
        else
            {
             matrix[i][k] = matrix[i][k-1] + del_ik;
            }

       }

       }

// Calculate and Print Block 2

      for (k=0; k<=NK; k++)
       {

        jdisp.set(0., 0., 0.);

      for (j=0; j<=(NW+NAW); j++)
        {

          for (i=0; i<=NC; i++)
            {
                point = matrix[i][k] + jdisp;
                point.print(ofile);
            }
```

```
                if (j<=NW)
                  del_j.set(0., weir_ht/NW, 0.);
                else
                  del_j.set(0., (froth_ht-weir_ht)/NAW, 0.);

                jdisp = jdisp + del_j;
            }
        }
// Calculate and Print Block 3

        ofile << "/* VERTEX CO-ORDS(X,Y,Z) FOR BLOCK   3 */\n" ;

        del_j.set(0. , downcomer/NLD, 0.);

        for (k=0; k<=NK; k++)
          {

            jdisp.set(0., -downcomer, 0.);

        for (j=0; j<=NLD; j++)
            {

              for (i=0; i<=NC; i++)
                  {
                        point = matrix[i][k] + jdisp;
                        point.print(ofile);
                  }
                jdisp = jdisp + del_j;
            }
      }


//Clean-up and Exit

            ofile.close();
            file.close();
            return(0);
}
```

Appendix III

Statistical Definitions

Statistical Definitions:

1. Mean Liquid Velocity:

$$\bar{v} = \frac{Q_L}{\alpha_{L,avg} h_f L_w}$$

2. Standard Error (absolute):

$$E_{st} = \sqrt{\frac{\sum \left(v_{actual} - v_{predicted} \right)^2}{n-2}}$$

3. Standard Error (percent):

$$E_{st\%} = \left(\frac{E_{st}}{\bar{v}} \right) \times 100$$

Appendix IV

Data Sets

DATA SETS

Velocity and Flow Pattern Evaluation

SET A:

Author(s): Solari Saez D'Apollo Bellet
Title: Velocity Distribution and Liquid Flow Patterns on Industrial Sieve Trays
Reference: Chem. Eng. Commun.
Volume: 13
Pages: 369 - 384
Year: 1982
Abbreviation: SSDB-82

Chemical System: air-water

Case	Dia. (m)	Lw (m)	hw (m)	Hole Area	Ql (m3/s)	Fs	Flv
A1	1.250	0.726	0.050	0%	1.262E-02	0.000	#DIV/0!
A2	1.250	0.726	0.000	0%	6.310E-03	0.000	#DIV/0!
A3	1.250	0.726	0.000	0%	1.135E-02	0.000	#DIV/0!
A4	1.250	0.726	0.000	0%	1.577E-02	0.000	#DIV/0!
A5	1.250	0.726	0.000	0%	2.208E-02	0.000	#DIV/0!
A6	1.250	0.726	0.000	8%	6.310E-03	0.518	0.346
A7	1.250	0.726	0.000	8%	1.135E-02	0.518	0.623
A8	1.250	0.726	0.000	8%	1.577E-02	0.518	0.866
A9	1.250	0.726	0.000	8%	2.208E-02	0.518	1.212
A10	1.250	0.726	0.100	8%	1.577E-02	0.649	0.691
A11	1.250	0.726	0.100	8%	2.208E-02	0.649	0.967
A12	1.250	0.726	0.050	8%	1.640E-02	0.410	1.137
A13	1.250	0.726	0.050	8%	1.325E-02	0.410	0.919
A14	1.250	0.726	0.050	8%	1.104E-02	0.410	0.766
A15	1.250	0.726	0.050	8%	1.640E-02	0.910	0.512
A16	1.250	0.726	0.050	8%	1.325E-02	0.910	0.414
A17	1.250	0.726	0.050	8%	1.104E-02	0.910	0.345

SET B:

Author(s): Solari Bell
Title: Fluid Flow Patterns and Velocity Distribution on Commercial-Scale Sieve Trays
Reference: AIChEJ
Vol: 32
No: 4
Pages: 640-649
Year: 1986
Abbreviation: SB-86

Chemical System: air-water

Case	Dia. (m)	Lw (m)	hw (m)	Hole Area	Ql (m3/s)	Fs	Flv
B1	1.213	0.925	0.050	5%	6.940E-03	1.015	0.246
B2	1.213	0.925	0.050	5%	6.940E-03	1.464	0.170
B3	1.213	0.925	0.050	5%	1.780E-02	0.462	1.385
B4	1.213	0.925	0.050	5%	1.780E-02	0.801	0.799

DATA SETS

Velocity and Flow Pattern Evaluation

SET A:

Author(s): Solari Saez D'Apollo Bellet
Title: Velocity Distribution and Liquid Flow Patterns on Industrial Sieve Trays
Reference: Chem. Eng. Commun.
Volume: 13
Pages: 369 - 384
Year: 1982
Abbreviation: SSDB-82

Chemical System: air-water

Case	Dia. (m)	Lw (m)	hw (m)	Hole Area	Ql (m3/s)	Fs	Flv
A1	1.250	0.726	0.050	0%	1.262E-02	0.000	#DIV/0!
A2	1.250	0.726	0.000	0%	6.310E-03	0.000	#DIV/0!
A3	1.250	0.726	0.000	0%	1.135E-02	0.000	#DIV/0!
A4	1.250	0.726	0.000	0%	1.577E-02	0.000	#DIV/0!
A5	1.250	0.726	0.000	0%	2.208E-02	0.000	#DIV/0!
A6	1.250	0.726	0.000	8%	6.310E-03	0.518	0.346
A7	1.250	0.726	0.000	8%	1.135E-02	0.518	0.623
A8	1.250	0.726	0.000	8%	1.577E-02	0.518	0.866
A9	1.250	0.726	0.000	8%	2.208E-02	0.518	1.212
A10	1.250	0.726	0.100	8%	1.577E-02	0.649	0.691
A11	1.250	0.726	0.100	8%	2.208E-02	0.649	0.967
A12	1.250	0.726	0.050	8%	1.640E-02	0.410	1.137
A13	1.250	0.726	0.050	8%	1.325E-02	0.410	0.919
A14	1.250	0.726	0.050	8%	1.104E-02	0.410	0.766
A15	1.250	0.726	0.050	8%	1.640E-02	0.910	0.512
A16	1.250	0.726	0.050	8%	1.325E-02	0.910	0.414
A17	1.250	0.726	0.050	8%	1.104E-02	0.910	0.345

SET B:

Author(s): Solari Bell
Title: Fluid Flow Patterns and Velocity Distribution on Commercial-Scale Sieve Trays
Reference: AIChEJ
Vol: 32
No: 4
Pages: 640-649
Year: 1986
Abbreviation: SB-86

Chemical System: air-water

Case	Dia. (m)	Lw (m)	hw (m)	Hole Area	Ql (m3/s)	Fs	Flv
B1	1.213	0.925	0.050	5%	6.940E-03	1.015	0.246
B2	1.213	0.925	0.050	5%	6.940E-03	1.464	0.170
B3	1.213	0.925	0.050	5%	1.780E-02	0.462	1.385
B4	1.213	0.925	0.050	5%	1.780E-02	0.801	0.799